

Brown, M. C., Hervé, G., Korte, M., Genevey, A. (2021):
Global archaeomagnetic data: The state of the art and
future challenges. - Physics of the Earth and Planetary
Interiors, 318, 106766.

<https://doi.org/10.1016/j.pepi.2021.106766>

Global archaeomagnetic data: the state of the art and future challenges

Maxwell C. Brown^{*,a,b}, Gwenaël Hervé^{c,d,e}, Monika Korte^f, Agnès Genevey^g

^a*Institute for Rock Magnetism, Department of Earth and Environmental Sciences, University of Minnesota, 150 John T. Tate Hall, 116 Church St SE, Minneapolis, MN 55455, USA*

^b*Institute of Earth Sciences, University of Iceland, Sturlugata 7, 101 Reykjavík, Iceland*

^c*Université Bordeaux Montaigne, 33607 Pessac, France*

^d*Université Rennes 1, 2 rue du Thabor, 35065 Rennes, France*

^e*Laboratoire des Sciences du Climat et de l'Environnement/IPSL, CEA, CNRS, UVSQ, Université Paris-Saclay, Orme des Merisiers, Bat. 714, 91190, Gif-sur-Yvette, France*

^f*GFZ German Research Centre for Geosciences, Telegrafenberg, 14473 Potsdam, Germany*

^g*Sorbonne Université, CNRS, Laboratoire d'Archéologie Moléculaire et Structurale (LAMS), F-75005 Paris, France*

Abstract

Archaeomagnetic data are fundamental for our understanding of the evolution of Earth's magnetic field on centennial to millennial timescales. From the earliest studies of the Thelliers, Aitken, Nagata and others in the 1950s and 1960s, archaeomagnetic data have been vital for extending our knowledge of the field to times prior to observational measurements. Today, many thousands of archaeomagnetic data allow us to explore the geomagnetic field in more detail than ever before. Both regional time series of archaeomagnetic data and the inclusion of archaeomagnetic data in time-varying global spherical harmonic field models have revealed a range of newly discovered field

*Corresponding author

Email address: mcbrown@umn.edu (Maxwell C. Brown)

behaviour. More sophisticated approaches to developing regional curves and global models have allowed us to resolve the field in certain regions more robustly and with greater resolution than previously possible. In this review we give an overview of the widely used global archaeomagnetic database GEOMAGIA50, discuss the methods used to obtain archaeomagnetic data, their challenges, and explore progress over the past twenty years in developing regional secular variation curves and global spherical harmonic models of the archaeomagnetic field. We end the review by covering what we see as the “grand challenges” in archaeomagnetism, including which regions of the world should be focussed on with regards to data acquisition.

Key words: archaeomagnetism, GEOMAGIA50, global models

1. Introduction

Archaeomagnetism is the study of the past direction and intensity of Earth’s magnetic field recorded by any type of manmade artefact or fired material. It is dependent on archaeological discoveries and advances that lead to a better description and understanding of our history and heritage. Although it was recognized at the end of the 19th century that fired materials can record Earth’s magnetic field (Folgheraiter, 1899), it was not until the pioneering work of Émile and Odette Thellier beginning in the 1930s that the physical principles, methods and instrumentation necessary to accurately obtain the past direction and intensity of the geomagnetic field recorded by archaeological materials were developed (Thellier, 1938, 1941; Thellier and Thellier, 1959). Reviews by Thellier (1977), Le Goff et al. (2006) and Dunlop (2011) give excellent English language overviews of the Thelliers’

14 most important contributions to the subject.

15 Archaeomagnetism established itself as a research field through the 1950s
16 and 1960s, with proponents of the subject obtaining data from fired materials
17 from locations globally. Studies from these decades reported data from Eu-
18 rope (e.g., Burlatskaya, 1961; Aitken and Weaver, 1962; Belshé et al., 1963;
19 Chelidze, 1965; Bucha, 1967; Kovacheva, 1969), Northern Africa (Athavale,
20 1969), India (Athavale, 1966), China (Deng and Li, 1965), Japan (Watanabe,
21 1958; Nagata et al., 1963; Sasajima, 1965), North America (e.g., Watanabe
22 and Dubois, 1965; Schwarz and Christie, 1967) and South America (e.g.,
23 Nagata et al., 1965; Kitazawa and Kobayashi, 1968). Research continued
24 though the 1970s, but it was not until the 1980s that there was a general
25 increase in the number of studies reporting new archaeomagnetic data each
26 year (Fig. 1); a trend that continued through to the 2010s. This has resulted
27 in a large compilation of global data that has greatly improved our under-
28 standing of how Earth’s magnetic field has varied spatially and temporally
29 on centennial to millennial timescales.

30 To date close to 700 studies reporting archaeomagnetic data have been
31 published. The majority of studies have concentrated on specific regions,
32 with data from Europe, the Middle East, China, Japan and North America
33 dominating the global database (see section 2.3). A peak in productivity in
34 the 2000s coincided with the successful European Commission funded Ar-
35 chaeomagnetic Applications for the Rescue of Cultural Heritage (AARCH)
36 research and training network. Data from Europe vastly outweighs that
37 from any other region (section 2.3). Since the early 2000s the development
38 of temporally continuous global spherical harmonic models of the geomag-

39 netic field (see section 4.2) and an interest in the development of the South
40 Atlantic Anomaly on archaeomagnetic timescales has led to a number of
41 studies focussed on obtaining data from archaeological sites in the South-
42 ern Hemisphere and equatorial regions (e.g., Tarduno et al., 2015; Hartmann
43 et al., 2019). Significant new studies have been published for Africa (Gómez-
44 Paccard et al., 2012b; Neukirch et al., 2012; Mitra et al., 2013; Tarduno
45 et al., 2015; Donadini et al., 2015; Hare et al., 2018; Kapper et al., 2017,
46 2020; Tchibinda Madingou et al., 2020), South America (e.g., Hartmann
47 et al., 2010, 2011, 2019; Goguitchaichvili et al., 2011, 2015, 2019; Poletti
48 et al., 2016; Capdeponet et al., 2019; Cejudo et al., 2019; Gómez-Paccard
49 et al., 2019) and West Oceania (Stark et al., 2010; Turner et al., 2020).
50 These areas are ripe for expanding our global data set. However, there are
51 limitations on the availability of archaeological materials for analyses from
52 these areas. As archaeomagnetism is a destructive method (artefacts must
53 be cut and often heated), there can be restrictions on the materials available
54 for laboratory analyses.

55 The majority of archaeomagnetic data have been dated to within the past
56 3000 years, with the number of data on the whole decreasing with increasing
57 age (section 2.4). This has led an increasing number of studies to focus on
58 obtaining archaeomagnetic data from materials between 6000 BCE (Before
59 the Current Era) and 1000 BCE (e.g., Kovacheva et al., 2009a; Fanjat et al.,
60 2013; Gallet et al., 2014, 2015; Shaar et al., 2016, 2020; Cai et al., 2020);
61 however, almost all data are from Eurasia, limiting our global knowledge of
62 the field at older archaeological times. Extending archaeological time series to
63 older ages is an exciting direction of research for the coming years. Although,

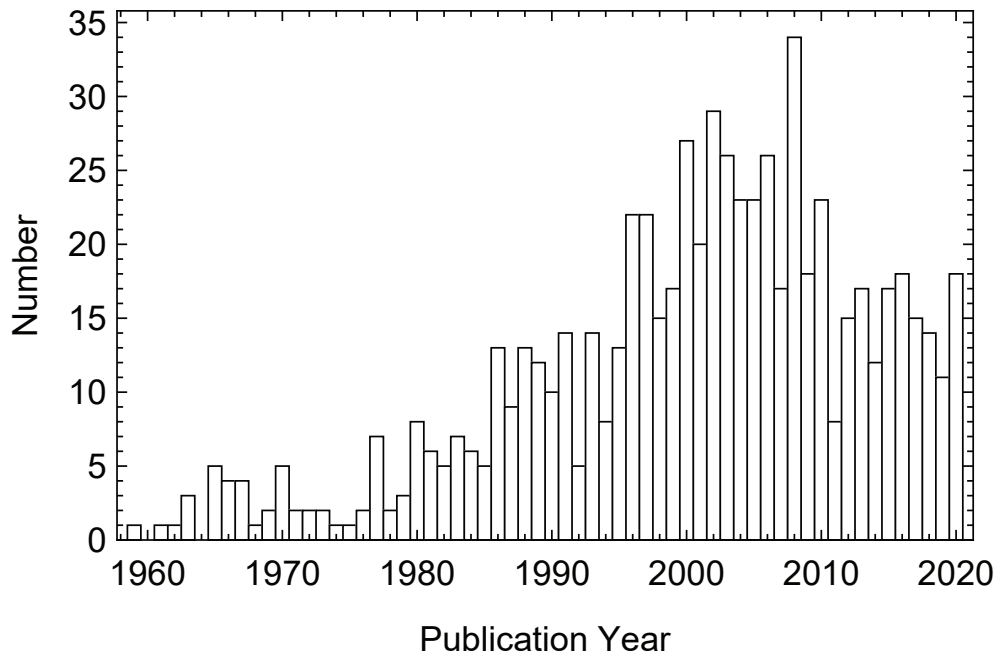


Figure 1: Histogram of the number of archaeomagnetic studies published per year in the GEOMAGIA50.v3.4 database that contain data dated to the past 10,000 years (accurate as of December 2020). The total number of studies is 685. This excludes studies that employed archaeomagnetic dating as the sole dating method. NB (1) there are additional studies that have published data in non-tabulated form, which have not been added to the database and do not contribute to the total number of studies reported here (e.g., Aitken and Weaver, 1965; Aitken et al., 1989); (2) not all archaeomagnetic studies from Japan have been fully integrated in the current version of GEOMAGIA50 (see section 2.3).

64 as with improving the global distribution of data, limitations on the materials
65 available for analysis impact the time periods that can be studied further.

66 The usefulness of compiling regional and global archaeomagnetic data for
67 understanding the evolution of the geomagnetic field was recognized early on
68 in the development of the subject (e.g., Cook and Belshé, 1958; Watanabe,
69 1958; Aitken and Weaver, 1965; Kawai and Hirooka, 1967). This has contin-
70 ued through today, with country or regional specific archaeomagnetic data
71 compilations (e.g., Thellier, 1981; Márton, 2003; Tema et al., 2006; Márton,
72 2010; Carrancho et al., 2013; Hervé et al., 2013a; De Marco et al., 2014;
73 Kovacheva et al., 2014; Batt et al., 2017; Molina-Cardín et al., 2018; Gogui-
74 tchaichvili et al., 2019; Schnepf et al., 2020b,a; Rivero-Montero et al., 2021).
75 Such regional data sets have been used to develop secular variation (or ref-
76 erence) curves (see section 4.1), using evermore sophisticated mathematical
77 approaches (recent examples include Lodge and Holme, 2009; Thébault and
78 Gallet, 2010; Helliö et al., 2014; Batt et al., 2017; Livermore et al., 2018;
79 Genevey et al., 2021; Kapper et al., 2020). Compilations of global archaeoin-
80 tensity data have also been used to infer global dipole moment evolution
81 (e.g., McElhinny and Senanayake, 1982; Aitken et al., 1989; Yang et al.,
82 2000; Genevey et al., 2008; Knudsen et al., 2008; Usoskin et al., 2016).

83 Over the past 20 years (alongside the construction of direction and in-
84 tensity curves), has been the development of temporally continuous global
85 palaeomagnetic field models (see section 4.2). These data-based inverse mod-
86 els employ spherical harmonic methods initially developed to analyze and
87 depict the present day field (e.g., Bloxham and Gubbins, 1985; Bloxham and
88 Jackson, 1992) and the historical field (from 1590 CE onwards, based on

89 shipboard and ground based measurements) (Jackson et al., 2000). They
90 have been adapted to suit archaeomagnetic and palaeomagnetic data to pro-
91 duce maps of the geomagnetic field at Earth’s surface and the core-mantle
92 boundary (CMB). The earliest global models were developed by Hongre et al.
93 (1998), Constable et al. (2000), Korte and Constable (2003) and Korte and
94 Constable (2005) and combined a variety of data sources (archaeomagnetic,
95 volcanic and sediment data). Global models based on primarily archaeo-
96 magnetic data (but also including volcanic data) were not developed until
97 the construction of ARCH3k.1 (Korte et al., 2009) (a three thousand year
98 model), which was recently updated to a 10,000 year model (Constable et al.,
99 2016). Spherical harmonic cap approaches using archaeomagnetic data have
100 also been used to create regional models (e.g., Pavón-Carrasco et al., 2008;
101 Pavón-Carrasco et al., 2009). Varying approaches to modelling the archaeo-
102 magnetic field have been applied since, including Licht et al. (2013), Pavón-
103 Carrasco et al. (2014), Sanchez et al. (2016), Hellio and Gillet (2018), Arneitz
104 et al. (2019) and Mauerberger et al. (2020).

105 Concurrent to regional compilations of data and the development of global
106 models there have been continued efforts to create global databases of ar-
107 chaeomagnetic data. The first global archaeomagnetic databases were paper
108 lists of results, the first likely being the historical and archaeointensity compi-
109 lation of Smith (1967). With the development of digital database structures,
110 archaeomagnetic data could be compiled and updated more easily. Early
111 efforts included those of Burlatskaya et al. (1986), Liritzis and Lagios (1993)
112 and Daly and Goff (1996), although the data were not available in a digital
113 form. The first digital archaeomagnetic database that was easily accessi-

114 ble was the Plymouth archaeomagnetic directional database (ARCHEO97
115 and ARCHEO00) compiled by Don Tarling and last released in 1999. This
116 was one of seven International Association of Geomagnetism and Aeronomy
117 (IAGA) databases available online to download as stand-alone programs.
118 Two major efforts to compile all global archaeomagnetic data have been the
119 ArcheoInt database (Genevey et al., 2008) and the GEOMAGIA50 database
120 (Donadini et al., 2006; Korhonen et al., 2008; Brown et al., 2015b). Although
121 GEOMAGIA50 largely subsumes the data within ArcheoInt, ArcheoInt con-
122 tains additional fields that place archaeomagnetic results in their archaeo-
123 logical context and provides greater descriptive information regarding the
124 acquisition of the data sets. The databases can be viewed as complemen-
125 tary. In addition, there is the HISTMAG database of Arneitz et al. (2017),
126 which combines historical and archaeomagnetic data. There are also numer-
127 ous archaeomagnetic data in the MagIC database (described in part in Tauxe
128 et al., 2016); however, GEOMAGIA50 is currently the primary database for
129 archaeomagnetic data. Unlike MagIC, GEOMAGIA50 includes only aver-
130 age data and is not designed to include results at the specimen level or raw
131 measurements. The site level data from GEOMAGIA50 has been used in
132 numerous studies. In addition to being used to construct secular variation
133 curves and global and regional field models, it has been used to understand
134 solar activity during the Holocene (Usoskin et al., 2016) and to calibrate
135 cosmogenic nuclide production stacks through the use of intensity data (e.g.,
136 authigenic $^{10}\text{Be}/^9\text{Be}$ ratios, Simon et al., 2016).

137 An important consideration when using archaeomagnetic data for any
138 purpose is the reliability of the data. This includes chronological controls

139 and archaeomagnetic components (direction and intensity), which are most
140 commonly determined from a thermoremanent magnetization (TRM): a mag-
141 netization acquired on cooling from firing temperature to room temperature.
142 Archaeomagnetic directions can be influenced by post-cooling displacement
143 and magnetic refraction (section 3.1.1) and obtaining reliable archaeointen-
144 sities requires that numerous factors are considered (section 3.1.2). These in-
145 cludes thermal alteration during palaeointensity experiments (section 3.1.3),
146 the influence of non-ideal magnetic remanence carriers (e.g., multi-domain
147 (MD) grains, section 3.1.4), remanence anisotropy (section 3.1.5) and dif-
148 ferences between natural and experimental cooling rates (section 3.1.6). All
149 chronological determinations have an associated uncertainty, whether an ar-
150 chaeological age, determined through physical measurements (e.g., by radio-
151 carbon dating or luminescence methods), or by a combination of approaches
152 (section 3.2). Documenting such uncertainties is a challenge (section 5.1.1)
153 and uncertainties should be carefully considered in any study looking to in-
154 vestigate field behaviour.

155 In this review we cover the current status of the global archaeomagnetic
156 database (GEOMAGIA50; section 2), provide an overview of archaeomag-
157 netic procedures, data quality, uncertainties and chronological controls (sec-
158 tion 3) and explore advances in regional secular variation curve construction
159 and global archaeomagnetic field modelling (section 4). The review ends with
160 a discussion on the future challenges of the subject (section 5).

161 **2. Overview of the GEOMAGIA50 archaeomagnetic database**

162 In the following sections we give a brief history of the GEOMAGIA50
163 database (section 2.1), cover the abundance of archaeomagnetic data within
164 the most recent version of the database (GEOMAGIA50.v3.4) (section 2.2),
165 discuss the spatial and temporal distribution of data (section 2.3 and sec-
166 tion 2.4), and provide an overview of the archaeological materials used to
167 obtain archaeomagnetic data (section 2.5). The methods used to obtain ar-
168 chaeomagnetic and age data, as well as their uncertainties, are discussed in
169 section 3.

170 In this review we consider purely archaeomagnetic data. Data from vol-
171 canic materials (lava, volcanic ashes, obsidian) and speleothems (i.e. Latham
172 et al., 1986; Trindade et al., 2018), although stored in GEOMAGIA50.v3.4,
173 are neglected for the purpose of this study. We also restrict our analysis
174 to materials dated between 8000 BCE and today, and we do not include
175 materials that have been dated using archaeomagnetic dating.

176 *2.1. History of GEOMAGIA50 and its most recent compilation*

177 Version 1 of GEOMAGIA50 primarily focused on compiling palaeointen-
178 sity data and contained data from both archaeological materials and lava
179 flows. Directional data were added only if they accompanied intensity data.
180 Version 1 integrated the ArcheoInt database of Genevey et al. (2008) and the
181 IAGA ARCHEO00 database (<http://www.ngdc.noaa.gov/geomag/paleo.shtml>)
182 compiled by Don Tarling. Data from other country- or region-specific compi-
183 lations were also added (see Brown et al. (2015b) for a list of compilations).
184 Further details of version 1 of the database can be found in Donadini et al.

185 (2006), Korhonen et al. (2008) and Brown et al. (2015b). After numerous
186 updates since original publication, 2762 archaeomagnetic entries from 109
187 studies remain from version 1 in the most up-to-date version of the database.

188 No publication accompanied version 2 of the database; however, the data
189 compilation is described in Donadini et al. (2009). Around 100 archaeo-
190 magnetic entries from version 1 of the database were updated in version 2.
191 Archaeomagnetic directional results were added independently of whether
192 they accompanied intensity data. This greatly increased the amount of data
193 in version 2 of the database, with 3072 data from 130 studies added at this
194 time that remain in the most recent update of the database (5834 entries
195 from 240 studies in total).

196 The current version of the database is version 3, which was initially pub-
197 lished in 2015 (Brown et al., 2015b). It marked a change from being hosted at
198 the Scripps Institution of Oceanography, University of California-San Diego,
199 to GFZ Potsdam (<https://geomagia.gfz-potsdam.de/>). Sediment data were
200 also added in version 3 (Brown et al., 2015a). 1006 entries from 100 archaeo-
201 magnetic studies were added to version 3.1 of the database; 498 entries from
202 220 studies were added to version 3.2 (released in 2017); and 1717 entries
203 from 109 studies in version 3.3 (released in 2019). GEOMAGIA50.v3.2 also
204 incorporated a number of legacy studies (studies published prior to the in-
205 ception of the database in 2004) that were missing in previous versions of
206 the database. This included 141 studies from the UK, which was part of a
207 major revision of all UK entries (Batt et al., 2017). It also included 75 UK
208 studies published since 2004.

209 The most up-to-date version of GEOMAGIA50 (v3.4) was released in

210 December 2020. To our knowledge, it includes nearly all archaeomagnetic
211 studies with independent age constraints published to date, with the excep-
212 tion of a large number of entries in the Japanese archaeomagnetic database
213 (<http://mag.center.ous.ac.jp/en>) and some entries from HISTMAG (Arneitz
214 et al., 2017), which have not yet been integrated into GEOMAGIA50. In
215 total 1188 archaeomagnetic entries from 29 studies were added to GEOMA-
216 GIA50.v3.4 in 2020 and the current database contains 9981 archaeomagnetic
217 entries from 685 studies. This is 87% of all entries within the database as a
218 whole. This includes 528 French directional entries determined in the Thel-
219 lier laboratory at Saint Maur over the past 25 years (Le Goff et al., 2020) and
220 a re-evaluation of the French directional compilations of Thellier (1981) and
221 Bucur (1994) (170 entries). It also contains a significant new compilation
222 of central European archaeomagnetic data, both directional data (Schnepp
223 et al., 2020b) and intensity data (Schnepp et al., 2020a) (188 new entries
224 and 18 updates). Data from China have also been significantly increased
225 with 64 entries published in Cai et al. (2020). Improvements to the Southern
226 Hemisphere/equatorial compilation were made, with new data from Kenya
227 (Tchibinda Madingou et al., 2020), Burkina Faso and Ivory Coast (Kapper
228 et al., 2020), Ecuador (Herrero-Bervera et al., 2020), Colombia (Cejudo et al.,
229 2019), Uruguay (Capdepont et al., 2019) and New Zealand (Turner et al.,
230 2020). Changes in the distribution of data with each version of GEOMA-
231 GIA50, both globally and for Europe, are shown in Fig. 2 and Fig. 3.

232 *2.2. Overview of archaeomagnetic data*

233 Out of the 9981 archaeomagnetic entries in GEOMAGIA50.v3.4, 5931
234 archaeomagnetic entries contain either declination or inclination and 4528

235 entries have both. The majority of entries that only have inclination are from
236 the Russian school (e.g., Burlatskaya et al., 1986) (85% of inclination only
237 entries). Although 5231 entries contain archaeointensity, only 651 entries
238 contain full vector information (declination, inclination and intensity); 533
239 entries report intensity and inclination without declination; and 4047 entries
240 list intensity without accompanying directions.

241 In addition to archaeomagnetic results, GEOMAGIA50 contains age and
242 age uncertainty information (see section 3.2) and a variety of meta data that
243 outline the directional, intensity and dating methods used. It also includes
244 the number of samples/specimens and specimen types investigated, and the
245 types of archaeological materials the data were obtained from (section 2.5).
246 Full details of the fields within GEOMAGIA50 are given in Brown et al.
247 (2015b).

248 *2.3. Spatial distribution of archaeomagnetic data*

249 There is a large disparity in the global distribution of archaeomagnetic
250 data (Fig. 2). Data from Europe dominates the database (Fig. 3 and Fig. 4a-
251 c): 59% of all entries (including Russia), 51% without Russian data. The
252 UK (10% of entries), France (9%), Russia (8%) and Georgia (5%) contribute
253 to a significant portion the European entries (Fig. 3 and Fig. 4b). Many
254 European countries individually contribute between 2% and 4% of the total
255 number of entries. The UK comprises the largest number of all entries (961),
256 which are primarily directional data (905). See Batt et al. (2017) for further
257 details on the UK contribution. France is the second largest contributor with
258 890 entries (770 with directions, 162 with intensity). A large amount of data
259 was added (520 entries) following the publication of Le Goff et al. (2020).

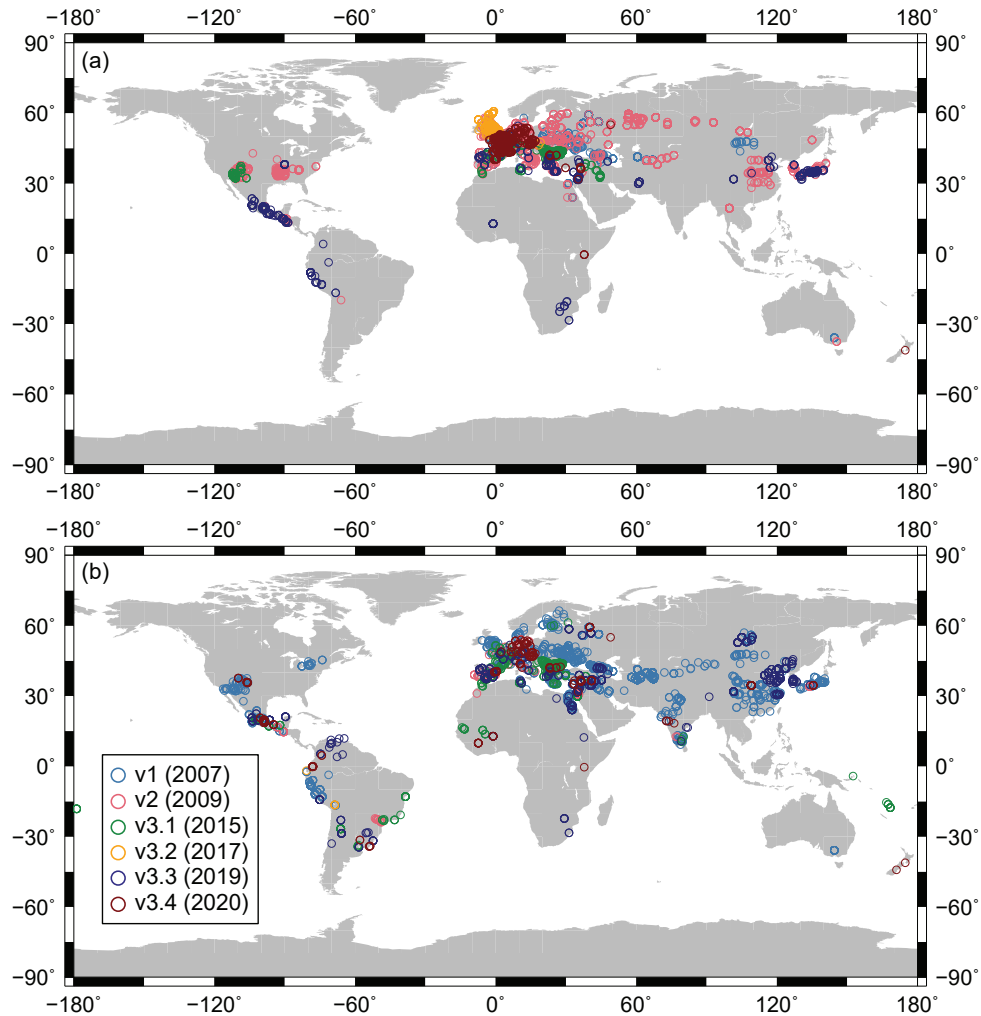


Figure 2: Geographical distribution of archaeomagnetic sites given in the six versions of GEOMAGIA50 to date (date range from 8000 BCE to 2000 CE; archaeomagnetically dated sites are excluded). Colours denote when the data were added to the database. (a) sites with directional data; (b) sites with intensity data. Some version 1 (v1) sites were updated with directional information and are shown in (a) as belonging to v1, although they were updated after the initial release of v1. If sites were removed during revisions of subsequent versions, they are not shown on the figure.

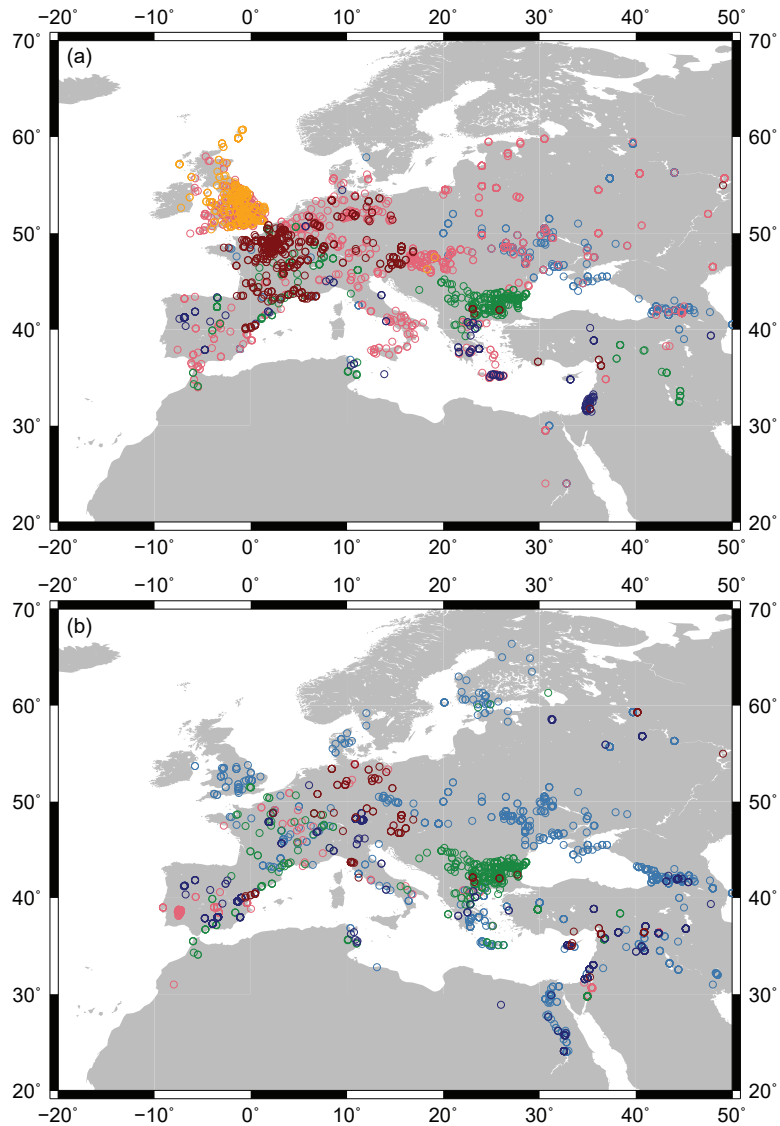


Figure 3: Geographical distribution of archaeomagnetic sites given in the six versions of GEOMAGIA50 to date for Europe and surrounding regions (date range from 8000 BCE to 2000 CE; archaeomagnetically dated sites are excluded). (a) sites with directional data; (b) sites with intensity data. See Fig 2 for legend and other details.

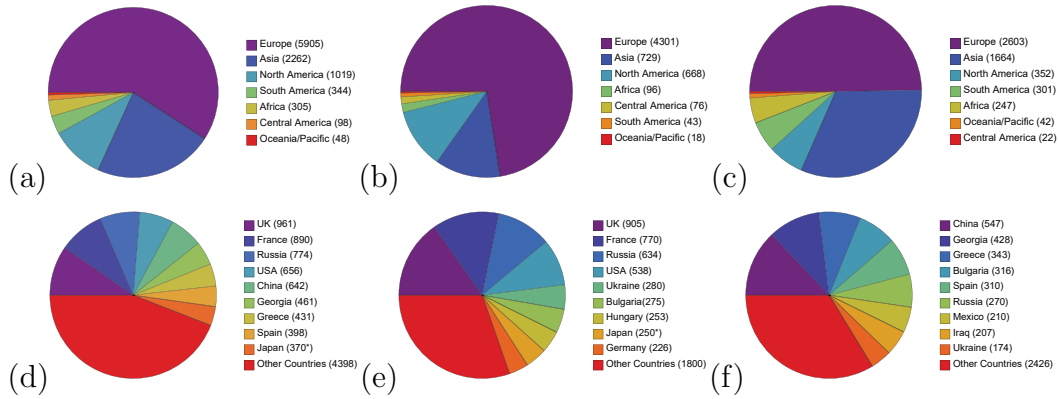


Figure 4: Pie charts of the number of archaeomagnetic entries (in brackets) in GEOMAGIA50.v3.4 by region (a-c) and by country (d-f) by data type: (a,d) directional and intensity, (b,e) directional, and (c,f) intensity. Country plots list the top nine countries by number of entries, with all other entries grouped into a single pie segment.*The data within GEOMAGIA50.v3.4 does not contain all known Japanese data, which total around 800.

260 It is worth noting that although 72% of directional entries come from
 261 Europe (omitting Russia), this region covers only 1-2% of Earth's surface
 262 (depending on the definition of Europe) (Fig. 4b). Data from regions adjacent
 263 to Europe are also dense, with the Levant (Israel, Syria, Jordan), Egypt and
 264 Iraq contributing significantly to the database. The distribution of data
 265 (directions and intensities) from Europe and these regions is shown in Fig. 3.

266 Outside of Europe the United States of America (7% of entries), China
 267 (6%), Japan (4%) and Mexico (3%) are the main contributors. All other
 268 nations make up 29% of entries. Although the number of Japanese entries in
 269 GEOMAGIA50 totals 370, the Japanese archaeomagnetism database of T.
 270 Hatakeyama (Okayama University, Japan) (<http://mag.center.ous.ac.jp/en>)
 271 lists 744 directional data and 59 intensity data, placing it third in the list

272 of country entries. We aim to integrate this significant contribution with
273 GEOMAGIA50 in the future.

274 Although there have been recent efforts to improve the global distribution
275 of data, the Southern Hemisphere is currently poorly represented, with only
276 400 entries or 4% of all archaeomagnetic entries. 76 entries contain a direction
277 and 340 an intensity. The disparity in data distribution is stark when it is
278 considered that Africa and South America, which cover 9% of Earth's surface
279 when combined (32% of the land area), provide only 7% of the entries in the
280 database (Fig. 4a). However, the amount of Southern Hemisphere data con-
281 tinues to improve. In Fig. 2 we show the increase of Southern Hemisphere
282 data with each new version of GEOMAGIA50. Notable studies have that
283 have obtained data from southern Africa are Neukirch et al. (2012), Tarduno
284 et al. (2015) and Hare et al. (2018). Previously only one study had pub-
285 lished data from this region (Henthorn et al., 1979) and this was not added
286 to GEOMAGIA50 until version 3.3. A number of South American countries
287 have garnered new data. In the first version of GEOMAGIA50, there were
288 no entries from Brazil, Argentina, Uruguay and Chile. In the past 10 years
289 data have been obtained from all four: Brazil, 49 intensity entries (Hart-
290 mann et al., 2010, 2011, 2019; Poletti et al., 2016), Argentina, 44 entries
291 (e.g., Gómez-Paccard et al., 2019; Goguitchaichvili et al., 2019), Uruguay, 6
292 entries (Capdeponet et al., 2019) and Chile, 1 entry (Roperch et al., 2015).
293 In addition, data have been obtained from other South American countries
294 south of the Equator. By far the most number of entries come from Peru,
295 with 191 (e.g., Gunn and Murray, 1980; Yang et al., 1993). Smaller contri-
296 butions come from Bolivia (13 entries) (e.g., Nagata et al., 1965; Kitazawa

297 and Kobayashi, 1968) and Ecuador (23 entries) (Kitazawa and Kobayashi,
298 1968; Bowles et al., 2002; Herrero-Bervera et al., 2020).

299 The area between the tropics fairs better than the Southern Hemisphere,
300 with nearly 10% of all entries coming from this latitude band. This includes
301 the large and growing data set from Mexico (see, Hervé et al., 2019b,c; Mah-
302 goub et al., 2019). New studies from India (Basavaiah et al., 2019; Deena-
303 dayalan et al., 2020), western Africa (Kapper et al., 2017, 2020) and eastern
304 Africa (Osete et al., 2015) have contributed important intensity data from
305 areas that are isolated from others globally. As we move closer to the equa-
306 tor the amount of available data shrinks with $< 2\%$ of database entries from
307 between $\pm 10^\circ$ latitude. Six studies have produced new data in this latitude
308 band over the past 10 years, with the first archaeomagnetic data from Kenya
309 (Tchibinda Madingou et al., 2020) and the Ivory Coast (Kapper et al., 2020),
310 and others building on small data sets from Ecuador (Herrero-Bervera et al.,
311 2020) and Colombia (Cejudo et al., 2019).

312 The spatial distribution of directional and intensity data are distinctly
313 different (Fig. 2, Fig. 3 and Fig. 4). Countries that produce numerous direc-
314 tional data do not always produce large amounts of intensity data and vice
315 versa. As stated already, the UK has the most directional entries, but few
316 intensity entries. Conversely, China has the most abundant intensity data
317 by country, but does not make the top ten countries for directional data.
318 Russia, east of the Black Sea has abundant directional data, but sparser
319 intensity data. To a lesser extend the same is true for the Ukraine, which
320 produces the 5th most directional data (5% of all directional entries), but
321 far fewer intensity data than other countries. India and Brazil have no di-

322 rectional data, but numerous intensity data. This disparity can be crucial
323 in areas with sparse data coverage, where full vector data are particularly
324 important for constraining field models, e.g., sites in West Africa, where few
325 directional data have been obtained (Burkina Faso; Donadini et al., 2015),
326 whereas intensity data are more plentiful (Mitra et al., 2013; Kapper et al.,
327 2017, 2020). The greater abundance of intensity data can be related to the
328 availability of material to study (see section 2.5).

329 *2.4. Temporal distribution of archaeomagnetic data*

330 There is a large variability in the temporal distribution of data in GE-
331 OMAGIA50.v3.4 over the past 10,000 years (Fig. 5). Both the number of
332 archaeomagnetic directions and intensity in general decrease with age. This
333 is most stark for BCE data, with 35% of all entries from this time. The
334 number of BCE directions is substantially less (20% of total directions) than
335 for CE (Common Era) directions. The contrast is less abrupt for archaeoin-
336 tensity data. Although the number of BCE intensity entries per century is
337 in general less than for CE entries, 54% of all intensity data span 8000 BCE
338 to 1 BCE.

339 There are notable spikes in the number of directional and intensity entries
340 for certain time periods. For directional data there are peaks in the number
341 of directional data between 100 CE and 300 CE, 700 CE and 900 CE, 1100
342 and 1400 BCE, and 1700 BCE and 2000 (Fig. 5a). The most populous
343 century for directional results is the 19th (410 entries from 31 studies). Some
344 peaks can be attributed to certain cultural periods, e.g., the high number of
345 entries between 100 CE and 300 CE are from the peak of the Roman Empire,
346 with the data set dominated by entries from present day England, France,

347 Hungary, Bulgaria and Spain. Other peaks are associated with concerted
348 research initiatives in specific countries (or by certain research groups with
349 dedicated focuses), e.g., the 700 CE to 900 CE peak is dominated by data
350 from France for the High Middle Ages (Le Goff et al., 2020).

351 There is a peak in archaeointensity age entries during the first millennium
352 BCE, where there has been concerted efforts to characterize the Levantine
353 intensity spike (see section 4.1.2). There are notable minor peaks in the
354 number of intensity entries during the Neolithic, with notable studies from
355 the Neolithic and Bronze age from China (207 entries) (see Cai et al., 2020),
356 Iraq (179 entries) (Sakai, 1980; Nachasova and Burakov, 1995, 1998; Yutsis-
357 Akimova et al., 2018a,b) and the rest of the Middle East (148 entries) (e.g.,
358 Kawai et al., 1972; Gallet et al., 2014; Stillinger et al., 2015; Shaar et al., 2016;
359 Gallet et al., 2020), Bulgaria (136 entries) (e.g., Kovacheva, 1997; Kovacheva
360 et al., 2009a, 2014; Kostadinova-Avramova et al., 2020) and Spain (79 entries)
361 (Nachasova et al., 2002, 2007; Carrancho et al., 2013).

362 We note that there are very few BCE data from the Southern Hemisphere.
363 There are only a few data per century back to 6000 BCE (Fig. 5d). In contrast
364 the Northern Hemisphere (Fig. 5c) has 10 times or more data per century.

365 *2.5. Overview of archaeological materials*

366 A wide range of archaeological materials and structures can be used to
367 obtain directional and intensity information (Fig. 6). Almost all data from ar-
368 chaeological material ($\sim 99\%$) were recovered from baked clays that acquired
369 a TRM roughly parallel and proportional to the ambient geomagnetic field
370 at the time of their firing. A few other archaeological materials can carry
371 a remanent magnetization acquired through different processes. In mural

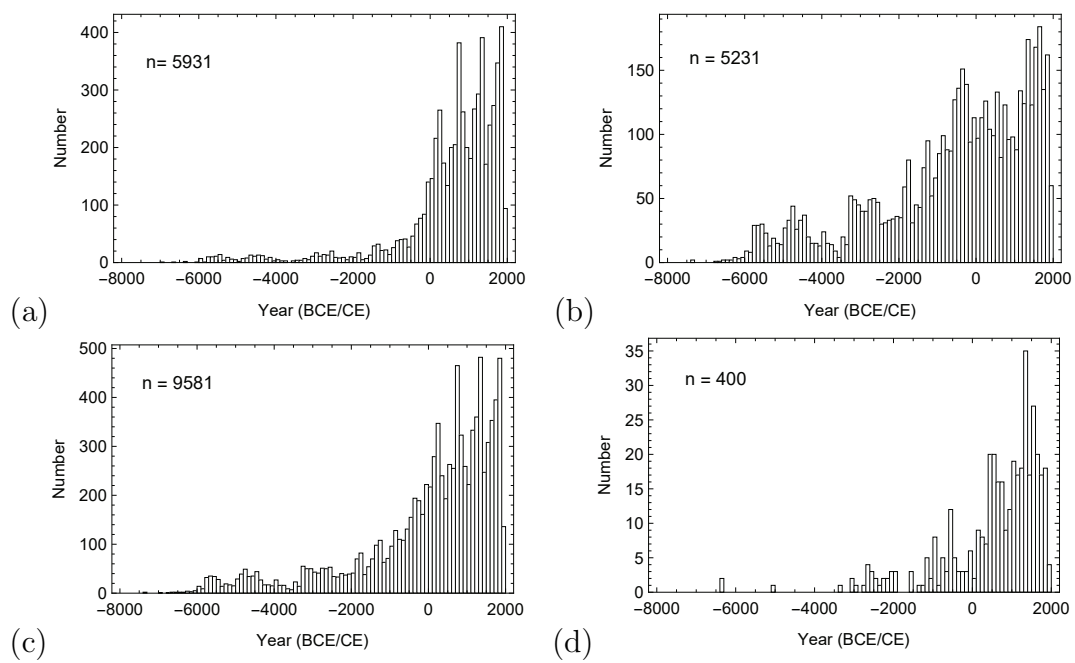


Figure 5: Archaeomagnetic entries in GEOMAGIA50.v3.4 by age in 100 year bins. (a) directions, (b) intensity, (c) Northern Hemisphere data and (d) Southern Hemisphere data.

372 paintings, e.g., frescoes, red pigments with hematite can acquire a so-called
373 pictorial remanent magnetization when paint is sufficiently liquid to enable
374 hematite grains to orientate parallel to the geomagnetic field (e.g., Chiari
375 and Lanza, 1997; Zanella et al., 2000). Through a related process, lime-
376 plasters (e.g., Hueda-Tanabe et al., 2004) and unburnt adobe bricks (e.g.,
377 Games, 1977) can also acquire a remanent magnetization, when the plaster
378 or the clay is mixed with water. These materials are promising, even though
379 experimental uncertainties are generally higher than for baked clays.

380 Fifty types of materials and structures are listed in the current version
381 of GEOMAGIA50; however, there are some that have been sampled more
382 frequently than others. In Fig. 6 we list the 8 most commonly used. In some
383 cases (13% of entries) the type of material that was used is not given in the
384 database. There are clear differences in the materials used for directional and
385 intensity studies. For directional analysis, in-place oriented structures are
386 necessary. Therefore kilns, ovens and hearths, bricks, and burnt structures
387 are frequently used. For intensity the materials do not need to be in-situ,
388 which allows a more diverse array of materials to be pooled from. Pottery
389 and ceramics, owing to their abundance and ease of sampling are therefore
390 the most common for intensity analysis. Over recent years copper slags
391 have been used owing to their magnetically appropriate characteristics for
392 intensity experiments (Shaar et al., 2010).

393 Materials suitable for intensity are often easier to access, because the
394 material has already been sampled and the collections they are from are
395 well-studied. Sampling of these objects is also less invasive. For directional
396 studies, it is necessary to be reactive to an archaeological excavation. In-situ

397 structures are uncovered and maybe destroyed when working on rescue exca-
398 vations. Sometimes kiln-type structures are preserved because of an obvious
399 archaeological interest; however, sampling is invasive and possibly incom-
400 patible with heritage conservation. These issues may partially explain why
401 the proportion of direction and intensity studies varies in different countries
402 (section 2.3).

403 **3. Experimental considerations and data quality**

404 In this section we outline the methods that have been used to obtain
405 archaeomagnetic data and date archaeological materials. We discuss how
406 experimental methods and practices affect the accuracy and precision of
407 archaeomagnetic and chronological data and address how uncertainties are
408 represented in the database. For intensity experiments we cover alteration
409 during heating, the influence of multi-domain grains, remanence anisotropy
410 and the effect of cooling rate.

411 Dating methods applied to archaeological materials are varied and we
412 group them into two categories: those that directly or indirectly date a mate-
413 rial. We discuss the nuances of these methods when applied to archaeological
414 materials, how they can be combined to create a site chronology, and their
415 age uncertainties.

416 *3.1. Archaeomagnetic measurements*

417 *3.1.1. Directions*

418 Three approaches have commonly been used to recover directional data
419 from archaeological materials. The first two involve stepwise removal (demag-
420 netization) of a TRM by either heating to increasing temperatures (thermal

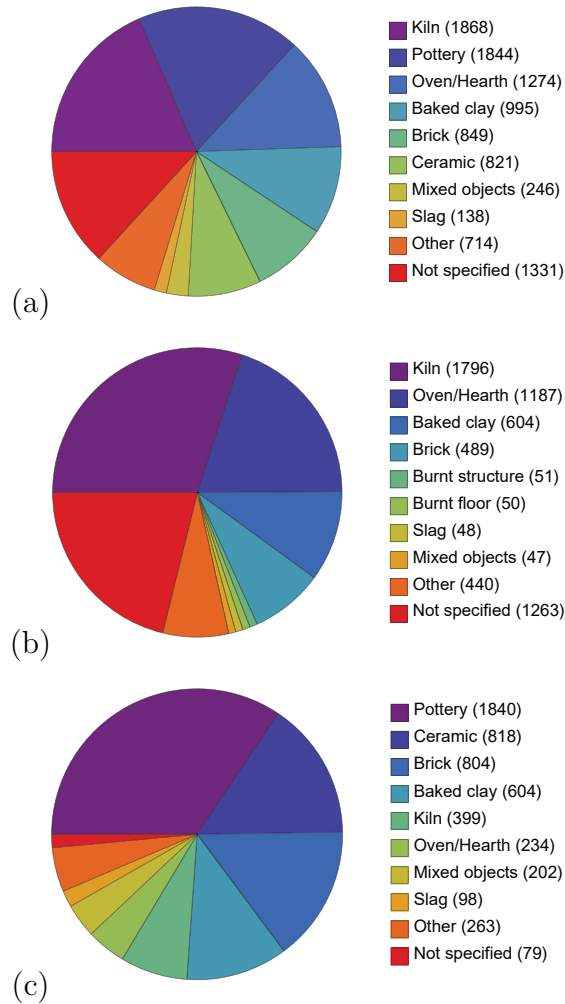


Figure 6: Pie charts of the number of mentions (in brackets) of the archaeomagnetic materials used to determine (a) direction and/or intensity, (b) directions, (c) intensity. The eight most used materials are shown in each subplot, remaining material types are grouped under “Other”. Note in (b), most inclination data only come from displaced bricks, making the assumption that they were fired on one of their sides. The number of directional and intensity entries do not match the number of materials given in the plots, as numerous entries were determined from multiple materials.

421 demagnetization) or by increasing the alternating current of a field coil (al-
422 ternating field (AF) demagnetization). For some entries in the database both
423 approaches have been used in conjunction. An alternative approach is to use
424 viscosity cleaning. Developed by Émile Thellier (see, Thellier, 1981), viscos-
425 ity cleaning has proven to be as effective as a complete demagnetization in
426 isolating directions, when a sample records a single TRM component. See
427 Le Goff et al. (2020) for an overview of this two-step method. Unfortunately,
428 56% of entries in the database do not report the demagnetization method
429 used. Of entries that do list a demagnetization method, alternating field
430 (AF) demagnetization is the most commonly used (33%), followed by viscos-
431 ity cleaning (28%) (largely from entries from France, Le Goff et al., 2020),
432 a mixture of AF and thermal demagnetization (23%), and solely thermal
433 demagnetization (16%).

434 There are various factors that are likely to interfere with the accurate
435 recovery of past field directions. First is the precision of the sampling and
436 sample orientation, which is critical in archaeomagnetism where one tries
437 to recover small directional variations. Conservation of structures and me-
438 chanical problems, such as the inward or outward sagging of the walls or a
439 slight tilting of the kiln sole, can influence the precision and reliability of
440 the archaeomagnetic direction. The direction recorded by a structure can
441 be further perturbed by magnetic refraction, whereby the magnetization of
442 a structure can distort the magnetic field recorded, in particular when the
443 magnetization is strong (e.g., Aitken and Hawley, 1970; Hus et al., 2004).
444 This can also result from differential cooling as, for instance, may occur in
445 large structures (Lanos, 1987). Understanding magnetic refraction requires

446 dense sampling across all parts of a structure. Too much localized sampling
447 can lead to a precise but biased mean direction.

448 Another factor that may bias remanence directions is the anisotropy of
449 TRM. For bricks or tiles used to mason all or parts of a kiln, this effect results
450 in a recorded direction that may deviate from the ancient field. Taking
451 this effect into account requires the determination of an anisotropy tensor
452 (see details on the correction for anisotropy effects in section 3.1.5). For
453 baked clay ovens or hearths, the degree of anisotropy is usually considered
454 to be weak, and does not impact the remanence direction, e.g., Kovacheva
455 et al. (2009b) and Le Goff et al. (2020). However, it should be noted that a
456 significant shallowing of inclinations of up to 13° was recently documented
457 for thin oven soles (Palencia-Ortas et al., 2017, 2021). We further note that
458 the GEOMAGIA50 database does not yet make it possible to assess whether
459 or not the anisotropy effect has been evaluated and taken into account in the
460 directional studies.

461 On the whole the precision of directional data within GEOMAGIA50.v3.4
462 is variable, but is in general of statistically good quality, with 80% of entries
463 having $0^\circ \leq \alpha_{95} \leq 5^\circ$ (the cone of confidence at 95%; Fisher, 1953) and 90%
464 with $0^\circ \leq \alpha_{95} \leq 10^\circ$ (Fig. 7). Some data have particularly low α_{95} (30% of
465 entries have $0^\circ \leq \alpha_{95} \leq 2^\circ$) and values of k (the precision parameter; Fisher,
466 1953) into the thousands. Conversely, some α_{95} values are notably high and
467 some k are very low. The precision of directional data can be difficult to
468 quantify for some entries as α_{95} is not specified for 6% of directional entries
469 and k is given for only 50%. We also note that the method of calculating
470 α_{95} is not always noted in publications. There are two forms of the α_{95}

471 equation; the original equation in Fisher (1953) and an approximation for a
472 large number of samples (see, e.g., Butler, 1992). These can result in different
473 values of α_{95} if the number of samples is less than approximately 10.

474 Less than 2% of entries are based on the successful analysis of only one
475 or two samples and have no associated α_{95} or k . When the number of suc-
476 cessfully measured samples is at least equal to 3, k is greater than 100 for
477 80% of the entries reporting k (40% of the all directional results). Any study
478 wishing to use directional data should assess the uncertainty that they are
479 comfortable in incorporating into the analysis.

480 *3.1.2. Archaeointensity determinations*

481 The linearity at low fields ($< 150 \mu\text{T}$) between geomagnetic field strength
482 and the intensity of a TRM acquired on cooling in this field is the physical
483 basis for intensity estimates. A detailed description of the protocols is beyond
484 the scope of this article as there are numerous approaches and derivatives
485 that can be used (e.g., Dunlop, 2011; Tauxe and Yamazaki, 2015; Tauxe
486 et al., 2018), but we give an overview of those used for archaeological entries
487 in GEOMAGIA50 and review the different experimental strategies used to
488 detect and/or possibly mitigate various effects that influence the intensity
489 measurements.

490 GEOMAGIA50.v3.4 lists 25 palaeointensity methods and variants; how-
491 ever, these can be primarily classed into five main types, as listed in Fig. 8a.
492 Thellier-type approaches that use double heating steps to impart a labora-
493 tory induced TRM as proposed by Thellier and Thellier (1959) make up 87%
494 of all intensity entries in the database. Of the Thellier-type approaches, the
495 original Thellier and Thellier (1959) method has been used more than any

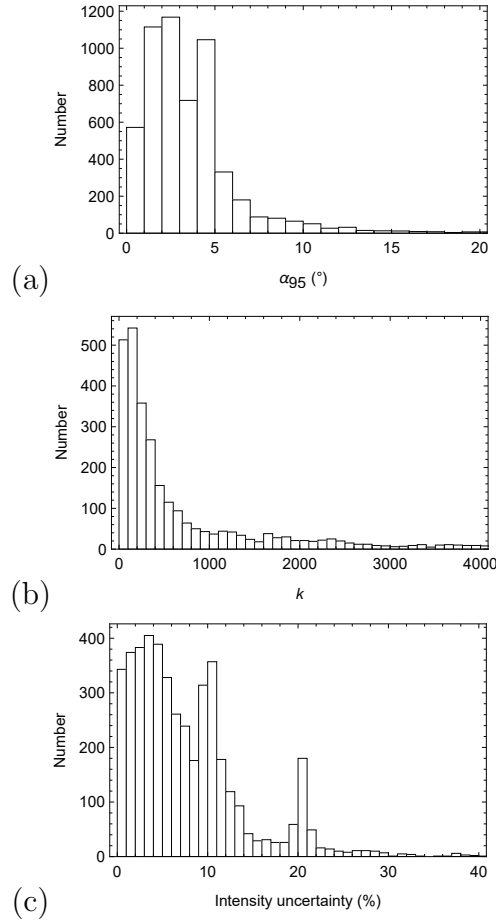


Figure 7: Measures of uncertainty and precision (Fisher, 1953) on archaeomagnetic directional and intensity entries within GEOMAGIA50.v3.4: (a) 95% cone of confidence (α_{95}) (bin size = 1 degree); (b) precision parameter (k) (bin size = 100 k). Only α_{95} values < 20 are shown, corresponding to 5542 entries or 99% of all entries with an α_{95} or 93% of all directional entries. Only k values < 4000 are plotted, totalling 2769 values (91% of all entries with k ; 47% of all directional entries). Whether α_{95} is calculated using the full equation of Fisher (1953) or an approximation (see, Butler, 1992) is not noted in the database as it is commonly not stated. (c) Uncertainty on archaeointensity estimates expressed as a percentage of the archaeointensity value (bin size = 1%). Note that the uncertainties plotted here are those given by the author and result from different approaches to calculating uncertainty.

496 other method, followed by the Coe-Thellier approach (Coe, 1967). The IZZI
497 protocol (Yu et al., 2004) has increasingly been used over recent years as the
498 revised order of the in-field and zero-field steps during the experiment aids in
499 the identification of non-ideal (MD) grains that can bias intensity estimates
500 (section 3.1.4). It currently makes up 11% of Thellier-type entries, but we
501 anticipate it will be used increasingly over coming years. Other Thellier-
502 type variants, such as that of Aitken et al. (1988), MT4 of Leonhardt et al.
503 (2004), and the two specimen approach of Domen (1977), make up only a
504 minor contribution to the database.

505 The remaining 13% of palaeointensity estimates were determined by vari-
506 ants of the Shaw (1974) method (5%), the Triaxe approach (Le Goff and
507 Gallet, 2004) (4%) (derived from a technique proposed by Wilson (1961)),
508 microwave variants of Thellier-type protocols (Shaw et al., 1999; Hill and
509 Shaw, 1999, 2007; Stark et al., 2010) (2%) and the two variants of the mul-
510 tispecimen parallel differential partial TRM (pTRM) method (Dekkers and
511 Böhnell, 2006; Fabian and Leonhardt, 2010) (1%). The calibrated pseudo-
512 Thellier method (de Groot et al., 2013) and the approach of Walton (1977)
513 contribute less than 1% of entries.

514 *3.1.3. Checking and/or correcting for thermal alteration*

515 As noted above, most archaeointensity data have been obtained using
516 protocols derived from the original Thellier and Thellier (1959) method. Its
517 principle is based on the stepwise thermal demagnetization of the natural
518 remanent magnetization (NRM, assumed to be a TRM) and its progressive
519 replacement by a new TRM acquired in a laboratory field whose direction
520 and intensity are controlled. The ratio between the remaining NRM and

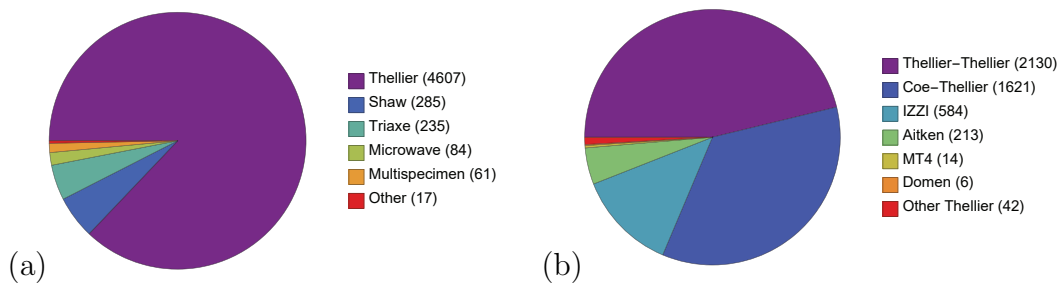


Figure 8: Pie charts of the number of entries (in brackets) within GEOMAGIA50.v3.4 associated with different palaeointensity methods. (a) All palaeointensity methods (note that the total number of entries exceeds 5231 as multiple palaeointensity entries were derived from measurements using one or more methods). Thellier methods by type are given in (b): Original Thellier-Thellier method (Thellier and Thellier, 1959), Coe-Thellier (Coe, 1967), Aitken (Aitken et al., 1988), IZZI (Yu et al., 2004), MT4 method (Leonhardt et al., 2004), the two specimen approach of Domen (1977) and other non-specific Thellier-based methods. Note that for three entries two Thellier-type methods were used for the mean intensity given in the entry, therefore the individual mentions of Thellier-type methods totals 4610. Shaw methods include the original procedure (Shaw, 1974) and modified versions by Kono (1978), Rolph and Shaw (1985), Shaw et al. (1995), Tsunakawa and Shaw (1994), Yamamoto et al. (2003). Triaxe method is that of Le Goff and Gallet (2004). Microwave methods are based on versions of the Thellier-type approaches listed above (see, e.g., Hill and Shaw, 1999, 2007). The multispecimen entries include both Dekkers and Böhnelt (2006) and Fabian and Leonhardt (2010) approaches. Other methods are the approach of Walton (1977) and the calibrated pseudo-Thellier method (de Groot et al., 2013).

521 the partial TRM acquired after each heating/cooling step, with data usually
522 displayed on an Arai-Nagata diagram (Nagata et al., 1963), allows an estima-
523 tion of the past geomagnetic field intensity. The comparison of NRM lost to
524 TRM gained requires the magnetic mineralogy of the specimen to remain un-
525 changed during the thermal treatment. In order to assess alteration, Thellier
526 suggested as early as 1946 a partial-TRM check (a pTRM check) (Thellier,
527 1946). During the stepwise heating-cooling cycle, additional pTRM acqui-
528 sition steps are added. After a number of heating steps, a lower temperature
529 step is repeated and the pTRMs compared. This is done multiple times
530 throughout the experiment, e.g., after every three heating steps, the first
531 step of the three will be repeated. This alteration test is now common and
532 always required for modern intensity studies using the Thellier method and
533 derivatives (i.e. Coe, 1967; Aitken et al., 1988; Yu et al., 2004). It is im-
534 portant to underline that different approaches have been used to calculate
535 the degree of alteration at each pTRM check (commonly expressed as a per-
536 centage) and the associated cut-off values to accept or reject a check or an
537 intensity determination. 44% of Thellier-type intensity entries are accom-
538 panied by a pTRM check; however, this number hides the variability in the
539 statistical cutoffs used (see Genevey et al., 2008; Paterson et al., 2014).

540 Monitoring magnetic susceptibility during heating has been used to check
541 for the stability of the magnetic mineralogy; however, it must be noted that
542 slight changes in susceptibility may not relate to changes in remanence car-
543 rying minerals or the formation of new remanence carriers (rather changes
544 in the susceptibility of magnetic minerals that do not have the capacity to
545 hold or acquire a remanence). This approach was for example used for the

546 part of the Bulgarian data set acquired in the 70s and 80s (Kovacheva et al.,
547 2014). Susceptibility monitoring was only used for 1.5% of intensity entries
548 in the database.

549 Instead of rejecting samples for which alteration is judged too strong,
550 another possibility is to correct for this effect. This was proposed by Burakov
551 and Nachasova (1985), with a protocol that additionally takes into account
552 anisotropy of TRM. Several sets of data were acquired using this protocol
553 (26 studies spanning 1986 to the present day). This protocol which has not
554 been used in other laboratories is viewed with caution.

555 For $\sim 30\%$ of database entries listing the use of a Thellier-type protocol, no
556 alteration test was performed to check or correct for alteration: the linearity
557 of the data points in the Arai-Nagata diagram over a large proportion of the
558 unblocking temperatures was judged sufficient to testify of the absence of
559 this effect. This concerns mainly studies published before the 1990s.

560 In the Triaxe method (Le Goff and Gallet, 2004) measurements are made
561 continuously in temperature, through successive series of heating and cooling,
562 in zero field or laboratory field. The stability of the magnetic mineralogy
563 is assessed by checking the stability of the ratio between the demagnetized
564 NRM fraction and the acquired TRM fraction at each increasing temperature
565 step. This approach corresponds in a similar way to testing the linearity in
566 an Arai-Nagata diagram, but the steps are spaced only 5°C apart: the data
567 are therefore numerous (e.g., 60 data for a 300°C temperature interval) and
568 the linearity is thus finely checked and also assessed through specific linearity
569 tests (Le Goff and Gallet, 2004).

570 To mitigate the risk of magnetic alteration, alternative methods have

571 been developed. From the oldest to the most recent: the Shaw technique
572 and derivatives (Shaw, 1974; Tsunakawa and Shaw, 1994; Yamamoto et al.,
573 2003), the microwave technique (e.g., Walton et al., 1996; Hill and Shaw,
574 1999) and the multispecimen protocol and adaptations (Dekkers and Böhnell,
575 2006; Fabian and Leonhardt, 2010).

576 Most data obtained with the Shaw technique were acquired between 1975
577 and 1995 (e.g., Liritzis and Thomas, 1980; Shaw et al., 1995), but the method
578 has seen a revival in recent years (Kitahara et al., 2018, 2020) in the form of
579 the modified Tsunakawa-Shaw approach (Yamamoto et al., 2003). The Shaw
580 method involves only one heating in which the sample is heated above its
581 Curie temperature allowing the acquisition of a full TRM. Prior to heating
582 the NRM is stepwise demagnetized using increasing alternating field (AF)
583 steps. After heating the sample is again demagnetized using the AF steps as
584 for the NRM. The linear relationship of the demagnetized NRM to TRM is
585 then used to calculate an estimate of palaeointensity. Alteration is assessed
586 through a comparison of coercivity spectra. Changes in an AF demagnetized
587 anhysteretic magnetization (ARM) given before and after heating are com-
588 pared. Later modifications to the method incorporated corrections to take
589 into account alteration to the pre- and post-heating ARM spectra (Kono,
590 1978; Rolph and Shaw, 1985).

591 The microwave method follows the protocols of Thellier and Thellier and
592 modified variants, e.g., the perpendicular single heating method (Hill and
593 Shaw, 2007), but thermal demagnetization is replaced by microwave demag-
594 netization. The rationale is that microwave power should limit the rise in
595 temperature of the sample matrix and reduce the possibility of alteration.

596 However, some conversion to thermal energy to heat the matrix is likely and
597 pTRM-checks test are now integrated in the microwave technique. Recent
598 studies have also included checks for evaluating the cooling rate effect (e.g.,
599 Poletti et al., 2013; Ertepinar et al., 2020).

600 The multispecimen parallel differential partial pTRM method (Dekkers
601 and Böhnell, 2006) started life as essentially a very simple method. Multi-
602 ple specimens from a site were heated at the same temperature (below the
603 temperature of alteration, but high enough for an appreciable decrease in
604 NRM), but with a different field for each specimen aligned with the spec-
605 imens NRM. However, shortcomings in the method were evident and the
606 method was expanded upon by Fabian and Leonhardt (2010). It was elabo-
607 rated upon to correct for differences in the fraction of the pTRM imparted
608 in each specimen, a specimen's domain state, and included a step to monitor
609 alteration.

610 *3.1.4. Checking or correcting for the presence of multi-domain grains*

611 Another possible factor for the failure of intensity determinations is linked
612 to the presence of MD grains for which the laws of reciprocity and additiv-
613 ity of the partial TRMs are not obeyed (Néel, 1949). Although the influ-
614 ence of MD grains on volcanic palaeointensity estimates has been investi-
615 gated in detail, it has received less attention in archaeomagnetic studies.
616 This is primarily a result of the different grain size distributions found in
617 archaeomagnetic materials compared with volcanic rocks: archaeomagnetic
618 materials are commonly dominated by pseudo-single domain grains, which
619 are not effected by pTRM tails, whereas volcanic rocks frequently contain a
620 MD fraction where pTRM tails are significant (where a pTRM-tail results

621 from a non-reciprocity between the blocking and unblocking temperatures).
622 The influence of MD grains can be recognized on Arai-Nagata diagrams as
623 a concave-up curve, whose misinterpretation can lead to underestimates or
624 overestimates of intensity depending on which portion of the curve was used
625 to calculate palaeointensity (e.g., Levi, 1977; Dunlop, 2011). The linearity of
626 the data in the Arai diagram was often considered as a sufficient criterion to,
627 if not exclude, at least consider that the proportion of MD grains is too small
628 to critically affect the intensity determination. The presence of MD grains is
629 now more directly investigated with either rock magnetic measurements, such
630 as hysteresis curves, backfield curves and first order reversal curves (see, e.g.,
631 Day et al., 1977; Dunlop, 2002; Roberts et al., 2019), or through additional
632 tests implemented during Thellier-type methods and microwave protocols,
633 such as pTRM-tail checks (aiming at testing the independence of pTRM;
634 Riisager and Riisager, 2001) and additivity checks (Krása et al., 2003). Only
635 5% of intensity entries in the database list an MD check.

636 The IZZI protocol (Yu et al., 2004), a variant on the Thellier method,
637 was designed to accentuate the influence of MD tails, evident by pronounced
638 zig-zagging in the Arai-Nagata plot. However, this method is sensitive to
639 the direction of the laboratory field relative to the orientation of the NRM
640 leading to over- or under- estimation of the pTRM-tail and with the field
641 aligned with the direction of the NRM, MD tails can be suppressed.

642 In comparison to other protocols, the MSP-DSC method of Fabian and
643 Leonhardt (2010) has the advantage to (partially) correct intensities for do-
644 main state effect. The Triaxe protocol (Le Goff and Gallet, 2004) mitigates
645 the spurious effect of large grains because the laboratory TRM is almost a full

646 one, mimicking the acquisition of the original TRM. The Shaw derivative of
647 Yamamoto et al. (2003) aims to remove all MD contributions by incorporat-
648 ing a low-temperature demagnetization step after each remanence acquisition
649 and prior to AF demagnetization.

650 3.1.5. TRM anisotropy

651 An important parameter that may affect intensity determinations when
652 analyzing baked clay artefacts is anisotropy of TRM (already touched upon
653 in section 3.1.1). This anisotropy arises from the stretching of clay during the
654 process of shaping an object, resulting in a preferential alignment of magnetic
655 grains in the clay matrix (e.g., Rogers et al., 1979; Aitken et al., 1981). This
656 effect may be particularly intense for pottery fragments and thin tiles and to
657 a lesser extent to thick bricks, with biases up to several dozens of micro Tesla
658 (e.g., Genevey et al., 2008; Hervé et al., 2017; Gómez-Paccard et al., 2019).
659 Conversely, it has been observed that this effect is generally less critical when
660 analysing fragments made of clay, which are coarsely assembled, as they are
661 usually taken from in situ structures (e.g., Kovacheva et al., 2009b).

662 For 38% of archaeointensity entries in the database remanence anisotropy
663 was not investigated (Fig. 9a). In some cases data were obtained from less
664 anisotropic materials and no measure of anisotropy was pursued. In a small
665 number of entries where anisotropy was estimated, a correction was not nec-
666 essary. This is most likely as the anisotropy was not considered to be sig-
667 nificant. Different approaches have been proposed to evaluate remanence
668 anisotropy. Determination of a TRM anisotropy tensor for each analysed
669 sample allows to evaluate the importance of this effect and to accurately cor-
670 rect the raw intensity determinations (Veitch et al., 1984; Selkin and Tauxe,

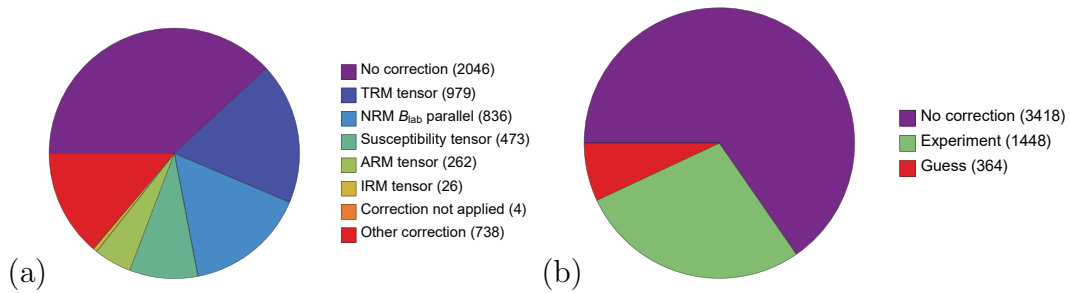


Figure 9: Pie charts of the intensity entries in the GEOMAGIA5.v3.4 database noting (a) remanence anisotropy corrections and (b) cooling rate corrections. Number of uses of an approach are given in brackets. In (a) TRM = thermoremanent magnetization; ARM = anhysteretic remanent magnetization; IRM = isothermal remanent magnetization; NRM B_{lab} parallel = laboratory field applied parallel to specimen natural remanent magnetization (NRM) direction during the palaeointensity method; other corrections are generally approaches that were insufficiently defined in a publication). See more details in section 3.1.5 and Section 3.1.6,

2000). This approach was used for 30% of entries considering anisotropy in
the database. The drawback of this approach is the time-consuming multiple
heating steps (usually six), which increases the risk of mineralogical alter-
ation. Aligning the laboratory field direction with the original NRM (25%
of entries considering anisotropy) is an adequate alternative, as long as the
degree of anisotropy is not too strong to bias significantly the direction (e.g.,
Aitken et al., 1981). Ideally, the laboratory field direction should be aligned
with the ancient ambient field. This is achieved with the Triaxe protocol
and MSP protocols where the direction of the laboratory field is adjusted so
a TRM is imparted parallel to the primary TRM (see, Le Goff and Gallet,
2004). To minimize the effect of TRM anisotropy, Morales et al. (2009) pro-
posed to average the intensity values obtained for 6 specimens from the same

683 fragment: here the specimens are oriented in such a way that the TRM is
684 acquired in 6 orthogonal directions relative to a fixed arbitrary orientation.
685 However, Poletti et al. (2016) and Hervé et al. (2019b) demonstrated that
686 this approach results in larger standard deviations and possibly significant
687 inaccuracies as high as 10-15 μT .

688 As an alternative to the full determination of the TRM anisotropy ten-
689 sor, it has been suggested to use other tensors to evaluate and correct for
690 anisotropy; namely tensors of magnetic susceptibility (AMS; 14% of anisotropy
691 assessed entries), anhysteretic remanent magnetization (ARM; 8%) or isother-
692 mal remanent magnetization (IRM; $< 1\%$). These substitutes are often
693 quicker and easier to implement and avoid the six additional heatings during
694 the thermal protocol. However, the respective ellipsoids significantly differ
695 in their shape and anisotropy degree from TRM ellipsoids (e.g., Chauvin
696 et al., 2000). AMS can underestimate TRM anisotropy by several dozens
697 of percent (Gómez-Paccard et al., 2019). In 22% of entries other types of
698 anisotropy corrections have been applied, but either a method was not listed
699 in the database or the method was not described in the publication.

700 *3.1.6. Cooling rate effect*

701 Another possible biasing factor for intensity determinations is the cooling
702 rate dependence of TRM intensity (Fox and Aitken, 1980). Ideally, to avoid
703 such systematic bias, the cooling duration used for the acquisition of the
704 laboratory TRM should be chosen to be identical to the original one when
705 the primary TRM was recorded by the archaeological object. This is rarely
706 possible as the original cooling time is usually long, ranging typically from
707 half a day to a few days (with the notable exception of the slags, Shaar et al.,

708 2010), while the laboratory cooling time is faster, generally from 0.5 up to 2
709 hours, depending of the type of oven and the size of the specimens.

710 For Thellier-Thellier data, the cooling rate effect can be evaluated through
711 a comparison of the TRM acquired with a rapid cooling time (the one used
712 routinely during the experiment) and a slow cooling time chosen to be close
713 to the original one (e.g., Chauvin et al., 2000; Leonhardt et al., 2006; Poletti
714 et al., 2013). This is performed for 28% of the intensity entries in the database
715 and comprises 80% of entries that used a cooling rate correction (Fig. 9b).
716 Precisely evaluating the duration of the past cooling is the main difficulty of
717 the correction protocol. Experimental archaeology has provided constraints
718 on this issue (e.g., Morales et al., 2011; Calvo-Rathert et al., 2019; Genevey
719 et al., 2016; Schnepf et al., 2016; Hervé et al., 2019a; Jones et al., 2020).
720 Archaeological information concerning, e.g., the estimated size of kilns, their
721 morphology, and the type of firing (open or closed), may also help to assess
722 the original cooling conditions. Another approach is to measure the cool-
723 ing rate effect on TRM acquisition with increasingly slow cooling duration
724 (therefore exploring different conditions of cooling) and to infer from this the
725 error that would be made by under or over estimating the original cooling
726 rate (Genevey et al., 2003; Hartmann et al., 2010).

727 A different possibility is to apply a fixed correction for all samples from
728 the same archaeomagnetic site, usually 5% or 10%. This “educated guess”
729 concerns 7% of intensity data or 20% of entries which applied a cooling rate
730 correction (Fig. 9b). This approach is based on the assumption that all
731 fragments of the same archaeological object show the same TRM intensity
732 dependence on cooling rate. Experimental studies have, however, pointed

733 out that this effect is variable from one sample to another and (as predicted
734 by theory) that the TRM intensity increases following a logarithmic law as
735 a function of the ratio between an increasingly slow cooling time and a fixed
736 rapid one (Genevey et al., 2008; Hervé et al., 2019a). To avoid applying
737 an educated guess correction to all fragments, it has been suggested to esti-
738 mate at least for part of the collection the cooling rate effect and to apply
739 an average correction to the other fragments (Kostadinova-Avramova and
740 Jordanova, 2019).

741 Another important question is at what temperature to estimate the effect
742 of cooling rate. In particular, Hervé et al. (2019a) showed too high of a tem-
743 perature could greatly overestimate this effect and therefore underestimate
744 the intensity value. This appears to depend on the magnetic mineralogy of
745 the material analysed (see also Kostadinova-Avramova and Jordanova, 2019).

746 The cooling rate effect is a challenging parameter to estimate and many
747 studies have not explored this question (over 70% of entries in the database).
748 However, some of these data were obtained with a relatively slow cooling time
749 as part of routine intensity experiments (for example for Bulgarian dataset;
750 Kovacheva et al., 2014): the cooling rate effect is therefore expected to affect
751 them less strongly.

752 Optimally, we would like to be able to dispense with the question of the
753 cooling rate effect. It has been observed experimentally that the Triaxe pro-
754 tocol accounts for cooling rate (Le Goff and Gallet, 2004; Genevey et al.,
755 2009; Hartmann et al., 2010; Hervé et al., 2017; Salnaia et al., 2017). The
756 multispecimen parallel differential pTRM method also seems to be insensi-
757 tive to cooling rate (e.g., Schnepf et al., 2016; Calvo-Rathert et al., 2019),

758 possibly because in this technique all pTRMs are acquired at medium tem-
759 peratures. However, this question still needs to be further explored (Schnepp
760 et al., 2020a).

761 *3.1.7. Intensity uncertainties*

762 On the whole archaeomagnetic data within GEOMAGIA50.v3.4 have rea-
763 sonably well constrained uncertainties (Fig. 7c). The majority of estimates
764 have an uncertainty of less than 10% of the intensity estimate (60% of inten-
765 sity entries that report uncertainties), i.e. a few μT on most measurements.
766 Some intensity measurements, however, have high uncertainties, ranging up
767 to 40 μT . They require careful evaluation prior to their inclusion in reference
768 curves or for field modelling.

769 A caveat to all intensity uncertainties in the database is that they have
770 been calculated in a variety of ways. Uncertainties may be reported as stan-
771 dard deviations (to 1 or 2 σ), standard errors or they could be weighted.
772 The type of intensity uncertainty is not noted in the database. Care must
773 therefore be taken when using intensity uncertainties when constructing field
774 models and reference curves and using this field as a selection criteria.

775 *3.2. Dating methods*

776 Dating and its accuracy and precision are key elements for any archaeo-
777 magnetic study. For archaeological artefacts, the dating methods used and
778 listed in GEOMAGIA50 are based on archaeological or historical constraints,
779 or chronometric methods involving mainly radioisotopic and physicochemical
780 measurements (Fig. 10). See Aitken (2014) for an overview of scientific dat-
781 ing methods. We briefly describe the most salient aspects of these methods

782 and their caveats in section 3.2.1.

783 The archaeological approach remains the most common and concerns al-
784 most 60% of the database. Behind the term “archaeological dating” is often
785 hidden the use of a relative chronology, which itself is constrained by elements
786 of absolute dating. The different types of dating methods are clearly comple-
787 mentary and the quality of the two approaches cannot be simply ranked, i.e.
788 scientific dating does not always outrank archaeological observations, it de-
789 pends on the specific context and an understanding of an archaeological site.
790 The importance of sampling in close collaboration with an archaeologist is
791 paramount for selecting materials whose TRM acquisition can be dated with
792 the maximum precision and confidence. Two categories of methods to date
793 TRM acquisition are distinguished here, either direct, i.e. directly concern-
794 ing the analyzed material itself, or indirect, i.e. the material is dated by
795 association with another dating element.

796 *3.2.1. Direct dating of TRM*

797 One of the main sources to directly date TRM are document archives. A
798 well-known example is the eruption of Vesuvius first described by Pliny the
799 Younger, which destroyed the city of Herculaneum and Pompeii in 79 CE
800 (Evans, 1991; Evans and Hoye, 2005). But more commonly, these archives
801 are used, for example, to precisely date the edification of religious or civil
802 buildings (e.g., Schnepf et al., 2003; Osete et al., 2015; Salnaia et al., 2017;
803 Genevey et al., 2019) or short periods of activity of ceramics workshops (e.g.,
804 Genevey et al., 2009). Other objects, such as some amphoras, can be precisely
805 dated directly through the identification of stamps (Ben-Yosef et al., 2017).

806 Among the chronometric methods used in archaeology, thermolumines-

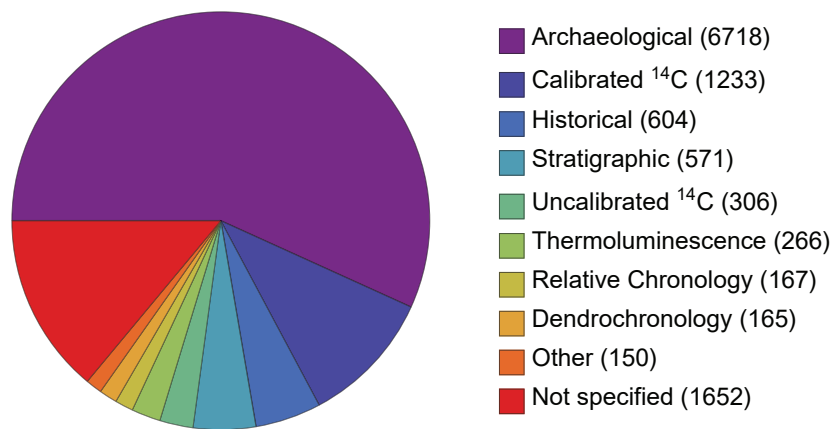


Figure 10: Pie chart of the 8 most commonly used methods to date archaeological materials in GEOMAGIA50.v3.4. Note, the numbers in brackets do not sum to the total number of entries in the database, as numerous entries have been dated using multiple methods. “Other” methods include whether accelerator mass spectrometry was used to obtain radiocarbon ages (133 entries, with frequent overlap with the calibrated and uncalibrated radiocarbon age entries), and if optically stimulated luminescence (OSL; 9 entries) or rehydroxylation (5 entries) were used.

807 cence (TL) and optically stimulated luminescence (OSL) are directly asso-
808 ciated to the TRM acquisition. A firing above 400°C is time-zero of the
809 method as at above this temperature the electron traps in quartz or feldspar
810 grains in baked clays are emptied (Aitken, 1985). From this moment, traps
811 progressively fill again under irradiation from the surrounding environment
812 (mainly related to ^{40}K , ^{238}U , ^{235}U and ^{232}Th radioactive isotopes). In spite of
813 the advantage of dating the same instance as the TRM acquisition, lumines-
814 cence methods constitute only $\sim 3\%$ of entries in the database. However, this
815 method has been used in recent studies (e.g., Gómez-Paccard et al., 2012a;
816 Schnepf et al., 2003; Kondopoulou et al., 2015; Cai et al., 2015; Aidona
817 et al., 2021). Accurate luminescence dating requires a careful reconstitution
818 of the radioactive environment of the baked clay since the last firing. The
819 resulting long measurement time limits the use of the techniques (Roberts
820 et al., 2015). Another caveat of luminescence methods are age uncertainties
821 of $\pm 5\text{-}10\%$ (1σ), corresponding to $\pm 100\text{-}200$ years for a 0 CE baked clay for
822 example. However, this can be reduced if multiple TL measurements are
823 made. It is worth noting that OSL does not always provide a direct dat-
824 ing of the TRM acquisition because time-zero of this technique can also be
825 the last exposure to sunlight, offering the possibility to date the deposit of
826 sedimentary layers around the studied baked clays.

827 Another method to directly date baked clay artefacts was proposed by
828 Wilson et al. (2009). It is based on the process of rehydroxylation (RHX) of
829 fired-clay ceramics after production. Similar to luminescence methods, the
830 principle is to start from a zero point by heating a sample up to $\sim 500^\circ\text{C}$ (de-
831 hydroxylation) and then monitor precisely the sample's weight gain in known

832 environmental conditions over several weeks (through rehydroxylation). This
833 allows the kinetics of the rehydroxylation process to be determined. Although
834 promising for archaeologists, and in turn for archaeomagnetists, the relation-
835 ship between mass gain and time has proved more complex than initially
836 thought, with kinetics that appear to depend on the nature and/or firing
837 conditions of the ceramic (in addition to the environmental conditions), and
838 the applicability of the RHX method appears clearly compromised (Bowen
839 et al., 1971; Le Goff and Gallet, 2014, 2015). So far it has only been applied
840 to two archaeomagnetic studies, both on Spanish ceramics (Nachasova and
841 Burakov, 2012; Burakov and Nachasova, 2013).

842 *3.2.2. Indirect dating of TRM*

843 As mentioned in the introduction to this section, the archaeological ap-
844 proach remains the most used method of indirect dating. Archaeological
845 dating is however a very generic term that integrates many different ele-
846 ments. The first is stratigraphy, which is essential for building chronologies
847 for ancient multi-layered sites in the Middle East (Shaar et al., 2011; Gallet
848 et al., 2020) and Eastern Europe (e.g., Kostadinova-Avramova et al., 2014).
849 Elements such as coins, fragments of ceramics or metallic artefacts (e.g.,
850 swords and fibulae) are also key for dating, if the evolution of their typol-
851 ogy is well known. Together, these elements make it possible to define a
852 post quem and ante quem terminus for an archaeological level or artefact.
853 It is also important to understand whether there has been any mixing of the
854 layers in the stratigraphy, which can limit chronological control. The central
855 question is to precisely understand how the object analysed for archaeomag-
856 netism is reliably related to these chronological constraints. This question

857 is far from trivial, e.g., for settlements occupied over a long period. For in-
858 tensity determination, one way to overcome this issue is to work directly on
859 dated pottery fragments, i.e. those whose shape or decoration is recognized
860 and can be linked to a known local/regional typo-chronology.

861 The relative chronology given by the stratigraphy is fixed to the calendar
862 scale by historical events or chronometric methods. Their precision and re-
863 liability are mainly related to the state of the art of archaeological research
864 in the region for a certain period. For example, in Western Europe, precise
865 typo-chronologies are firm for the Roman period (0-500 CE), but are “float-
866 ing” for the Neolithic period (6000-2000 BCE). These typo-chronologies, and
867 more generally archaeological dating, are also likely to evolve according to
868 the progress of knowledge. This is not a weakness insofar as the archaeomag-
869 netic results remain accurate. However, it is important that dates associated
870 with archaeomagnetic measurements reflect revisions to archaeological ages.
871 For some regions there have been recent revisions to GEOMAGIA50 to ac-
872 commodate new age information, e.g., Bulgaria (Kovacheva et al., 2014),
873 United Kingdom (Batt et al., 2017), Greece (De Marco et al., 2014), USA
874 (Bowles et al., 2002; Jones et al., 2020) and France (Le Goff et al., 2020).
875 It must also be recognized that there are likely ages within GEOMAGIA50
876 that do not reflect advances in archaeological age determinations for specific
877 times, regions or sites. Work can continue on sites for years to decades and
878 the archaeomagnetic aspect of the excavation/project may not be the pri-
879 mary objective; new ages may come to light after the final publication of the
880 archaeomagnetic work.

881 Another common method used to indirectly date archaeological materials

882 is radiocarbon dating. Approximately 15% of entries have used radiocarbon
883 dating as the sole chronological control or in conjunction with other dating
884 methods. Charcoals from carbonaceous or ashy layers that are related to the
885 last use of a kiln/fireplace or located in different horizons of the stratigraphy
886 have frequently been used for dating (e.g., Shaar et al., 2015), but other
887 materials such as seeds and bones have also been used. In comparison to the
888 typochronological approach, its advantage is to give a precise date bound by
889 experimentally derived uncertainties. However, the significance of this date
890 relative to the TRM acquisition is not guaranteed. For example, the date can
891 be affected by an old carbon/wood effect. Radiocarbon dates the formation of
892 the organic cell and dating charcoals from reused woods or central tree rings
893 can result in earlier dates up to a few centuries. A preliminary anthracological
894 study is useful to identify such samples and select, if possible, materials with
895 a short lifetime as burnt twigs, grasses or seeds.

896 A limitation of the method is that the abundance of radiocarbon within
897 a sample can not be simply related to a specimen's age, through comparison
898 to a decay product, as for example in $^{40}\text{K}/^{39}\text{Ar}$ dating; nitrogen produced
899 by the decay of ^{14}C is not captured by the majority of materials (Reimer
900 et al., 2020). Radiocarbon dating is based on measuring the amount of ^{14}C
901 still present in the sample, but the initial concentration of atmospheric ra-
902 diocarbon has varied through time and this variation must be accounted
903 for in the calculation of a final radiocarbon age (also known as a calendar
904 age). This process is called calibration and there has been a sustained effort
905 by the radiocarbon community over the past 40 years to develop curves of
906 atmospheric radiocarbon variations that can be used to transfer ^{14}C ages

907 based on the measurement of radiocarbon present in a specimen, expressed
908 in years Before Present (0 BP = 1950 CE) to an age on a calendar timescale
909 in calibrated BCE/CE. The last versions of calibration curves being IntCal20
910 (for the Northern Hemisphere; Reimer et al., 2020), SHCal20 (for the South-
911 ern Hemisphere; Hogg et al., 2020) and Marine20 (for the oceans; Heaton
912 et al., 2020). As atmospheric radiocarbon variations vary rapidly and non-
913 linearly, this leads to highly variable and complex calibration curves. This in
914 turn results in calibrated radiocarbon ages that have a non-Gaussian error
915 and in some cases result in very broad uncertainties with multiple age ranges.
916 Plateau effects at certain periods result in irreducible date intervals of several
917 centuries, such as 8200-7600 BCE, 4300-4000 BCE, 3400-2900 BCE, 800-400
918 BCE or the past four centuries.

919 Finally, we underline that the best way to minimize the risk that the true
920 date of the TRM acquisition is not included in the given interval of age is
921 to combine several chronometric and/or archaeological dates. This is often
922 done by an archaeologist who has an overarching understanding of the site
923 and its positioning in the regional fabric. More recently, mathematical tech-
924 niques such as Bayesian chronological modelling (e.g., Bronk Ramsey, 2009;
925 Lanos and Philippe, 2018) have brought additional insights into developing
926 archaeological chronologies, especially for sites with complex stratigraphies
927 (e.g., Shaar et al., 2011).

928 *3.2.3. Age uncertainties in GEOMAGIA50*

929 Age uncertainties (expressed here as age ranges to accommodate the mul-
930 timodal age probability distributions of calibrated radiocarbon ages) vary
931 widely within the database, ranging from 0 years for some historically and

932 archaeologically dated entries (1.4% of data) to 2900 years for an archaeo-
933 logically dated oven from Germany (Schnepp et al., 2020b) (Fig. 11). Ap-
934 proximately 6% of data (627 entries) have an age range ≤ 10 years; $\sim 30\%$
935 have an age range ≤ 50 years; and $\sim 50\%$ of entries have age ranges of 100
936 years or less. Nearly all age ranges are less than 500 years ($\sim 90\%$). There
937 are spikes in the age ranges, with ranges of 100, 200, 300, 400 and 500 being
938 more populous than others (Fig. 11b). The majority of these ranges are from
939 archaeological dated materials and are assignments to specific centuries or
940 across multiple centuries. In general, there is no correlation between age and
941 age range. It is important to note that age ranges can be reported at differing
942 precisions (e.g., 1 or 2 standard deviations) and they do not have the same
943 form. For example, some age distributions will follow a normal distribution
944 (e.g., uncalibrated radiocarbon ages and luminescence techniques), some a
945 multimodal distribution (calibrated radiocarbon ages) and others a uniform
946 distribution (e.g., archaeological ages assigned to a specific archaeological
947 period). For a specific age within an age range, this means there will be
948 differing probabilities of this age depending on the dating method used.

949 **4. Archaeomagnetic field reconstructions**

950 As described in section 2.3 and section 2.4 archaeomagnetic data are
951 inhomogeneous in space and time. Furthermore, little can be garnered about
952 the large scale geomagnetic field from individual data. Regional or global
953 compilations of data are therefore necessary to gain a greater understanding
954 of the temporal and spatial evolution of the field. This section will give an
955 overview of the two main approaches to reconstructing the geomagnetic field

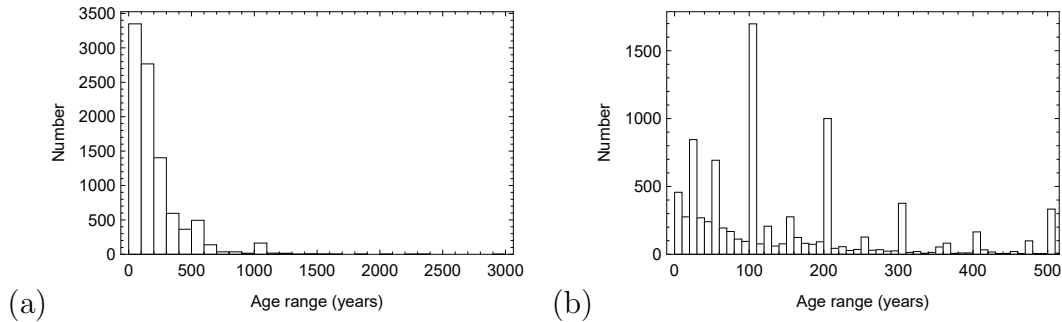


Figure 11: Archaeomagnetic age ranges within GEOMAGIA50.v3.4, binned by (a) 100 year age ranges and (b) 10 year age ranges. (a) the full span of age ranges; (b) truncated to age ranges ≤ 500 years.

956 on centennial to millennial time scales: regional secular variation curves and
 957 global spherical harmonic models.

958 *4.1. Regional secular variation curves*

959 The potential to combine individual archaeomagnetic data from different
 960 locations into composite archaeomagnetic curves for dating purposes was
 961 recognized in the 1950s (e.g., Cook and Belshé, 1958; Watanabe, 1958) and
 962 a variety of reference curves have been obtained for several parts of the
 963 world since then (see Korte et al. (2019) for a detailed review). Because the
 964 geomagnetic field cannot be considered purely dipolar, field variations at one
 965 location (or in one region) are not representative of the evolution of the field
 966 as a whole. Smaller-scale non-dipole contributions lead to deviations from
 967 a dipolar geometry, resulting in variations in direction and intensity that
 968 can vary from one region to another. Combining all global archaeomagnetic
 969 data into composite curves will not fully capture the evolution of the field
 970 and may obscure regional field structures. Therefore it has been common to

971 develop regional archaeomagnetic curves. It is generally assumed that data
972 within a radius of several 100 to a few 1000 km reflect similar field variations
973 and can be combined to form a reference curve for a region (e.g., Tarling,
974 1989; Tema and Lanos, 2020). A review by Korte et al. (2019) included an
975 investigation of the spatial correlation length of geomagnetic variations and
976 the possible influence of the distance to a curve for dating accuracy. However,
977 strict guidelines cannot be given owing to the complex spatial and temporal
978 evolution of the geomagnetic field over short time scales.

979 Archaeomagnetic reference curves of field directions, intensity, or all three
980 field components have been developed over a number of decades for several
981 European countries (e.g., Kovacheva et al., 2009a; Tema and Lanos, 2020;
982 Schnepp et al., 2020b,a), Japan (e.g., Watanabe, 1958; Nagata et al., 1963;
983 Kitazawa, 1970; Sakai and Hirooka, 1986), China (e.g., Wei et al., 1982, 1986;
984 Batt et al., 1998; Yang et al., 1993; Shaw et al., 1995), and the United States
985 of America (e.g., Watanabe and Dubois, 1965; Sternberg, 1989a; Hagstrum
986 and Blinman, 2010; Jones et al., 2020) (see Constable and Korte (2015) for a
987 more detailed list with comprehensive references). Several curves have been
988 frequently updated with new data as they become available, e.g., France
989 (e.g., Thellier, 1981; Bucur, 1994; Chauvin et al., 2000; Genevey and Gallet,
990 2002; Genevey et al., 2009, 2016; Gallet et al., 2002; Hervé et al., 2013a,b; Le
991 Goff et al., 2020). With efforts to improve data coverage for other regions,
992 there are now curves for China (Cai et al., 2017), the Near East (Gallet et al.,
993 2015; Stillinger et al., 2015; Shaar et al., 2020; Livermore et al., 2021), Mexico
994 (Soler Arechalde et al., 2019; Mahgoub et al., 2019) and South America
995 (Goguitchaichvili et al., 2019).

996 *4.1.1. Approaches to curve construction*

997 The first step to building a reference curve is to relocate the distributed
998 data to a central location (also known a reference location) to eliminate
999 differences that result in directions or intensity at different locations purely
1000 from a dipole field geometry. For directions, this is commonly done by using
1001 the conversion-via-pole (CVP) method, whereby a directional pair with one
1002 set of geographic coordinates is transformed to a virtual geomagnetic pole
1003 (VGP) and the subsequent VGP is then transformed to a new directional
1004 pair using the geographic coordinates selected for the reference curve (Shuey
1005 et al., 1970; Noel and Batt, 1990). Alternative approaches have also been
1006 used, which assume an axial dipole (a dipole aligned with Earth’s rotation
1007 axis where the geographic and magnetic pole are coincident) (Aitken and
1008 Hawley, 1966; Thellier, 1981), though this method is no longer common. In
1009 addition, average curves have been calculated using VGPs and not relocated
1010 directions (e.g., in the USA; Sternberg, 1989b; Lengyel and Eighmy, 2002).
1011 It is important to note that the non-dipolar nature of the archaeomagnetic
1012 field means that all relocation methods have an associated uncertainty (Shuey
1013 et al., 1970; Casas and Inconato, 2007).

1014 For archaeointensities, curves are typically constructed using intensity
1015 transformed to either a virtual dipole moment (VDM) or a virtual axial
1016 dipole moment (VADM) (e.g., Daly and Goff, 1996; Yang et al., 2000). A
1017 VDM is analogous to a VGP, as it uses inclination assuming a tilted dipole.
1018 VADM assumes a geocentric axial dipole configuration and allows intensity
1019 data lacking inclination to be compared. As with relocated directions, there
1020 is an intrinsic uncertainty when calculating a V(A)DM assuming a dipole

1021 field configuration when the field can have noticeable non-dipolar compo-
1022 nents. This can result in a dispersion between sites that is a reflection of
1023 non-dipolar field behaviour and not related to issues with how estimates of
1024 archaeointensity were obtained.

1025 Different data fitting and smoothing methods have been employed to
1026 derive regional secular variation curves. Some early curves relied on hand
1027 drawn fits through the data (see, Thellier, 1981; Clark et al., 1988). How-
1028 ever, through time increasingly sophisticated mathematical approaches have
1029 been used to construct curves, applying methods that not only derive single
1030 curves through time (or through inclination and declination), but calculate
1031 uncertainties. Simple interpolation of individual field components (or means
1032 across time interval bins) with or without the estimation of curve uncertain-
1033 ties has been common (e.g., Sternberg, 1989a; Yang et al., 2000), but over
1034 the past thirty years a variety of mathematical approaches have been taken.
1035 Methods such as bivariate extensions of Fisher Statistics (Le Goff et al., 1992)
1036 continue to be used to produce curves for Europe, e.g., France (Hervé et al.,
1037 2013a; Le Goff et al., 2020). Recently bootstrap or Bayesian methods have
1038 been used to obtain curves, uncertainty estimates, and/or probability dis-
1039 tributions (Thébault and Gallet, 2010; Hellio et al., 2014; Livermore et al.,
1040 2018). The Bayesian method of Lanos (2004) and Lanos et al. (2005) is
1041 notable as it produces consistent curves for all three field components and
1042 provides curve uncertainties that consider uncertainties on the archaeomag-
1043 netic data and ages, and the data distribution. This approach has been used
1044 in the creation of a number of archaeomagnetic curves across Europe, e.g.,
1045 Austria and Germany (Schnepp and Lanos, 2005), and Bulgaria (Kovacheva

1046 et al., 2014). The method of Livermore et al. (2018), which is published
1047 alongside open source code, also produces curve uncertainties for intensity
1048 and the posterior sample age distributions as a direct output.

1049 *4.1.2. Examples of regional field variations*

1050 There are two features noticed in several regions that have received atten-
1051 tion in the last decades: archaeomagnetic jerks and intensity spikes. Rapid
1052 changes in directional variations seen in Bauer plots (declination against
1053 inclination) associated with an increase in intensity in French and Middle
1054 East data have been named “archaeomagnetic jerks” (Gallet et al., 2003,
1055 2005, 2009). Gallet et al. (2005) suggested that if archaeomagnetic jerks
1056 are global features, they could be associated with episodes of a tilted and
1057 enhanced dipole. Later, Gallet et al. (2009) noted that they may corre-
1058 spond to maximum geomagnetic field hemispheric asymmetry, leading to
1059 most-eccentric dipole events, related to the dynamics of flux patches at mid-
1060 to high-latitudes. If archaeomagnetic jerks are regional, they may result from
1061 a recurring non-dipole field structure that influences Western Europe. Using
1062 the global field model CALS7k.2 (Korte and Constable, 2005), Dumberry
1063 and Bloxham (2006) inferred that archaeomagnetic jerks are associated with
1064 a change in the dominant azimuthal flow direction at the top of the outer
1065 core below Europe. It is important to note that there is a clear difference
1066 in timescales between archaeomagnetic and geomagnetic jerks (e.g., Man-
1067 dea and Olsen, 2009). Archaeomagnetic jerks do not appear unusually rapid
1068 compared to what we know from the present field. An archaeomagnetic jerk
1069 may last 100–200 years, whereas a geomagnetic jerk lasts ~ 1 year.

1070 In contrast, the intensity variations during geomagnetic intensity spikes

1071 during the Iron Age derived from archaeological materials in the Levant (e.g.,
1072 Ben-Yosef et al., 2009; Shaar et al., 2011), are much faster than field changes
1073 observed for recent and historical times. The intensity of the field was also
1074 far greater than seen today, exceeding twice today's field strength (Shaar
1075 et al., 2016, 2018) (Fig 12). Livermore et al. (2021) suggest that six inten-
1076 sity spikes are required by the Levant data sets. Increases in intensity were
1077 also associated with a directional anomaly (most notably in inclination) and
1078 the combined directional-intensity anomaly is referred to as the Levantine
1079 Iron Age Anomaly (Shaar et al., 2018). As with archaeomagnetic jerks, it is
1080 currently unclear whether the Iron Age anomaly is regional or global in ex-
1081 tent. Data from areas surrounding the Levant (e.g., Georgia, Turkmenistan,
1082 Uzbekistan, Cyprus, Greece, Bulgaria and Egypt) indicate there is some
1083 evidence of an increase in intensity at the same (or similar) times to the
1084 Levantine spikes; however, although intensity reaches twice the present day
1085 field's at these locations, the increase spans a broader time (a few hundred
1086 years) (Fig. 12). This maybe a true representation of the field behaviour
1087 during the Iron Age or it may reflect dating inaccuracies.

1088 There is some evidence globally of an intensity increase coincident with
1089 the Iron Age anomaly and of spikes at other times (see, Korte and Constable,
1090 2018). Their origin is under discussion (Livermore et al., 2014; Davies and
1091 Constable, 2017; Korte and Constable, 2018; Troyano et al., 2020) and dif-
1092 ficult to explain given our current knowledge of the geodynamo. To further
1093 understand the driving mechanisms that generate high intensity spikes more
1094 high-quality archaeomagnetic data from several regions are necessary to fully
1095 characterize their regional or global behaviour.

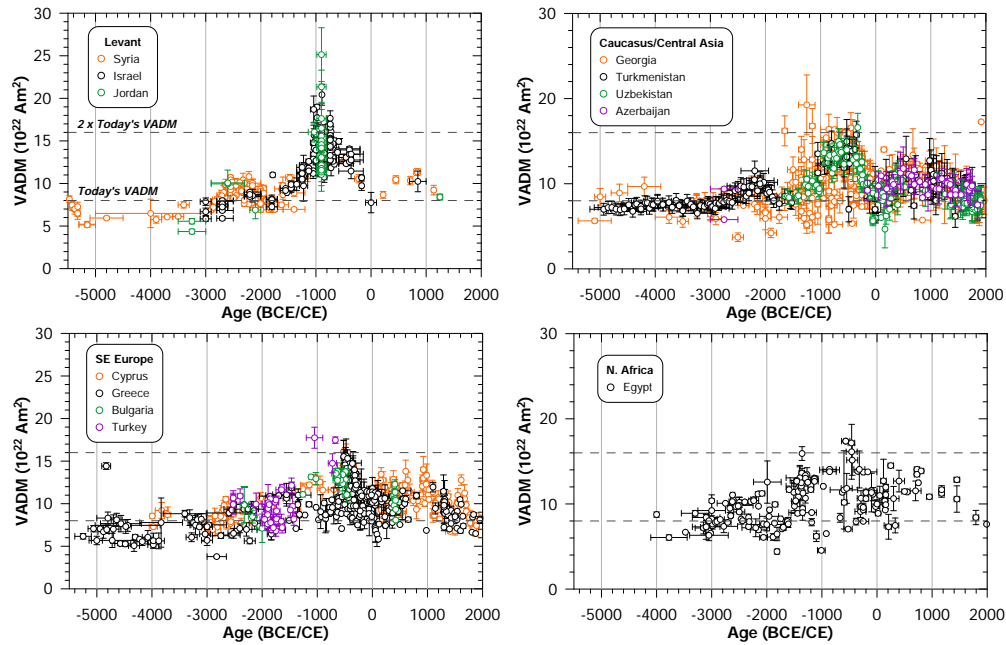


Figure 12: Virtual axial dipole moment (VADM) for the Levant and surrounding regions calculated from data in GEOMAGIA50.v3.4. Note that the data shown in (a) do not reflect the most recent interpretations (compilations) of Shaar et al. (2016), Shaar et al. (2020) and Livermore et al. (2021) as GEOMAGIA50 includes all data and a data selection protocol is not applied. The reader is referred to the above compilations for rationales related to data selection.

1096 *4.2. Global archaeomagnetic field models*

1097 Given its source in Earth’s outer core, the geomagnetic field is a global
1098 phenomenon and any studies that aim to decipher its driving processes must
1099 consider the global evolution of the field. In addition, variations in global field
1100 strength, expressed as a dipole moment are also of interest, e.g., in the context
1101 of estimating geomagnetic shielding against solar wind, galactic cosmic ray
1102 production, atmospheric ionization and solar activity (e.g., Usoskin et al.,
1103 2006, 2008, 2010, 2016). A range of global archaeomagnetic field models
1104 have been derived over the past decades, from which maps of the field can
1105 be generated for Earth’s surface (e.g., Fig. 13) and core-mantle boundary
1106 (CMB) (e.g., Fig. 14). In the following sections we give an overview of the
1107 history of global archaeomagnetic field models, how modelling approaches
1108 have evolved over the past twenty years, and the current state of the art. We
1109 discuss how data selection and data uncertainties influence global models and
1110 how these have been treated in the most recent models. We describe some of
1111 the major findings that global modelling has facilitated, but also note caveats
1112 to the modelling approaches.

1113 *4.2.1. Dipole moment reconstructions*

1114 According to the International Geomagnetic Reference Field (IGRF 13th
1115 generation; Alken et al., 2020) the present core field is dominated to about
1116 93% by a dipole centered in the middle of the Earth and tilted with respect
1117 to Earth’s rotation axis, and to about 91% percent by an axial dipole, i.e. a
1118 dipole aligned with the rotation axis. For a purely axially aligned dipole field,
1119 the global dipole moment can be determined from a single intensity value
1120 and the latitude of the observation. For the moment of a tilted dipole, the

1121 inclination at the observation site is additionally required (see, e.g., Merrill
1122 et al., 1996). However, when non-dipole field contributions are present, any
1123 dipole moment values determined in this way are biased depending on the
1124 strength of the local non-dipole field. It is often assumed that non-dipole
1125 field contributions average out when enough individual VDMs or VADM are
1126 averaged in space and/or time, so that such an average V(A)DM is considered
1127 a valid approximation of the actual dipole moment (e.g., Merrill et al., 1996).
1128 However, the validity of this assumption is unclear and at least for short
1129 intervals or a strongly inhomogeneous global data distribution, the resulting
1130 averaged V(A)DM is likely biased.

1131 Several V(A)DM reconstructions from archaeomagnetic data (which also
1132 in general include volcanic data) span the past 10 to 50 kyr (McElhinny and
1133 Senanayake, 1982; Yang et al., 2000; Genevey et al., 2008; Knudsen et al.,
1134 2008; Valet et al., 2008; Usoskin et al., 2016). Genevey et al. (2008) showed
1135 that based on the ArcheoInt database, VADM or mixed VADM/VDM curves
1136 from Eurasia differ notably from curves for the rest of the world and they
1137 constructed global curves for the past 3 kyr using equally weighted regional
1138 curves to avoid biasing from a heterogeneous data distribution. Knudsen et al.
1139 (2008) used GEOMAGIA50 (version 1) for a VADM reconstruction over the
1140 past 50 kyr, in time windows increasing from 500 years for the past 4 kyr to
1141 4 kyr prior to 24 ka, and noted that field strength through the Holocene is
1142 higher than during the preceding 40 kyr.

1143 *4.2.2. History of archaeomagnetic field models*

1144 Although early attempts to construct global archaeomagnetic field models
1145 date back to the early 1970s (e.g., Márton, 1970; Braginskiy and Burlatskaya,

1146 1979), they have only received considerable attention over the past 20 years,
1147 when the data basis had become large enough to allow for more spatial de-
1148 tail and temporally continuous reconstructions. The recent history of purely
1149 archaeomagnetic field models is closely linked to models including palaeo-
1150 magnetic sediment records in addition to archaeomagnetic and also volcanic
1151 data. A surge of models spanning back to 2 to 12 ka followed the publication
1152 of Hongre et al. (1998). This includes a series of 100-year snapshot models for
1153 the past 3000 years by Constable et al. (2000), and its first continuous equiv-
1154 alent (Korte and Constable, 2003). Several recent reviews include overviews
1155 of all these models (Constable and Korte, 2015; Korte and Constable, 2018;
1156 Korte et al., 2019), and we focus on archaeomagnetic models (including vol-
1157 canic data, but no sediment records) in the following discussion.

1158 The first such models were ARCH3k.1 and ARCH3k.cst.1 (Korte et al.,
1159 2009) for the time interval 1000 BCE to 1990 CE. ARCH3k.1 was initially
1160 based on all available archaeomagnetic and volcanic data that the authors
1161 were aware of (9605 values), with iterative outlier rejection. ARCH3k.cst.1
1162 was based on a smaller data set (6211 values) with prior data selection, ex-
1163 cluding data with directional uncertainty $\alpha_{95} > 10^\circ$, intensity uncertainty
1164 $\sigma_{VADM} > 2 \times 10^{22} \text{ Am}^2$, and age uncertainty $\sigma_{Age} > 100 \text{ yr}$. Licht et al.
1165 (2013) presented model A_FM based on 9660 data, spanning 1000 BCE to
1166 2000 CE. Similar to the two ARCH3k models, this was part of a study
1167 comparing archaeomagnetic data only models to models including sediment
1168 records. A model derived with the main purpose of archaeomagnetic dating is
1169 SHA.DIF.14k (Pavón-Carrasco et al., 2014), spanning nearly the past 14 kyr
1170 based on 12779 data and following from a series of regional European mod-

1171 els by the same group (e.g., Pavón-Carrasco et al., 2009). ARCH10k.1 was
1172 derived mainly as a starting model for a reconstruction including sediment
1173 records for 8000 BCE to 1990 CE (Constable et al., 2016). A model with
1174 somewhat improved Southern Hemisphere data coverage due to recent efforts
1175 to improve the global data coverage and a data weighting scheme according
1176 to archaeomagnetic quality criteria, named SHAWQ2k, was presented by
1177 Campuzano et al. (2019). New modelling methods were explored for mod-
1178 els AmR, spanning 1200 BCE to 2000 CE in 40-year snapshots (Sanchez
1179 et al., 2016), COV-ARCH, a continuous model for the past 3 kyr (Hellio and
1180 Gillet, 2018), BIGMUDI4k.1, an iterative approach simultaneously inverting
1181 palaeomagnetic, archaeomagnetic and historical records for the past 4,000
1182 years (Arneitz et al., 2019), and a proof-of-concept model for the past 1000
1183 years (Mauerberger et al., 2020).

1184 *4.2.3. Range of modelling approaches*

1185 Most global geomagnetic field models, whether covering recent, historical,
1186 archaeo- or palaeomagnetic times, are based on series of spherical harmonic
1187 (SH) functions that are fit to the data by mathematical inversion techniques.
1188 The geomagnetic field is conveniently described by a series of coefficients
1189 that scale with field contributions that can be described by a (tilted) dipole,
1190 quadrupole, octupole and increasingly shorter wavelength parts. Moreover,
1191 when assuming that Earth’s mantle is electrically insulating, the SH represen-
1192 tation can be downward-continued to provide an image of the field morphol-
1193 ogy at the top of Earth’s outer core, the CMB. For continuous models over
1194 certain time intervals the coefficients are smoothly varying time-dependent
1195 functions, mostly based on cubic B-splines when constructing historical to

1196 millennial scale models (see, e.g., Korte and Constable, 2003; Korte et al.,
1197 2009).

1198 As a result of uncertainties in data and age (see section 3) a model cannot
1199 and should not fit all data exactly, and some form of smoothing constraint
1200 is implemented in the modelling. The simplest form is a truncation of the
1201 SH expansion at low degrees to limit the spatial variability of the model and
1202 a temporal parameterisation allowing only slow temporal changes. However,
1203 most modellers prefer a more flexible form of regularization, where the model
1204 parameterisation allows for more variability than expected to be resolved by
1205 the data, and the fit to the data is traded off against additional smoothness
1206 constraints in space and time.

1207 Methodological differences among most archaeo- and palaeomagnetic SH
1208 models mainly lie in the choice and strength of smoothing constraints, and
1209 the treatment of outlying data. Helliö and Gillet (2018) in a new approach
1210 used statistical information about geomagnetic field evolution from satellite
1211 and observatory observations in temporal cross-covariance functions as a con-
1212 straint in a Bayesian modelling frame. The method results in an ensemble
1213 of models with statistically coherent errors on the parameters. Arneitz et al.
1214 (2019) also used a Bayesian approach when directly combining archaeomag-
1215 netic data with historical observations.

1216 Two recent studies investigate new methods for snapshots in time as a
1217 step towards improved continuous models. Sanchez et al. (2016) use statis-
1218 tics from a numerical dynamo simulation as mean and covariance background
1219 constraints, which avoids subjective choices of regularization parameters and
1220 provides an improved understanding what global spatial resolution can be

1221 retrieved from the data. Mauerberger et al. (2020) implemented a Bayesian
1222 non-parametric approach, assuming the geomagnetic potential to be a Gaus-
1223 sian process rather than using SH basis functions. The method provides
1224 realistic regional model uncertainties depending on data distribution.

1225 New modelling approaches provide additional relevant information on
1226 model resolution and model uncertainties. Models in general agree for re-
1227 gions or parameters that are well constrained by data, as can be seen in the
1228 maps of Fig. 13 and Fig. 14, where the different models appear more similar
1229 (panels in a) and have smaller uncertainties (panels in b) in the Northern,
1230 than the Southern Hemisphere. This can also be seen in time series from
1231 Europe and South Africa, where there is a better agreement of the models
1232 for Paris (dense data) than South Africa (sparse data) (Fig. 15). Differences
1233 in the data basis, outlier treatment and how uncertainties are weighted have
1234 a stronger influence on the models than the method used (Sanchez et al.,
1235 2016; Korte and Constable, 2018). When creating a field model (and assess-
1236 ing site dependent output), the underlying data basis should be considered,
1237 especially how well a model is constrained for a certain region and time or
1238 for a certain purpose. Moreover, all available models are smoothed represen-
1239 tations of the actual field variability in both space and time. The amplitudes
1240 of rapid field changes in field models are not fully resolved and are likely
1241 underestimated.

1242 *4.2.4. Influence of data selection and distribution on global models*

1243 Data selection, weighting and distribution have a significant influence on
1244 the output of global models. Data selection follows two philosophies. The
1245 first is to use all available data without any prior selection, hoping that the

1246 signal to noise ratio will increase with the number of available data. The sec-
1247 ond philosophy is to make a prior data selection by imposing a set of quality
1248 criteria. This makes sense when the quality of the data is well understood
1249 and the information is available in global databases, e.g., studies from France
1250 (Le Goff et al., 2020) or the Levant (Shaar et al., 2016, 2020). However, this
1251 is currently not the case in many other regions of the world, where results are
1252 sparse and/or many of the results have been obtained decades ago, before
1253 some of the modern laboratory methods and tests providing modern quality
1254 criteria existed. It is worth noting that Korte et al. (2009) performed a com-
1255 parison of models with and without prior data selection based on data and
1256 dating uncertainties and found no notable improvement when data selection
1257 was imposed.

1258 Well distributed global data are the most relevant ingredient for an overall
1259 good global model. Recent models providing improved uncertainty estimates
1260 (Sanchez et al., 2016; HELLIO and Gillet, 2018; Mauerberger et al., 2020) quan-
1261 tify what has been qualitatively stated before (Korte et al., 2009): with the
1262 presently available data distribution (more precisely the scarcity of Southern
1263 Hemisphere data) archaeomagnetic field models provide limited information
1264 about the Southern Hemisphere geomagnetic field.

1265 In Fig. 13 and Fig. 14 we show intensity at Earth’s surface and the radial
1266 field at the CMB for one snapshot in time. Models based on archaeomagnetic
1267 (and volcanic) data (ARCH10k.1, SHAWQ2k, AmR and COV-ARCH) and
1268 archaeomagnetic, volcanic and sediment data (CAL10k.2; Constable et al.,
1269 2016) and (COV-LAKE; HELLIO and Gillet, 2018) can produce models with
1270 some broad similarities in intensity at Earth’s surface and radial field for

1271 the Southern Hemisphere, e.g., lower intensity patches extending across the
1272 Indian Ocean and southern Atlantic ocean. However, the precise locations
1273 and morphologies of intensity and radial field patches are different. This
1274 can be seen in the model COV-LAKE, which incorporates sediment data
1275 and includes more Southern Hemisphere data than its counterpart archaeo-
1276 magnetic model (COV-ARCH); the use of sediment data results in different
1277 global intensity and radial field morphologies. Using sediment data in ad-
1278 dition to archaeomagnetic data, but applying the same modelling approach,
1279 (e.g., COV-ARCH and COV-LAKE), results in reduced uncertainties on the
1280 model output for the Southern Hemisphere (Fig. 13b).

1281 The lack of Southern Hemisphere data was explicitly considered by earlier
1282 versions of the SHA.DIF.14k model, which were European models based on
1283 regional rather than global basis functions (Pavón-Carrasco et al., 2010). Few
1284 archaeomagnetic (and volcanic) data in the Southern Hemisphere highlight
1285 the importance of using sediment records from the Southern Hemisphere to
1286 constrain the field in this region. Several other models (not discussed in detail
1287 here) mitigate the problem by including high resolution (mainly lacustrine)
1288 sediment records (see Constable and Korte (2015) and Korte et al. (2019)
1289 for reviews of these).

1290 *4.2.5. Major findings*

1291 The main applications of purely archaeomagnetic models are for dating
1292 purposes and for the calibration of relative intensities obtained from sedi-
1293 ments. The advantage of models over regional reference curves for archaeo-
1294 magnetic dating lies in that models can generate directional and intensity
1295 curves for any location without the need for re-location of data. Pavón-

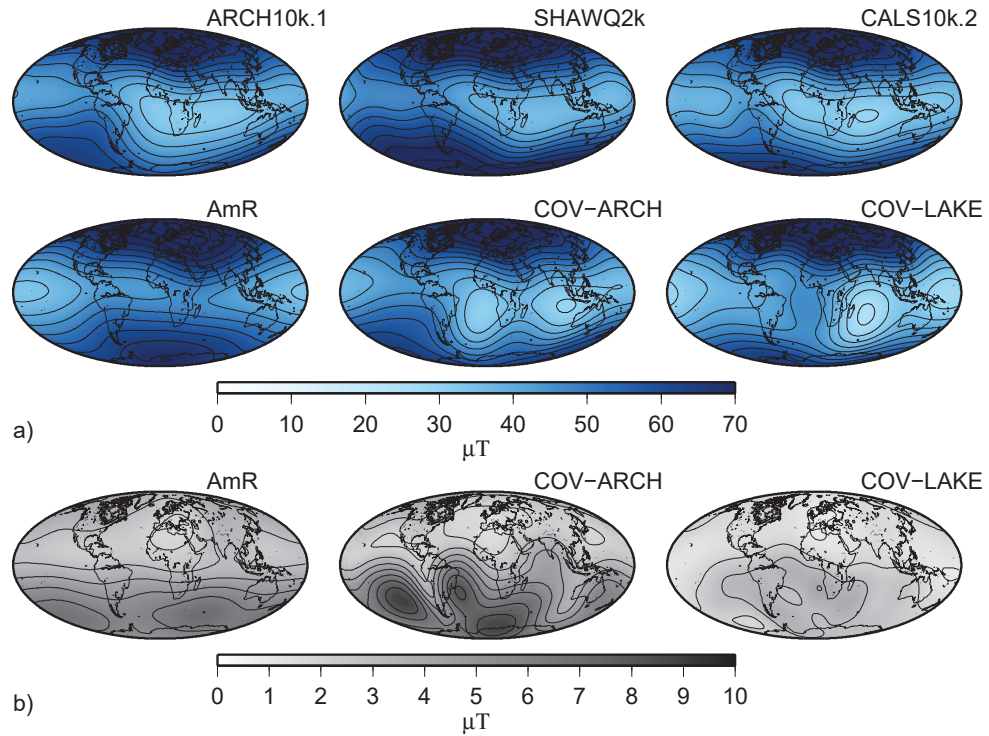


Figure 13: (a) Maps of intensity at Earth's surface at 900 CE from six global field models: ARCH10k.1 (Constable et al., 2016), SHAWQ2K (Campuzano et al., 2019), CALS10k.2 (Constable et al., 2016), AmR (Sanchez et al., 2016), and COV-ARCH and COV-LAKE (Hellio and Gillet, 2018). (b) Maps of intensity uncertainty for AmR, COV-ARCH and COV-LAKE.

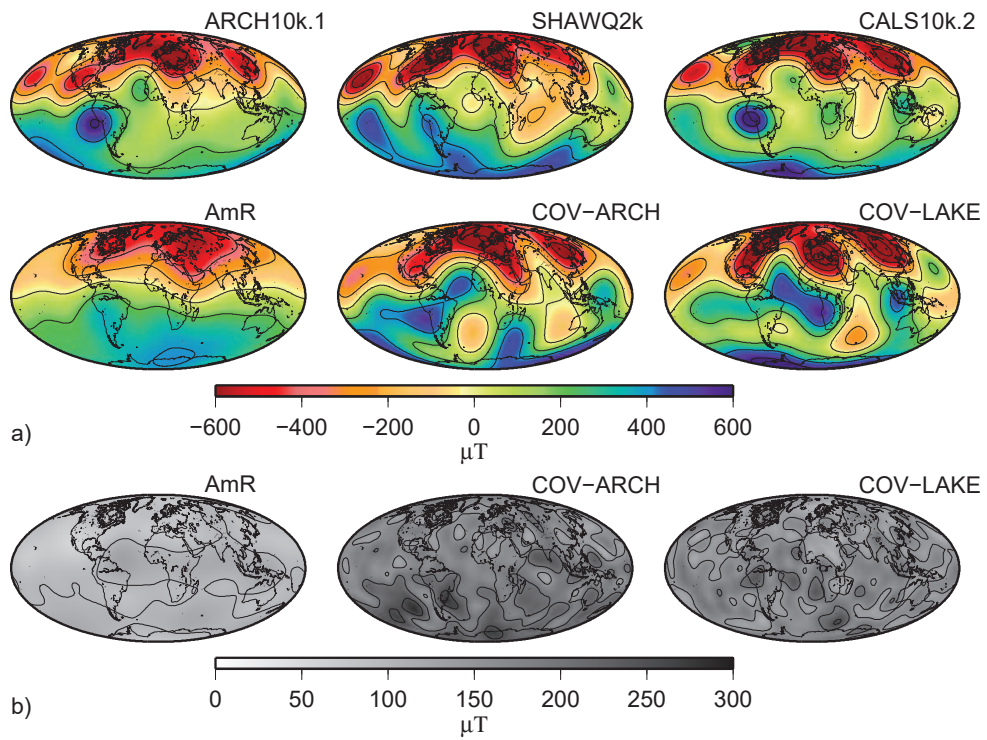


Figure 14: Maps of (a) the radial field (B_r) and (b) its uncertainty for the core-mantle boundary at 900 CE for different field models. See Fig. 13 for model references.

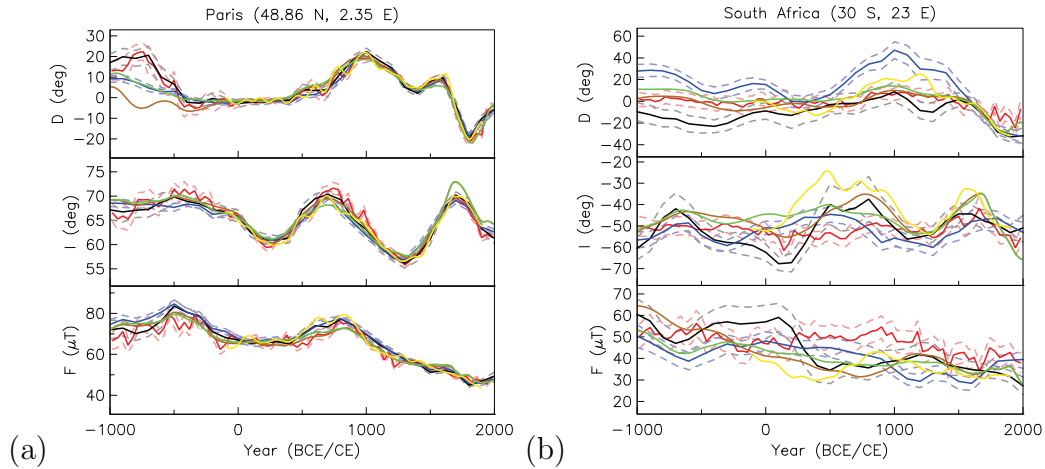


Figure 15: Time series of magnetic declination (D , top panels), inclination (I , middle panels) and intensity (F , bottom panels) for the past 3000 years at two locations as predicted by six different global magnetic field models. All models agree closely most of the time for Paris, where data coverage is good (a), whereas notable differences exist for South Africa, where there are limited data (b). The included models are the archaeomagnetic models ARCH10k.1 (brown), SHAWQ2k (yellow), AmR (red) and COV-ARCH (black), and the two models additionally including sediment records CALS10k.2 (green) and COV-LAKE (blue). We note that owing to the regularization applied in global modelling, all curves are reduced in temporal resolution in comparison to regional curves, e.g., intensity curves for Paris (Livermore et al., 2018).

1296 Carrasco et al. (2011) presented a convenient Matlab tool to obtain age
1297 probability density functions from any combination of declination, inclina-
1298 tion and intensity data. Estimated age ranges tend to be smaller if more
1299 than one field component is available. A range of published field models and
1300 reference curves are implemented in the published version of the tool, and
1301 additional ones can be incorporated by the user.

1302 As absolute field strength cannot be retrieved from sediments, archaeolog-
1303 ical materials and volcanic rocks are the only sources available for obtaining
1304 palaeointensity. Based on our current compilation of archaeomagnetic data,
1305 both dipole moment reconstructions and global models show that the dipole
1306 moment was high around 2 to 3 ka and greater than today’s field (e.g., Con-
1307 stable and Korte, 2015). The Holocene maximum seems high compared to
1308 the preceding 40 kyr, as noted by Knudsen et al. (2008) and the long-term
1309 palaeomagnetic average (Tauxe, 2006; Yamamoto and Tsunakawa, 2005).
1310 Geomagnetic intensity spikes, on the other hand, might be linked to strong
1311 dipole moment variations (Korte and Constable, 2018; Hervé et al., 2021),
1312 but their origin is not fully understood.

1313 Studies of global field characteristics, such as symmetry (e.g., Consta-
1314 ble et al., 2016) or the field morphology at the CMB (Dumberry and Finlay,
1315 2007; Nilsson et al., 2020), with relevance for the theoretical understanding of
1316 the geodynamo, are preferably based on models including sediment records,
1317 which provide improved data coverage, in particular for the Southern Hemi-
1318 sphere. Asymmetries seen in the modern field have been found to persist
1319 over at least 10 kyr: the field is weaker, but more variable on average in the
1320 Southern Hemisphere compared with the Northern Hemisphere, and secular

1321 variation tends to be stronger in the Atlantic and Indian Oceans compared
1322 with the Pacific (Constable et al., 2016). Although the magnetic flux mor-
1323 phology at the CMB changes notably with time, there are preferred or recur-
1324 rent long-term patterns evident in time-averaged models, in particular nearly
1325 symmetrical patches of intense flux at high latitudes in both hemispheres (for
1326 more details see, e.g., Amit et al. (2011) and the review by Constable and Ko-
1327 rte (2015)). Terra-Nova et al. (2017) more recently found recurring positions,
1328 but no preferred direction of motion and some correlation of flux evolution
1329 with lower mantle heterogeneities, supporting hypotheses of mantle control
1330 on the geodynamo (Bloxham and Gubbins, 1987; Bloxham, 2002). Although
1331 both westward and eastward azimuthal flow motions seem to occur in the
1332 core over archaeomagnetic times (Dumberry and Finlay, 2007; Wardinski and
1333 Korte, 2008), recent studies show a clear dominance of westward drift, with
1334 rates between $0.07^\circ/\text{yr}$ (Nilsson et al., 2014, 2020) and $0.25^\circ/\text{yr}$ (Hellio and
1335 Gillet, 2018; Nilsson et al., 2020).

1336 The South Atlantic Anomaly (SAA) is an area stretching from southern
1337 Africa over the Atlantic to South America where the geomagnetic field in-
1338 tensity is notably lower than at comparable latitudes. It is known to have
1339 deepened and moved westward from about 1700 onwards from historical data
1340 (Mandea et al., 2007; Hartmann et al., 2009). It is linked to the growth of
1341 patches of reversed flux at the CMB in the Southern Hemisphere (Gubbins
1342 and Bloxham, 1987; Terra-Nova et al., 2016) and has been discussed as a
1343 trigger for geomagnetic field reversals (Gubbins and Bloxham, 1987; Tar-
1344 duno et al., 2015). A unique connection to reversals is unclear as recent
1345 modelling of the field for times prior to the Holocene (Brown et al., 2018;

1346 Panovska et al., 2019) suggests that features similar to the SAA maybe re-
1347 current and do not necessarily lead to reversals. It is of great interest to
1348 know the longevity of the SAA, and whether it is a recurrent feature of
1349 the field, as it may be linked to structures at the CMB that influence core
1350 flow and hence geomagnetic field generation (Tarduno et al., 2015; Tarduno,
1351 2018). SHAWQ2k and other models indicate that reverse flux appeared in
1352 the Southern Hemisphere as early as 900 CE east of Africa and evolve into
1353 the SAA (Campuzano et al., 2019) (Fig. 14).

1354 5. Future challenges

1355 Challenges for the future include addressing current inadequacies in the
1356 GEOMAGIA50 database, how to improve the temporal and spatial distribu-
1357 tion of archaeomagnetic data, and advances in geomagnetic field modelling.

1358 5.1. GEOMAGIA50

1359 In previous sections we outlined some of the issues in using data from GE-
1360 OMAGIA50 for modelling purposes; especially for data selection. One chal-
1361 lenge is to homogenize the definition of intensity uncertainties (section 3.1.7)
1362 or at least indicate how it was calculated in a new database field. Further-
1363 more, a large number of directional entries are missing k values and some
1364 are missing α_{95} . All entries lacking these data need to be reassessed and the
1365 data added if missing; however, it is likely, especially for k , that the values
1366 were not given in the original publications.

1367 A major deficiency in GEOMAGIA50 is the treatment of chronological
1368 metadata and we outline these issues and possible solutions in section 5.1.1.
1369 The definition of numbers of samples and specimens also require greater

1370 clarification, because they can differ for displaced and in-situ archaeological
1371 materials, and for lava flows (section 5.1.2).

1372 Keeping the database up-to-date and useful for the scientific community
1373 remains a challenge. Given limited resources, it is not feasible to release a new
1374 update of the database when each new archaeomagnetic study is published.
1375 Instead over coming years, we intend to release an update at the end of
1376 each year containing all the new studies published that year. We note, for
1377 example, that the recent studies of Shaar et al. (2020) and Troyano et al.
1378 (2020) have yet to be included in version 3.4. of the database, but will be
1379 available in the 2021 release.

1380 *5.1.1. Archival of chronological data*

1381 Section 3.2.3 highlighted how complex the estimation of age uncertainties
1382 can be. All methods have caveats and the reliability of the age information is
1383 intimately linked to knowledge of the archaeological context. It is a difficult
1384 task to develop a hierarchy of dating methods and deduce/calculate dates,
1385 while preserving the complexity of the dating process in the database. This
1386 may only be partly achievable in future revisions to the database. It requires
1387 more metadata which de facto increases the complexity of the database and
1388 its searchability. Ideally, additional fields could be added to GEOMAGIA50
1389 giving more specific age information that could be used to sieve data for
1390 model or curve construction. However, owing to the range and complexity of
1391 dating methods, this is impractical. An alternative would be to add an ac-
1392 companying text field to each entry describing the chronological controls, e.g.
1393 the cultural name or period and a short description of the dating results (as
1394 is given in ArcheoInt database (Genevey et al., 2008)). This approach would

1395 not allow automatic data selection and would require manual assessments of
1396 the quality of data prior to modelling. Such functionality is not currently
1397 available and would require the assessment of all articles in GEOMAGIA50.

1398 Although attempts at incorporating greater radiocarbon information were
1399 made in version 2 of the database, there are numerous complications to suc-
1400 cessful implementation. Radiocarbon dates are currently entered in accor-
1401 dance with information provided in published articles, but not consistently
1402 and sometimes ambiguously. Ages maybe calibrated or not and calibrated
1403 dates can be reported with symmetrical or asymmetrical bounds (reflecting
1404 the calibrated age's non-gaussian distribution) and at 68 or 95% confidence.
1405 It is not always clear at what level uncertainty is reported.

1406 Calibration can result in significant shifts in age. It is therefore important
1407 that calibration is clearly documented. As the database stands, there are still
1408 uncalibrated ages that are used for the date of an entry. An initial goal will
1409 be to reexamine all the uncalibrated ages and, if there is enough information
1410 available, calibrate those ages. As noted in section 3.2, uncalibrated ages are
1411 just one of a number of methods that may have been used at a site, e.g., un-
1412 calibrated ages may have been combined with archaeological ages or relative
1413 stratigraphic ages. In these cases, the dates can not be simply recalibrated,
1414 as the radiocarbon ages may form only one aspect of the structural frame-
1415 work for the stratigraphy. This requires that every paper with radiocarbon
1416 ages is reexamined in detail to see what scope there is for age re-evaluation.

1417 Documenting calibration of radiocarbon dates is also problematic. GEO-
1418 MAGIA50 contains studies from the 1960s onwards and numerous improve-
1419 ments have been made in calibration methods since this time and new cali-

1420 bration curves are published every few years (e.g. Reimer et al., 2013, 2020)
1421 (section 3.2.2). Therefore, there are likely some differences in field varia-
1422 tions that are not geomagnetic in origin, but rather they relate to changes
1423 in calibration curves. Although there is minimal revision for the past 10,000
1424 years between the generations of calibration curves since 1998 (boundaries
1425 of the 95% intervals of date are generally modified by 5-10 years at the
1426 most), calibrated ages can be shifted up to several centuries for older periods
1427 (Reimer et al., 2020). Even if changes are small, radiocarbon ages should
1428 be recalibrated to keep them mutually consistent and to remove differences
1429 in field variations that stem from non-geomagnetic origins. At a minimum,
1430 the experimental radiocarbon ages should be reported accompanied by the
1431 calibration method.

1432 The uncertainties on calibrated ages are not treated ideally in the database.
1433 Currently only \pm uncertainties are given. Although this allows asymmetric
1434 uncertainties, i.e. the maximum and minimum ages at two standard devia-
1435 tions resulting from calibration, there is no way to record the full multi-modal
1436 probability distribution of a calibrated age. This is a significant limitation
1437 of the database, as it is important to take into account the irregular shape
1438 of the probability density function of calibrated radiocarbon dates in geo-
1439 magnetic modelling and regional secular variation curves (e.g., Hellio et al.,
1440 2014; Lanos, 2004; Hervé and Lanos, 2018; Tema et al., 2017; Yutsis-Akimova
1441 et al., 2018a). Systematically storing uncalibrated ages (when available) and
1442 updating all radiocarbon ages and uncertainties after calibration is a major
1443 undertaking, but is an aim for the future.

1444 *5.1.2. Clarification of site-sample-specimen hierarchy*

1445 Reporting of the number of samples and specimens used for directional
1446 and intensity analysis requires evaluation. The database aims to follow the
1447 standard palaeomagnetic hierarchy, whereby each entry in the database is
1448 considered to be a site, a group of data related to a geological unit or archae-
1449 ological context that has a unique age. A sample is treated as part of the site
1450 that was removed for further analysis. A specimen is a subdivision of a sam-
1451 ple and it is this that palaeomagnetic or archaeomagnetic measurements are
1452 made on. In palaeomagnetism, this hierarchy works well. A site would be,
1453 e.g., a lava flow; a sample, a palaeomagnetic core drilled out of the lava flow;
1454 and a specimen, the subdivision of the sample (core) that was measured and
1455 the directional or intensity data were obtained from. The number of sam-
1456 ples and specimens maybe similar, e.g., if one specimen was taken from each
1457 sample or the number of specimens could be more if multiple specimens were
1458 measured from a sample. In this case, the specimen numbers are averaged to
1459 give a sample mean and it is always the sample mean and number of samples
1460 that are used to calculate the site mean direction.

1461 In archaeointensity studies this may work differently. For example, a
1462 piece of pottery may be related to an instance in time, but might not belong
1463 to a context with other pieces of pottery of the same age (a context being a
1464 site, analogous, e.g., to a lava flow). In this case the piece of pottery could
1465 be treated as both a site or a sample. The piece of pottery can be further
1466 divided for measurement and these divisions could be considered to be either
1467 samples or specimens. If the piece of pottery were treated as if it were to
1468 belong to a context with many other pieces of pottery, then it is just one

1469 sample of possibly many, therefore the number of samples would be one and
1470 there would be multiple specimens. If the piece of pottery is treated as a
1471 site, then the number of samples would be multiple and equal to the number
1472 of specimens.

1473 Both approaches have their advantages, depending on how the data are
1474 to be used or from a consistency point of view (rigid use of the site, sam-
1475 ple, specimen hierarchy). For example, obtaining multiple measurements of
1476 intensity from a piece of pottery can provide an accurate mean intensity de-
1477 termination, valuable for secular variation or curve construction. This would
1478 require that the piece of pottery is treated as a site and that the number of
1479 specimens is treated as the number of samples. In the database, the number
1480 of archaeointensity measurements used for the mean value is therefore treated
1481 in the same way as the number of samples from, e.g., a lava flow: they would
1482 have equal value. However, this leads to a mismatch in how different ar-
1483 chaeological entries may be treated in the database (e.g., an in-situ structure
1484 versus a piece of pottery) and between archaeological and palaeomagnetic
1485 hierarchies, e.g., a lava flow would no longer be equal to a context, if the
1486 piece of pottery becomes the site. Treating a single artefact as belonging to
1487 a single context, regardless of whether there are other artefacts maintains the
1488 logic of the hierarchy, but may result in data not being included in further
1489 analyses if the number of samples is listed as one, e.g., if the data are filtered
1490 by the number of samples.

1491 The fact that there is no common system of hierarchy is a current weak-
1492 ness of the database. In the future, we propose (as in ArcheoInt) that N
1493 corresponds to the number of thermal units, i.e. the number of units that

1494 can be considered to have been magnetized at the same time. It is fixed to
1495 1 for a lava flow, an archaeological in-situ structure and a single fragment of
1496 pottery, or is higher than 1 for a group of baked clay fragments. A second
1497 number, n , would be the number of individual values from which the average
1498 and its uncertainty are calculated. Because the averages are not calculated
1499 homogeneously between data entries, either at the sample level or the speci-
1500 men level, this solution has the disadvantage to mix samples and specimens,
1501 but it would clearly make it easier for data selection.

1502 *5.2. Improvements in data distribution*

1503 As noted in Section 4.2.4 the most important factor in improving global
1504 models and our overall understanding of the global archaeomagnetic field
1505 is more data from regions with sparse data distributions. With $\sim 50\%$ of
1506 all data coming from Europe (Section 2.3), there is significant room for im-
1507 proving data coverage. Africa is a clear target given its large area and rich
1508 archaeological history. Studies on Burkina Faso, Ivory Coast, Mali, Ethiopia,
1509 Kenya, Zimbabwe and South Africa over the past 10 years have made sig-
1510 nificant steps in improving data coverage. However, an increased emphasis
1511 should be placed on developing archaeomagnetic research projects in Africa.
1512 Similarly, South America is well positioned to provide useful data. Data from
1513 both southern Africa and South America will be key to unraveling the long
1514 term evolution of the South Atlantic Anomaly. The Indian subcontinent has
1515 a rich archaeological history and yet no archaeomagnetic directional data
1516 have been produced. Given its unique position, new directional data could
1517 aid in understanding of westward drift of the field across the Indian Ocean.
1518 Australia, New Zealand and Pacific islands also have the potential to provide

1519 further archaeomagnetic data. This would be especially valuable as it could
1520 improve our understanding of field variations in the Southern Hemisphere
1521 and the Pacific, which are greatly lacking in data. It would be interesting
1522 to investigate/confirm the persistence of lower field variability in the west-
1523 ern Pacific (Constable et al., 2016). Finally, the large amount of Japanese
1524 directional data not in the database should be added. There are hundreds
1525 of entries in this data set and it will be of great interest to see how this
1526 influences our understanding of field evolution in eastern Asia.

1527 Acquiring data in regions with few data presents practical challenges. Ac-
1528 cess to in-situ structures is crucial for full vector studies. However, sampling
1529 must take place shortly after excavation and this is not always practical.
1530 In most countries archaeomagnetists are limited by several constraints (e.g.,
1531 travel, time, funding, and export licences). This explains why the spatial
1532 distribution of directions is fairly close to palaeomagnetic laboratories, as
1533 is the case with Europe. A solution would be to develop local laboratories
1534 and/or networks of researchers trained in archaeomagnetic sampling, as well
1535 as to collaborate with and train local archaeologists. However, such efforts
1536 take time to implement, so we may only see a gradual increase in the amount
1537 of data from poorly represented areas.

1538 Another aspect of improving the data distribution is to extend the database
1539 further back in time through the Iron Age, Bronze Age and the Neolithic.
1540 There is a tendency to focus on more dramatic field changes, e.g., spikes in
1541 intensity during the transition from the Iron to Bronze age in the Levant and
1542 surrounding areas; however, all times (or “quiet times”) are equally valuable
1543 to study, as all field variations relate to the underlying geodynamo process.

1544 Furthermore, more detailed descriptions of field evolution through time will
1545 allow for the development of more accurate archaeomagnetic dating curves.

1546 A consideration of the types of archaeological materials used to extend
1547 our knowledge of field variations to older times is also required. Baked clays
1548 are less frequent back through time, as are in situ structures, which are more
1549 likely to suffer eventual post-displacements. The baking degree of older clay-
1550 based materials is also usually lower, resulting in a less stable mineralogy
1551 prone to alteration and therefore less favourable for obtaining archaeoin-
1552 tensity results. Increasing the success rate of archaeointensity experiments
1553 on such materials is a major challenge that could be overcome in the next
1554 decade by new approaches, such as scanning magnetometry and computed
1555 tomography (de Groot et al., 2018). Furthermore, a better understanding of
1556 the magnetic mineralogy of archaeological materials will aid in this research
1557 (e.g., Lopez-Sanchez et al., 2020). To recover intensity variations in the early
1558 Holocene or even in the Pleistocene prior to apparition of ceramic produc-
1559 tion, an alternative to baked clays is the study of heated rock artefacts, such
1560 as burnt cherts (Kapper et al., 2014; Zeigen et al., 2019).

1561 Beyond the acquisition of data for older periods and/or for regions that
1562 are still poorly documented, an important challenge in archaeomagnetism
1563 remains to better understand the issue of data dispersion. Dispersion is
1564 characteristic for many data sets and hinders our ability to finely trace geo-
1565 magnetic field variations through time. Besides age uncertainty, the sources
1566 of dispersion are more numerous for intensity data (undetected alteration,
1567 MD effects, uncorrected TRM anisotropy and cooling rate) than for direc-
1568 tions. One major issue is the cooling rate correction because its absence

1569 can potentially result in a systematic overestimation. One could think to
1570 apply a correction factor to uncorrected data. On average, the correction
1571 factor seems to be 5-10% (Genevey et al., 2008). However, defining a suit-
1572 able rate of correction is difficult, because it depends on the specific rock
1573 magnetic properties of a specimen and the equipment and protocols used in
1574 each laboratory.

1575 Furthermore, what is the precision with which the direction and/or in-
1576 tensity of the geomagnetic field can be retrieved? Does dispersion reflect
1577 our current limitations in the acquisition of data? To better constrain these
1578 questions, one can ask whether there would be an interest in revisiting re-
1579 gions with a good data coverage and an active archaeological research, in
1580 order to acquire new precisely dated data, for example from the past few
1581 centuries where chronological constraints can be extremely tight. By limit-
1582 ing the influence of age uncertainties, this could help solve the above issues,
1583 which are crucial in using archaeomagnetism for archaeological purposes and
1584 for refining our knowledge of the evolution of the geomagnetic field.

1585 *5.3. Global geomagnetic field modelling*

1586 From a field modelling point of view, the above-mentioned improvements
1587 to the underlying data basis are paramount for improving the temporal res-
1588 olution and full global spatial reliability of models. Both these aspects are
1589 relevant when using field models to infer geodynamo processes in the core,
1590 or when using their predictions for regional reference curves. As noted in
1591 section 4.2.4, the lack of archaeomagnetic data in the Southern Hemisphere
1592 and equatorial areas can be partly compensated for by using sediment data.
1593 Similarly, a recently renewed interest in speleothems may produce new high

1594 resolution time series for the Holocene in the coming years from locations
1595 where it is not possible to obtain archaeological or sediment data. Lascu
1596 and Feinberg (2011) give a detailed overview of the potential for speleothems
1597 to recover detailed field variations, with the study of Trindade et al. (2018)
1598 providing a detailed Holocene record from Brazil and other studies resolv-
1599 ing other geomagnetically interesting times in great detail (e.g., Lascu et al.,
1600 2016; Chou et al., 2018).

1601 Continuing the efforts to improve the treatment of data and dating errors
1602 and translating them into realistic model errors through methodological de-
1603 velopments is also of interest for both these cases. Improved global archaeo-
1604 magnetic field models may contribute to answering open questions about,
1605 e.g., the maximum possible rate of geomagnetic field change and the influ-
1606 ences of lowermost mantle structure on the geodynamo (which is reflected in
1607 magnetic field morphology). They will also likely contribute to improved pre-
1608 dictions of future geomagnetic field evolution by assimilation of data-based
1609 models into numerical simulations (e.g., Fournier et al., 2010; Tangborn and
1610 Kuang, 2018).

1611 **Acknowledgments**

1612 We thank the archaeomagnetic community for providing data when re-
1613 quested, especially Elisabeth Schnepf, Patrick Arneitz and Mary Kovacheva.
1614 We acknowledge Fabio Donadini, Kimo Korhonen and Lauri Pesonen for
1615 the development and design of GEOMAGIA50. GH was supported by the
1616 Labex LsScArBx (Bordeaux Archaeological Sciences Labex, ANR-10-LABX-
1617 52). Development of GEOMAGIA50 was supported by DFG SPP-1488. This

1618 is Institute for Rock Magnetism contribution 2008.

1619 **References**

- 1620 Aidona, E., Polymeris, G., Kondopoulou, D., Spassov, S., Raptis, K., 2021.
1621 Archaeomagnetism and luminescence on Late Byzantine kilns in Thessa-
1622 loniki (N. Greece): Implications for geomagnetic field variations during the
1623 last two millennia. *Phys. Earth Planet. Inter.* 316, 106709.
- 1624 Aitken, M., Hawley, H., 1970. Archaeomagnetism: evidence for magnetic
1625 refraction in kiln structures. *Archaeometry* 13, 83–85.
- 1626 Aitken, M. J., 1985. Thermoluminescence dating. Academic Press.
- 1627 Aitken, M. J., 2014. Science-Based Dating in Archaeology. Longman Archae-
1628 ology Series. Routledge.
- 1629 Aitken, M. J., Alcock, P. A., Bussel, G. D., Shaw, C. J., 1981. Archaeo-
1630 magnetic determination of the past geomagnetic intensity using ancient
1631 ceramics: Allowance for anisotropy. *Archaeometry* 23 (1), 53–64.
- 1632 Aitken, M. J., Allsop, A. L., Bussell, G. D., Winter, M. B., 1988. Determi-
1633 nation of the intensity of the Earth’s magnetic field during archaeological
1634 times: Reliability of the Thellier technique. *Reviews of Geophysics* 26 (1),
1635 3–12.
- 1636 Aitken, M. J., Allsop, A. L., Bussell, G. D., Winter, M. B., 1989. Geomag-
1637 netic intensity variation during the last 4000 years. *Phys. Earth Planet.*
1638 *Inter.* 56 (1), 49 – 58.

- 1639 Aitken, M. J., Hawley, H. N., 1966. Magnetic dating-III: further archaeomag-
1640 netic measurements in Britain. *Archaeometry* 9, 187–199.
- 1641 Aitken, M. J., Weaver, G. H., 1962. Magnetic dating: Some archaeomagnetic
1642 measurements in Britain. *Archaeometry* 5 (1), 4–18.
- 1643 Aitken, M. J., Weaver, G. H., 1965. Recent archaeomagnetic results in Eng-
1644 land. *J. Geomag. Geoelectr.* 17, 391–394.
- 1645 Alken, P., Thébault, E., Beggan, C. D., Amit, H., Aubert, J., Baerenzung,
1646 J., Bondar, T. N., Brown, W., Califf, S., Chambodut, A., Chulliat, A.,
1647 Cox, G., Finlay, C. C., Fournier, A., Gillet, N., Grayver, A., Hammer,
1648 M. D., Holschneider, M., Huder, L., Hulot, G., Jager, T., Kloss, C., Korte,
1649 M., Kuang, W., Kuvshinov, A., Langlais, B., Léger, J. M., Lesur, V.,
1650 Livermore, P. W., Lowes, F. J., Macmillan, S., Mound, J. E., Nair, M.,
1651 Nakano, S., Olsen, N., Pavón-Carrasco, F. J., Petrov, V. G., Ropp, G.,
1652 Rother, M., Sabaka, T. J., Sanchez, S., Saturnino, D., Schnepf, N. R.,
1653 Shen, X., Stolle, C., Tangborn, A., Tffner-Clausen, L., Toh, H., Torta,
1654 J. M., Varner, J., Vervelidou, F., Vigneron, P., Wardinski, I., Wicht, J.,
1655 Woods, A., Yang, Y., Zeren, Z., Zhou, B., 2020. International Geomagnetic
1656 Reference Field: the thirteenth generation. Accepted to *Earth Planets and*
1657 *Space*.
- 1658 Amit, H., Korte, M., Aubert, J., Constable, C., Hulot, G., 2011. The time-
1659 dependence of intense archeomagnetic flux patches. *J. Geophys. Res.* 116,
1660 B12106.
- 1661 Arneitz, P., Egli, R., Leonhardt, R., Fabian, K., 2019. A Bayesian iterative

- 1662 geomagnetic model with universal data input: Self-consistent spherical
1663 harmonic evolution for the geomagnetic field over the last 4000 years. *Phys.*
1664 *Earth Planet. Inter.* 290, 57–75.
- 1665 Arneitz, P., Leonhardt, R., Schnepf, E., Heilig, B., Mayrhofer, F., Kovacs,
1666 P., Hejda, P., Valach, F., Vadasz, G., Hammerl, C., Egli, R., Fabian,
1667 K., Kompein, N., 2017. The HISTMAG database: combining historical,
1668 archaeomagnetic and volcanic data. *Geophys. J. Int.* 210 (3), 1347–1359.
- 1669 Athavale, R. N., 1966. Intensity of the geomagnetic field in India over the
1670 past 4000 years. *Nature* 210, 1310–1312.
- 1671 Athavale, R. N., 1969. Intensity of the geomagnetic field in prehistoric Egypt.
1672 *Earth Planet. Sci. Lett.* 6, 221–224.
- 1673 Basavaiah, N., Deenadayalan, K., Babu, J. M., Kanu, M., Kumar, K. N.,
1674 Demudu, G., Rao, K. N., Mallikarjunarao, N., 2019. Last 3000 years of
1675 geomagnetic field intensity from India: New reference palaeointensity data
1676 from two east coast archaeological sites and archaeomagnetic dating in-
1677 sights. *Journal of Archaeological Science: Reports* 27, 101943.
- 1678 Batt, C., Meng, Z., Noël, M., 1998. New archaeomagnetic studies near Xian,
1679 China. *Archaeometry* 40 (1), 169–175.
- 1680 Batt, C. M., Brown, M. C., Clelland, S.-J., Korte, M., Linford, P., Outram,
1681 Z., 2017. Advances in archaeomagnetic dating in Britain: New data, new
1682 approaches and a new calibration curve. *Journal of Archaeological Science*
1683 85, 66–82.

- 1684 Belshé, J. C., Cook, K., Cook, R. M., 1963. Some archaeomagnetic results
1685 from Greece. *The Annual of the British School at Athens* 58, 813.
- 1686 Ben-Yosef, E., Millman, M., Shaar, R., Tauxe, L., Lipschits, O., 2017. Six
1687 centuries of geomagnetic intensity variations recorded by royal Judean
1688 stamped jar handles. *Proceedings of the National Academy of Sciences*
1689 114 (9), 2160–2165.
- 1690 Ben-Yosef, E., Tauxe, L., Levy, T. E., Shaar, R., Ron, H., Najjar, M., 2009.
1691 Geomagnetic intensity spike recorded in high resolution slag deposit in
1692 Southern Jordan. *Earth Planet. Sci. Lett.* 287 (3), 529–539.
- 1693 Bloxham, J., 2002. Time-independent and time-dependent behaviour of high-
1694 latitude flux bundles at the core-mantle boundary. *Geophys. Res. Lett.* 29,
1695 1854.
- 1696 Bloxham, J., Gubbins, D., 1985. The secular variation of Earth’s magnetic
1697 field. *Nature* 317, 777–781.
- 1698 Bloxham, J., Gubbins, D., 1987. Thermal core-mantle interactions. *Nature*
1699 325, 511–513.
- 1700 Bloxham, J., Jackson, A., 1992. Time-dependant mapping of the magnetic
1701 field at the core-mantle boundary. *J. Geophys. Res.* 97, 19537–19563.
- 1702 Bowen, P., Ranck, H., Scarlett, T., Drelich, J., 1971. Rehydra-
1703 tion/rehydroxylation kinetics of a reheated XIX-Century Davenport
1704 (Utah) ceramic. *J. Am. Ceram. Soc.* 94, 2585–2591.

- 1705 Bowles, J., Gee, J., Hildebrand, J., Tauxe, L., 2002. Archaeomagnetic in-
1706 tensity results from California and Ecuador: evaluation of regional data.
1707 Earth Planet. Sci. Lett. 203 (3), 967–981.
- 1708 Braginskiy, S. I., Burlatskaya, S. P., 1979. Spherical analysis of the geomag-
1709 netic field based on archaeomagnetic data. *Izv. Earth Phys.* 15, 891–895.
- 1710 Bronk Ramsey, C., 2009. Bayesian analysis of radiocarbon dates. *Radiocar-*
1711 *bon* 51, 337–360.
- 1712 Brown, M., Korte, M., Holme, R., Wardinski, I., Gunnarson, S., 2018.
1713 Earth’s magnetic field is probably not reversing. *Proceedings of the Na-*
1714 *tional Academy of Sciences* 115 (20), 5111–5116.
- 1715 Brown, M. C., Donadini, F., Frank, U., Panovska, S., Nilsson, A., Korhonen,
1716 K., Schuberth, M., Korte, M., Constable, C. G., 2015a. GEOMAGIA50.v3:
1717 2. a new paleomagnetic database for lake and marine sediments. *Earth*
1718 *Planets Space* 67, 70.
- 1719 Brown, M. C., Donadini, F., Korte, M., Nilsson, A., Korhonen, K., Lodge,
1720 A., Lengyel, S. N., Constable, C. G., 2015b. GEOMAGIA50.v3: 1. general
1721 structure and modifications to the archeological and volcanic database.
1722 *Earth Planets Space* 67, 83.
- 1723 Bucha, V., 1967. Intensity of the Earth magnetic field during archeological
1724 times in Czechoslovakia. *Archaeometry* 10, 12–22.
- 1725 Bucur, I., 1994. The direction of the terrestrial magnetic field in France,
1726 during the last 21 centuries. recent progress. *Phys. Earth Planet. Inter.*
1727 87 (1), 95–109.

- 1728 Burakov, K. S., Nachasova, I. E., 1985. Correcting for chemical change during
1729 heating in archeomagnetic determinations of the ancient geomagnetic field
1730 intensity. *Izvestiya, Phys. Solid Earth* 21, 801–803.
- 1731 Burakov, K. S., Nachasova, I. E., 2013. Archaeomagnetic study and rehy-
1732 droxylation dating of fired-clay ceramics. *Izvestiya, Phys. Solid Earth* 49,
1733 105–112.
- 1734 Burlatskaya, S., Nachasova, I., Didenko, E., Shelestun, N., 1986. Archeomag-
1735 netic determinations of geomagnetic field elements of the USSR Academy
1736 of Sciences. Soviet Geophysical Committee of the USRR Academy of Sci-
1737 ences: Moskow, 168pp.
- 1738 Burlatskaya, S. P., 1961. Archeomagnetic evidence for the Earth's magnetic
1739 field near Tiflis during the past. *Geomagnetism and Aeronomy* 1, 707–708.
- 1740 Butler, R. F., 1992. *Paleomagnetism: Magnetic domains to geologic terrains.*
1741 Blackwell Science.
- 1742 Cai, S., Chen, W., Tauxe, L., Deng, C., Qin, H., Pan, Y., Yi, L., Zhu, R.,
1743 2015. New constraints on the variation of the geomagnetic field during the
1744 late Neolithic period: Archaeointensity results from Sichuan, southwestern
1745 China. *J. Geophys. Res.* 120 (4), 2056–2069.
- 1746 Cai, S., Tauxe, L., Paterson, G. A., Deng, C., Pan, Y., Qin, H., Zhu, R., 2017.
1747 Recent advances in Chinese archeomagnetism. *Frontiers in Earth Science*
1748 5, 92.
- 1749 Cai, S., Tauxe, L., Wang, W., Deng, C., Pan, Y., Yang, L., Qin, H., 2020.

- 1750 High-fidelity archeointensity results for the Late Neolithic Period from
1751 Central China. *Geophys. Res. Lett.* 47 (10), e2020GL087625.
- 1752 Calvo-Rathert, M., Morales Contreras, J., Carrancho, A., Camps, P., Go-
1753 guitchaichvili, A., Hill, M. J., 2019. Reproducibility of archaeointensity
1754 determinations with a multimethod approach on archaeological material
1755 reproductions. *Geophys. J. Int.* 218 (3), 1719–1738.
- 1756 Campuzano, S., Gómez-Paccard, M., Pavón-Carrasco, F., Osete, M., 2019.
1757 Emergence and evolution of the South Atlantic Anomaly revealed by the
1758 new paleomagnetic reconstruction SHAWQ2k. *Earth Planet. Sci. Lett.* 512,
1759 17–26.
- 1760 Capdepon, I., Sánchez Bettucci, L., Morales, J., Gogichaishvili, A., 2019.
1761 Archaeomagnetism applied to ceramics from coastal archaeological sites in
1762 Uruguay. In: Inda Ferrero, H., García Rodríguez, F. (Eds.), *Advances in*
1763 *Coastal Geoarchaeology in Latin America*. Springer International Publish-
1764 ing, pp. 157–176.
- 1765 Carrancho, A., Villalaín, J., Pavón-Carrasco, F., Osete, M., Straus, L.,
1766 Vergès, J., Carretero, J., Angelucci, D., González Morales, M., Arsuaga,
1767 J., Bermúdez de Castro, J., Carbonell, E., 2013. First directional European
1768 palaeosecular variation curve for the Neolithic based on archaeomagnetic
1769 data. *Earth Planet. Sci. Lett.* 380, 124–137.
- 1770 Casas, L., Incoronato, A., 2007. Distribution analysis of errors due to reloca-
1771 tion of geomagnetic data using the ‘Conversion via Pole’ (CVP) method:

- 1772 Implications on archaeomagnetic data. *Geophysical Journal International*
1773 169 (2), 448–454.
- 1774 Cejudo, R., Goguitchaichvili, A., Montejo, F., Ruiz, R. G., Ivaro Botiva,
1775 Morales, J., 2019. First archaeomagnetic results from Colombia (the Bo-
1776 gotá Savanna Pre-Hispanic sites): Implications for the Caribbean absolute
1777 geomagnetic intensity variation curve. *Journal of Archaeological Science:*
1778 *Reports* 26, 101898.
- 1779 Chauvin, A., Garcia, Y., Lanos, P., Laubenheimer, F., 2000. Paleointensity
1780 of the geomagnetic field recovered on archaeomagnetic sites from France.
1781 *Phys. Earth Planet. Inter.* 120 (1-2), 111–136.
- 1782 Chelidze, Z. A., 1965. Some results of a study of the past geomagnetic field in
1783 Georgian SSR by the archeomagnetic method. *Geomagnetism and Aeron-*
1784 *omy* 5, 744–746.
- 1785 Chiari, G., Lanza, R., 1997. Pictorial remanent magnetization as an indicator
1786 of secular variation of the Earth’s magnetic field. *Phys. Earth Planet. Inter.*
1787 101 (1), 79–83.
- 1788 Chou, Y.-M., Jiang, X., Liu, Q., Hu, H.-M., Wu, C.-C., Liu, J., Jiang, Z.,
1789 Lee, T.-Q., Wang, C.-C., Song, Y.-F., Chiang, C.-C., Tan, L., Lone, M. A.,
1790 Pan, Y., Zhu, R., He, Y., Chou, Y.-C., Tan, A.-H., Roberts, A. P., Zhao,
1791 X., Shen, C.-C., 2018. Multidecadally resolved polarity oscillations during
1792 a geomagnetic excursion. *Proceedings of the National Academy of Sciences*
1793 115 (36), 8913–8918.

- 1794 Clark, A. J., Tarling, D. H., Noel, M., 1988. Developments in archaeomag-
1795 netic dating in Britain. *Journal of Archaeological Science* 15 (6), 645–667.
- 1796 Coe, R. S., 1967. Paleo-intensities of the Earth’s magnetic field determined
1797 from Tertiary and Quaternary rocks. *J. Geophys. Res.* 72, 3247–3262.
- 1798 Constable, C., Korte, M., 2015. Centennial- to millennial-scale geomagnetic
1799 field variations. In: *Treatise on Geophysics, Second Edition*. Elsevier, Am-
1800 sterdam, Netherlands.
- 1801 Constable, C., Korte, M., Panovska, S., 2016. Persistent high paleosecular
1802 variation activity in southern hemisphere for at least 10 000 years. *Earth*
1803 *Planet. Sci. Lett.* 453, 78–86.
- 1804 Constable, C. G., Johnson, C. L., Lund, S. P., 2000. Global geomagnetic field
1805 models for the past 3000 years: transient or permanent flux lobes? *Phil.*
1806 *Trans. R. Soc. Lond. A* 358, 991–1008.
- 1807 Cook, R., Belshé, J., 1958. Archaeomagnetism. A preliminary report on
1808 Britain. *Antiquity* 32, 167.
- 1809 Daly, L., Goff, M. L., 1996. An updated and homogeneous world secular
1810 variation data base. 1. Smoothing of the archaeomagnetic results. *Phys.*
1811 *Earth Planet. Inter.* 93 (3), 159 – 190.
- 1812 Davies, C. J., Constable, C. G., 2017. Geomagnetic spikes on the core-mantle
1813 boundary. *Nat. Commun.* 8, 15593.
- 1814 Day, R., Fuller, M., Schmidt, V. A., 1977. Hysteresis properties of titano-

- 1815 magnetites: grain size and compositional dependence. *Phys. Earth Planet.*
1816 *Inter.* 13, 260–267.
- 1817 de Groot, L., Biggin, A., Dekkers, M., Langereis, C., Herrero-Bervera, E.,
1818 2013. Rapid regional perturbations to the recent global geomagnetic decay
1819 revealed by a new Hawaiian record. *Nature Communications* 4, 2727.
- 1820 de Groot, L. V., Fabian, K., Béguin, A., Reith, P., Barnhoorn, A.,
1821 Hilgenkamp, H., 2018. Determining individual particle magnetizations in
1822 assemblages of micrograins. *Geophysical Research Letters* 45 (7), 2995–
1823 3000.
- 1824 De Marco, E., Tema, E., Lanos, P., Kondopoulou, D., 2014. An updated
1825 catalogue of Greek archaeomagnetic data for the last 4500 years and a
1826 directional secular variation curve. *Stud. Geophys. Geod.* 58 (1), 121–147.
- 1827 Deenadayalan, K., Gawali, P. B., Lakshmi, B. V., Rai, M., 2020. Rock-
1828 magnetic and archaeomagnetic investigations on archaeological artefacts
1829 from Maharashtra, India. *Geological Society, London, Special Publications*
1830 497 (1), 9–26.
- 1831 Dekkers, M. J., Böhnell, H. N., 2006. Reliable absolute palaeointensities inde-
1832 pendent of magnetic domain state. *Earth Planet. Sci. Lett.* 248, 508–517.
- 1833 Deng, X. H., Li, D. J., 1965. The geomagnetic field in Peking region and
1834 its secular variation during the last 2000 years. *Acta Geophys. Sinica* 14,
1835 181–196.
- 1836 Domen, H., 1977. A single heating method of paleomagnetic field intensity

- 1837 determination applied to old roof tiles and rocks. *Phys. Earth Planet. Inter.*
1838 13 (4), 315 – 318.
- 1839 Donadini, F., Korte, M., Constable, C., 2009. Geomagnetic field for 0-3 ka:
1840 1. New data sets for global modeling. *Geochem. Geophys. Geosyst.* 10,
1841 Q06007.
- 1842 Donadini, F., Riisager, P., Korhonen, K., Pesonen, L., 2006. Database for
1843 Holocene geomagnetic intensity information. *Eos Trans. AGU* 87(14), 137–
1844 143.
- 1845 Donadini, F., Serneels, V., Kapper, L., El Kateb, A., 2015. Directional
1846 changes of the geomagnetic field in West Africa: Insights from the metal-
1847 lurgical site of Korsimoro. *Earth Planet. Sci. Lett.* 430, 349–355.
- 1848 Dumberry, M., Bloxham, J., 2006. Azimuthal flows in the Earth’s core and
1849 changes in length of day at millennial timescales. *Geophys. J. Int.* 165,
1850 32–46.
- 1851 Dumberry, M., Finlay, C. C., 2007. Eastward and westward drift of the
1852 Earth’s magnetic field for the last three millennia. *Earth Planet. Sci. Lett.*
1853 254, 146–157.
- 1854 Dunlop, D. J., 2002. Theory and application of the Day plot (M_{rs}/M_s versus
1855 H_{cr}/H_c) 1. Theoretical curves and tests using titanomagnetite data. *J.*
1856 *Geophys. Res.* 107 (B3), 2056.
- 1857 Dunlop, D. J., 2011. Physical basis of the Thellier-Thellier and related pale-
1858 ointensity methods. *Phys. Earth Planet. Inter.* 187, 118–138.

- 1859 Ertepinar, P., Hammond, M. L., Hill, M. J., Biggin, A. J., Langereis, C. G.,
1860 Herries, A. I. R., Yener, K. A., Akar, M., Gates, M.-H., Harrison, T.,
1861 Greaves, A. M., Frankel, D., Webb, J., Ozgen, I., Yazicioglu, G. B., 2020.
1862 Extreme geomagnetic field variability indicated by Eastern Mediterranean
1863 full-vector archaeomagnetic records. *Earth Planet. Sci. Lett.* 531, 115979.
- 1864 Evans, M., Hoyer, G., 2005. Archaeomagnetic results from southern Italy and
1865 their bearing on geomagnetic secular variation. *Phys. Earth Planet. Inter.*
1866 151 (1), 155–162.
- 1867 Evans, M. E., 1991. An archaeointensity investigation of a kiln at Pompeii.
1868 *J. Geomag. Geoelectr.* 43 (5), 357–361.
- 1869 Fabian, K., Leonhardt, R., 2010. Multiple-specimen absolute paleointen-
1870 sity determination: An optimal protocol including pTRM normalization,
1871 domain-state correction, and alteration test. *Earth Planet. Sci. Lett.* 297,
1872 84–94.
- 1873 Fanjat, G., Camps, P., Alva Valdivia, L. M., Sougrati, M. T., Cuevas-
1874 Garcia, M., M.Perrin, 2013. First archeointensity determinations on Maya
1875 incense burners from Palenque temples, Mexico: New data to constrain the
1876 Mesoamerica secular variation curve. *Earth Planet. Sci. Lett.* 363, 168–180.
- 1877 Fisher, R. A., 1953. Dispersion on a sphere. *Proc. R. Soc. Lond., A* 217,
1878 295–305.
- 1879 Folgheraiter, G., 1899. Sur les variations séculaires de l'inclinaison
1880 magnétique dans l'antiquité. *J. Phys. Theor. Appl.* 8, 660–667.

- 1881 Fournier, A., Hulot, G., Jault, D., Kuang, W., Tangborn, A., Gillet, N.,
1882 Canet, E., Aubert, J., Lhuillier, F., 2010. An introduction to data assim-
1883 ilation and predictability in geomagnetism. *Space Science Reviews* 155,
1884 247–291.
- 1885 Fox, J. M. W., Aitken, M. J., 1980. Cooling-rate dependency of thermore-
1886 manent magnetisation. *Nature* 283, 462–463.
- 1887 Gallet, Y., D’Andrea, M., Genevey, A., Pinnock, F., Le Goff, M., Matthiae,
1888 P., 2014. Archaeomagnetism at Ebla (Tell Mardikh, Syria). new data on
1889 geomagnetic field intensity variations in the Near East during the Bronze
1890 Age. *Journal of Archaeological Science* 42, 295–304.
- 1891 Gallet, Y., Fortin, M., Fournier, A., Le Goff, M., Livermore, P., 2020. Anal-
1892 ysis of geomagnetic field intensity variations in Mesopotamia during the
1893 third millennium BC with archeological implications. *Earth Planet. Sci.*
1894 *Lett.* 537, 116183.
- 1895 Gallet, Y., Genevey, A., Courtillot, V., 2003. On the possible occurrence of
1896 archaeomagnetic jerks in the geomagnetic field over the past three millen-
1897 nia. *Earth Planet. Sci. Lett.* 214 (1), 237–242.
- 1898 Gallet, Y., Genevey, A., Fluteau, F., 2005. Does earth’s magnetic field sec-
1899 ular variation control centennial climate change? *Earth Planet. Sci. Lett.*
1900 236 (1), 339–347.
- 1901 Gallet, Y., Genevey, A., Le Goff, M., 2002. Three millennia of directional
1902 variation of the Earth’s magnetic field in western Europe as revealed by
1903 archeological artefacts. *Phys. Earth Planet. Inter.* 131 (1), 81–89.

- 1904 Gallet, Y., Hulot, G., Chulliat, A., Genevey, A., 2009. Geomagnetic field
1905 hemispheric asymmetry and archeomagnetic jerks. *Earth Planet. Sci. Lett.*
1906 284, 179–186.
- 1907 Gallet, Y., Montaña, M. M., Genevey, A., García, X. C., Thébault, E., Bach,
1908 A. G., Goff, . M. L., Robert, B., Nachasova, I., 2015. New late neolithic
1909 (c. 7000-5000 BC) archeointensity data from Syria. Reconstructing 9000
1910 years of archeomagnetic field intensity variations in the Middle East. *Phys.*
1911 *Earth Planet. Inter.* 238, 89–103.
- 1912 Games, K. P., 1977. The magnitude of the paleomagnetic field: a new non-
1913 thermal, non detrital method using sun-dried bricks. *Geophys. J. R. astr.*
1914 *Soc.* 48, 315329.
- 1915 Genevey, A., Gallet, Y., 2002. Intensity of the geomagnetic field in western
1916 Europe over the past 2000 years: New data from ancient French pottery.
1917 *J. Geophys. Res.* 107, 2285.
- 1918 Genevey, A., Gallet, Y., Constable, C. G., Korte, M., Hulot, G., 2008.
1919 ArcheoInt: An upgraded compilation of geomagnetic field intensity data
1920 for the past ten millennia and its application to the recovery of the past
1921 dipole moment. *Geochem. Geophys. Geosyst.* 9, Q04038.
- 1922 Genevey, A., Gallet, Y., Jesset, S., Thébault, E., Bouillon, J., Lefèvre, A., Le
1923 Goff, M., 2016. New archeointensity data from French Early Medieval pot-
1924 tery production (6-10th century AD). Tracing 1500 years of geomagnetic
1925 field intensity variations in Western Europe. *Phys. Earth Planet. Inter.*
1926 257, 205–219.

- 1927 Genevey, A., Gallet, Y., Margueron, J.-C., 2003. Eight thousand years of ge-
1928 omagnetic field intensity variations in the eastern Mediterranean. *J. Geo-*
1929 *phys. Res.* 108.
- 1930 Genevey, A., Gallet, Y., Rosen, J., Le Goff, M., 2009. Evidence for rapid
1931 geomagnetic field intensity variations in Western Europe over the past
1932 800 years from new French archeointensity data. *Earth Planet. Sci. Lett.*
1933 284 (1), 132–143.
- 1934 Genevey, A., Gallet, Y., Thébault, E., Livermore, P., Fournier, A., Jesset,
1935 S., Lefèvre, A., Maé-Hourlier, N., Marot, E., Regnard, S., 2021. Archeo-
1936 magnetic intensity investigations of French medieval ceramic workshops:
1937 Contribution to regional field modeling and archeointensity-based dating.
1938 *Phys. Earth Planet. Inter.* 318, 106750.
- 1939 Genevey, A., Principe, C., Gallet, Y., Clemente, G., Le Goff, M., Fournier,
1940 A., Pallecchi, P., 2019. Refining the high-fidelity archaeointensity curve for
1941 Western Europe over the past millennium: analysis of Tuscan architectural
1942 bricks (Italy). *Geol. Soc. Lond. Spec. Pub.* 497 (1), 73–88.
- 1943 Goguitchaichvili, A., Greco, C., Garcia Ruiz, R., Pereyra Domingorena, L.,
1944 Cejudo, R., Morales, J., Gogorza, C., Scattolin, C., Tarrag, M., 2019. First
1945 archaeointensity reference paleosecular variation curve for South America
1946 and its implications for geomagnetism and archaeology. *Quaternary Re-*
1947 *search* 92 (1), 8197.
- 1948 Goguitchaichvili, A., Greco, C., Morales, J., 2011. Geomagnetic field in-
1949 tensity behavior in South America between 400 AD and 1800 AD: first

1950 archeointensity results from Argentina. *Phys. Earth Planet. Inter.* 186,
1951 191–197.

1952 Goguitchaichvili, A., Morales, J., Schavelzon, D., Vásquez, C., Gogorza,
1953 C. S., Loponte, D., Rapalini, A., 2015. Variation of the Earth’s magnetic
1954 field strength in South America during the last two millennia: New results
1955 from historical buildings of Buenos Aires and re-evaluation of regional data.
1956 *Phys. Earth Planet. Inter.* 245, 15–25.

1957 Gómez-Paccard, M., Chauvin, A., Albeck, M. E., Zaburlín, M. A., Basso,
1958 D. M., Pavón-Carrasco, F. J., Osete, M. L., Campuzano, S. A., 2019. New
1959 archeointensity data from NW Argentina (1300–1500 CE). *Phys. Earth
1960 Planet. Inter.* 286, 92–100.

1961 Gómez-Paccard, M., Chauvin, A., Lanos, P., Dufresne, P., Kovacheva, M.,
1962 Hill, M. J., Beamud, E., Blain, S., Bouvier, A., Guibert, P., 2012a. Improv-
1963 ing our knowledge of rapid geomagnetic field intensity changes observed
1964 in Europe between 200 and 1400 AD. *Earth Planet. Sci. Lett.* 355-356,
1965 131–143.

1966 Gómez-Paccard, M., McIntosh, G., Chauvin, A., Beamud, E., Pavón-
1967 Carrasco, F. J., Thiriot, J., 2012b. Archaeomagnetic and rock magnetic
1968 study of six kilns from North Africa (Tunisia and Morocco). *Geophys. J.
1969 Int.* 189 (1), 169–186.

1970 Gubbins, D., Bloxham, J., 1987. Morphology of the geomagnetic field and
1971 implications for the geodynamo. *Nature* 325, 509–511.

- 1972 Gunn, N. M., Murray, A. S., 08 1980. Geomagnetic field magnitude varia-
1973 tions in Peru derived from archaeological ceramics dated by thermolumi-
1974 nescence. *Geophys. J. Int.* 62 (2), 345–366.
- 1975 Hagstrum, J. T., Blinman, E., 2010. Archeomagnetic dating in western North
1976 America: An updated reference curve based on paleomagnetic and archeo-
1977 magnetic data sets. *Geochem. Geophys. Geosyst.* 11, Q06009.
- 1978 Hare, V. J., Tarduno, J. A., Huffman, T., Watkeys, M., Thebe, P. C.,
1979 Manyanga, M., Bono, R. K., Cottrell, R. D., 2018. New archeomagnetic
1980 directional records from Iron Age Southern Africa (ca. 425-1550 CE) and
1981 implications for the South Atlantic Anomaly. *Geophys. Res. Lett.* 45 (3),
1982 1361–1369.
- 1983 Hartmann, G. A., Genevey, A., Gallet, Y., Trindade, R. I., Goff, M. L.,
1984 Najjar, R., Etchevarne, C., Afonso, M. C., 2009. Time evolution of the
1985 South Atlantic magnetic anomaly. *Anais da Academia Brasileira de Cien-
1986 cias* 81 (2), 243–255.
- 1987 Hartmann, G. A., Genevey, A., Gallet, Y., Trindade, R. I., Goff, M. L., Naj-
1988 jar, R., Etchevarne, C., Afonso, M. C., 2011. New historical archeointensity
1989 data from Brazil: evidence for a large regional non-dipole field contribution
1990 over the past few centuries. *Earth Planet. Sci. Lett.* 306, 66–76.
- 1991 Hartmann, G. A., Genevey, A., Gallet, Y., Trindade, R. I. F., Etchevarne,
1992 C., Goff, M. L., Afonso, M., 2010. Archeointensity in Northeast Brazil over
1993 the past five centuries. *Earth Planet. Sci. Lett.* 296, 340–352.

- 1994 Hartmann, G. A., Poletti, W., Trindade, R. I., Ferreira, L. M., Sanches, P. L.,
1995 2019. New archeointensity data from South Brazil and the influence of the
1996 South Atlantic Anomaly in South America. *Earth and Planetary Science*
1997 *Letters* 512, 124 – 133.
- 1998 Heaton, T. J., Köhler, P., Butzin, M., Bard, E., Reimer, R. W., Austin, W.
1999 E. N., Bronk Ramsey, C., Grootes, P. M., Hughen, K. A., Kromer, B.,
2000 Reimer, P., Adkins, J., Burke, A., Cook, M., Olsen, J. and Skinner, L.,
2001 2020. Marine20 – the marine radiocarbon age calibration curve (0–55,000
2002 cal BP). *Radiocarbon* 62 (4), 779820.
- 2003 Hellio, G., Gillet, N., 2018. Time-correlation-based regression of the geo-
2004 magnetic field from archeological and sediment records. *Geophys. J. Int.*
2005 214 (3), 1585–1607.
- 2006 Hellio, G., Gillet, N., Bouligand, C., Jault, D., 2014. Stochastic modelling of
2007 regional archaeomagnetic series. *Geophys. J. Int.* 199 (2), 931–943.
- 2008 Henthorn, D. I., Parkington, J., Reid, R. C., Rüter, H., Fox, J. M. W., Mc-
2009 Fadden, P. L., 1979. An archaeomagnetic study of Mgungundlovu. *Good-*
2010 *win Series* (3), 149–158.
- 2011 Herrero-Bervera, E., Athens, S., Tema, E., Alva Valdivia, L. M., Camps,
2012 P., Trejo, A. R., 2020. First archaeointensity results from Ecuador with
2013 rock magnetic analyses and ^{14}C dates to constrain the geomagnetic field
2014 evolution in South America: Enhancing the knowledge of geomagnetic field
2015 intensity. *Journal of South American Earth Sciences* 103, 102733.

- 2016 Hervé, G., Chauvin, A., Lanos, P., 2013a. Geomagnetic field variations in
2017 Western Europe from 1500BC to 200AD. Part I: Directional secular vari-
2018 ation curve. *Phys. Earth Planet. Inter.* 218, 1–13.
- 2019 Hervé, G., Chauvin, A., Lanos, P., 2013b. Geomagnetic field variations in
2020 Western Europe from 1500BC to 200AD. Part II: New intensity secular
2021 variation curve. *Phys. Earth Planet. Inter.* 218, 51–56.
- 2022 Hervé, G., Chauvin, A., Lanos, P., Lhuillier, F., Boulud-Gazo, S., Denti, M.,
2023 Macario, R., 2021. How did the dipole axis vary during the first millennium
2024 BCE? New data from West Europe and analysis of the directional global
2025 database. *Phys. Earth Planet. Inter.* 315, 106712.
- 2026 Hervé, G., Chauvin, A., Lanos, P., Rochette, P., Perrin, M., Perrond’Arc, M.,
2027 2019a. Cooling rate effect on thermoremanent magnetization in archaeo-
2028 logical baked clays: an experimental study on modern bricks. *Geophys. J.*
2029 *Int.* 217 (2), 1413–1424.
- 2030 Hervé, G., Faßbinder, J., Gilder, S. A., Metzner-Nebelsick, C., Gallet, Y.,
2031 Genevey, A., Schnepf, E., Geisweid, L., Pütz, A., Reuß, S., Wittenborn,
2032 F., Flontas, A., Linke, R., Riedel, G., Walter, F., Westhausen, I., 2017.
2033 Fast geomagnetic field intensity variations between 1400 and 400 BCE:
2034 New archaeointensity data from Germany. *Phys. Earth Planet. Inter.* 270,
2035 143–156.
- 2036 Hervé, G., Lanos, P., 2018. Improvements in archaeomagnetic dating in West-
2037 ern Europe from the Late Bronze to the Late Iron Ages: An alternative to

- 2038 the problem of the Hallstattian radiocarbon plateau. *Archaeometry* 60 (4),
2039 870–883.
- 2040 Hervé, G., Perrin, M., Alva-Valdivia, L., Tchibinda, B. M., Rodriguez-Trejo,
2041 A., Hernandez-Cardona, A., Tello, M. C., Rodriguez, C. M., 2019b. Criti-
2042 cal analysis of the Holocene palaeointensity database in Central America:
2043 Impact on geomagnetic modelling. *Phys. Earth Planet. Inter.* 289, 1–10.
- 2044 Hervé, G., Perrin, M., Alva-Valdivia, L. M., Rodríguez-Trejo, A., Hernández-
2045 Cardona, A., Córdova Tello, M., Meza Rodriguez, C., 2019c. Secular vari-
2046 ation of the intensity of the geomagnetic field in Mexico during the first
2047 millennium BCE. *Geochem. Geophys. Geosyst.* 20 (12), 6066–6077.
- 2048 Hill, M. J., Shaw, J., 1999. Palaeointensity results for historic lavas from
2049 Mt Etna using microwave demagnetization/remagnetization in a modified
2050 Thellier-type experiment. *Geophys. J. Int.* 139, 583–590.
- 2051 Hill, M. J., Shaw, J., 2007. The use of the ‘Kono perpendicular applied field
2052 method’ in microwave palaeointensity experiments. *Earth Planets Space*
2053 59, 711–716.
- 2054 Hogg, A. G., Heaton, T. J., Hua, Q., Palmer, J. G., Turney, C. S. M.,
2055 Southon, J., Bayliss, A., Blackwell, P. G., Boswijk, G., Ramsey, C. B.,
2056 Pearson, C., Petchey, F., Reimer, P., Reimer, R., Wacker, L., 2020.
2057 SHCal20 Southern Hemisphere calibration, 0–55,000 years cal BP. *Ra-
2058 diocarbon* 62 (4), 759–778.
- 2059 Hongre, L., Hulot, G., Khokhlov, A., 1998. An analysis of the geomagnetic
2060 field over the past 2000 years. *Phys. Earth Planet. Inter.* 106, 311–335.

- 2061 Hueda-Tanabe, Y., Soler-Arechalde, A., Urrutia-Fucugauchi, J., Barba, L.,
2062 Manzanilla, L., Rebolledo-Vieyra, M., Goguitchaichvili, A., 2004. Archaeo-
2063 magnetic studies in central Mexico—dating of Mesoamerican lime-plasters.
2064 *Phys. Earth Planet. Inter.* 147 (2), 269–283.
- 2065 Hus, J., Geeraerts, R., Plumier, J., 2004. On the suitability of refractory
2066 bricks from a mediaeval brass melting and working site near Dinant (Bel-
2067 gium) as geomagnetic field recorders. *Phys. Earth Planet. Inter.* 147 (2),
2068 103–116.
- 2069 Jackson, A., Jonkers, A. R. T., Walker, M. R., 2000. Four centuries of ge-
2070 omagnetic secular variation from historical records. *Phil. Trans. R. Soc.*
2071 *Lond. A* 358, 957–990.
- 2072 Jones, S. A., Tauxe, L., Blinman, E., Genevey, A., 2020. Archeointensity of
2073 the Four Corners Region of the American Southwest. *Geochem. Geophys.*
2074 *Geosyst.* 21 (3), e2018GC007509.
- 2075 Kapper, K. L., Donadini, F., Mauvilly, M., Panovska, S., Hirt, A. M.,
2076 2014. New directional archaeomagnetic data of burned cave sediments from
2077 Switzerland and geomagnetic field variations in Central Europe. *Geophys.*
2078 *J. Int.* 198, 1208–1221.
- 2079 Kapper, L., Donadini, F., Serneels, V., Tema, E., Goguitchaichvili, A.,
2080 Morales, J. J., 2017. Reconstructing the geomagnetic field in West Africa:
2081 First absolute intensity results from Burkina Faso. *Scientific Reports*
2082 7 (45225).

- 2083 Kapper, L., Serneels, V., Panovska, S., Ruiz, R. G., Hellio, G., de Groot, L.,
2084 Goguitchaichvili, A., Morales, J., Ruiz, R. C., 2020. Novel insights on the
2085 geomagnetic field in West Africa from a new reference curve (0-2000 AD).
2086 Scientific Reports 10 (1121).
- 2087 Kawai, N., Hirooka, K., 1967. Wobbling motion of the geomagnetic dipole
2088 field in historic time during these 2000 years. *J. Geomag. Geoelectr.* 19 (3),
2089 217–227.
- 2090 Kawai, N., Hirooka, K., Nakajima, T., Tokieda, K., Tosi, M., 1972. Archaeo-
2091 magnetism in Iran. *Nature* 236, 223–225.
- 2092 Kitahara, Y., Nishiyama, D., Ohno, M., Yamamoto, Y., Kuwahara, Y.,
2093 Hatakeyama, T., 2020. Construction of new archaeointensity reference
2094 curve for East Asia from 2000 CE to 1100 CE. *Phys. Earth Planet. In-*
2095 *ter.*, 106596.
- 2096 Kitahara, Y., Yamamoto, Y., Ohno, M., Kuwahara, Y., Kameda, S.,
2097 Hatakeyama, T., 2018. Archeointensity estimates of a tenth-century kiln:
2098 first application of the Tsunakawa-Shaw paleointensity method to archeo-
2099 logical relics. *Earth Planets Space* 70, 79.
- 2100 Kitazawa, K., 1970. Intensity of the geomagnetic field in Japan for the past
2101 10,000 years. *J. Geophys. Res.* 75 (35), 7403–7411.
- 2102 Kitazawa, K., Kobayashi, K., 1968. Intensity variation of the geomagnetic
2103 field during the past 4000 years in South America. *J. Geomag. Geoelectr.*
2104 20, 7–19.

- 2105 Knudsen, M. F., Riisager, P., Donadini, F., Snowball, I., Muscheler, R.,
2106 Korhonen, K., Pesonen, L. J., 2008. Variations in the geomagnetic dipole
2107 moment during the Holocene and the past 50 kyr. *Earth Planet. Sci. Lett.*
2108 272, 319–329.
- 2109 Kondopoulou, D., Aidona, E., Ioannidis, N., Polymeris, G., Tsolakis, S.,
2110 2015. Archaeomagnetic study and thermoluminescence dating of Proto-
2111 byzantine kilns (Megali Kypsa, North Greece). *Journal of Archaeological*
2112 *Science: Reports* 2, 156–168.
- 2113 Kono, M., 1978. Reliability of palaeointensity methods using alternating field
2114 demagnetization and anhysteretic remanence. *Geophys. J. R. astr. Soc.* 54,
2115 241–261.
- 2116 Korhonen, K., Donadini, F., Riisager, P., Pesonen, L. J., 2008. GEOMA-
2117 GIA50: an archeointensity database with PHP and MySQL. *Geochem.,*
2118 *Geophys., Geosyst.* 9, Q04029.
- 2119 Korte, M., Brown, M. C., Gunnarson, S. R., Nilsson, A., Panovska, S.,
2120 Wardinski, I., Constable, C. G., 2019. Refining Holocene geochronologies
2121 using palaeomagnetic records. *Quaternary Geochronology* 50, 47–74.
- 2122 Korte, M., Constable, C., 2003. Continuous global geomagnetic field models
2123 for the past 3000 years. *Phys. Earth Planet. Inter.* 140, 73–89.
- 2124 Korte, M., Constable, C., 2018. Archeomagnetic intensity spikes: global or
2125 regional geomagnetic field features? *Frontiers in Earth Science* 6, 17.
- 2126 Korte, M., Constable, C. G., 2005. Continuous geomagnetic field models for
2127 the past 7 millenia: 2. CALS7K. *Geochem. Geophys. Geosyst.* 6, Q02H16.

- 2128 Korte, M., Donadini, F., Constable, C. G., 2009. Geomagnetic field for 0-
2129 3 ka: 2. a new series of time-varying global models. *Geochem. Geophys.*
2130 *Geosyst.* 10, Q06008.
- 2131 Kostadinova-Avramova, M., Jordanova, N., 2019. Study of cooling rate effect
2132 on baked clay materials and its importance for archaeointensity determi-
2133 nations. *Phys. Earth Planet. Inter.* 288, 9–25.
- 2134 Kostadinova-Avramova, M., Kovacheva, M., Boyadzhiev, Y., 2014. Contri-
2135 bution of stratigraphic constraints of Bulgarian prehistoric multilevel tells
2136 and a comparison with archaeomagnetic observations. *J. Arch. Sci.* 43,
2137 227–238.
- 2138 Kostadinova-Avramova, M., Kovacheva, M., Boyadzhiev, Y., Hervé, G.,
2139 2020. Archaeomagnetic knowledge of the Neolithic in Bulgaria with empha-
2140 sis on intensity changes. Geological Society, London, Special Publications
2141 497 (1), 89–111.
- 2142 Kovacheva, M., 1969. Inclination of the Earth’s magnetic field during the last
2143 2000 years in Bulgaria. *J. Geomag. Geoelectr.* 21 (3), 573–578.
- 2144 Kovacheva, M., 1997. Archaeomagnetic database from Bulgaria: the last
2145 8000 years. *Phys. Earth Planet. Inter.* 102 (3), 145–151.
- 2146 Kovacheva, M., Boyadzhiev, Y., Kostadinova-Avramova, M., Jordanova, N.,
2147 Donadini, F., 2009a. Updated archeomagnetic data set of the past 8 mil-
2148 lennia from the Sofia laboratory, Bulgaria. *Geochem. Geophys. Geosyst.*
2149 10 (5), Q05002.

- 2150 Kovacheva, M., Chauvin, A., Jordanova, N., Lanos, P., Karloukovski, V.,
2151 2009b. Remanence anisotropy effect on the palaeointensity results obtained
2152 from various archaeological materials, excluding pottery. *Earth Planets*
2153 *Space* 61, 711–732.
- 2154 Kovacheva, M., Kostadinova-Avramova, M., Jordanova, N., Lanos, P., Boy-
2155 adzhiev, Y., 2014. Extended and revised archaeomagnetic database and
2156 secular variation curves from Bulgaria for the last eight millennia. *Phys.*
2157 *Earth Planet. Inter.* 236, 79–94.
- 2158 Krása, D., Heunemann, C., Leonhardt, R., Petersen, N., 2003. Experimen-
2159 tal procedure to detect multidomain remanence during Thellier-Thellier
2160 experiments. *Phys. Chem. Earth* 28, 681–687.
- 2161 Lanos, P., 1987. The effects of demagnetizing fields on thermoremanent mag-
2162 netization acquired by parallel-sided baked clay blocks. *Geophys. J. Int.*
2163 91 (3), 985–1012.
- 2164 Lanos, P., 2004. *Bayesian Inference of Calibration Curves: Application to*
2165 *Archaeomagnetism*. Springer London, London, pp. 43–82.
- 2166 Lanos, P., Le Goff, M., Kovacheva, M., Schnepf, E., 2005. Hierarchical mod-
2167 elling of archaeomagnetic data and curve estimation by moving average
2168 technique. *Geophys. J. Int.* 160 (2), 440–476.
- 2169 Lanos, P., Philippe, A., 2018. Event date model: a robust Bayesian tool
2170 for chronology building. *Communications for Statistical Applications and*
2171 *Methods* 25 (2), 131–157.

- 2172 Lascu, I., Feinberg, J. M., 2011. Speleothem magnetism. *Quaternary Science*
2173 *Reviews* 30 (23), 3306–3320.
- 2174 Lascu, I., Feinberg, J. M., Dorale, J. A., Cheng, H., Edwards, R. L., 2016.
2175 Age of the Laschamp excursion determined by U-Th dating of a speleothem
2176 geomagnetic record from North America. *Geology* 44 (2), 139–142.
- 2177 Latham, A., Schwarcz, H., Ford, D., 1986. The paleomagnetism and U-Th
2178 dating of Mexican stalagmite, DAS2. *Earth Planet. Sci. Lett.* 79 (1), 195–
2179 207.
- 2180 Le Goff, M., Daly, L., Dunlop, D. J., Papusoi, C., 2006. Emile Thellier (1904-
2181 1987), a pioneer in studies of the “fossil” Earth’s magnetic field. Historical
2182 events and people in aeronomy, geomagnetism and solar-terrestrial physics,
2183 98–112.
- 2184 Le Goff, M., Gallet, Y., 2004. A new three-axis vibrating sample magnetome-
2185 ter for continuous high-temperature magnetization measurements: appli-
2186 cations to paleo- and archeo-intensity determinations. *Earth Planet. Sci.*
2187 *Lett.* 229, 31–43.
- 2188 Le Goff, M., Gallet, Y., 2014. Evaluation of the rehydroxylation dat-
2189 ing method: Insights from a new measurement device. *Quaternary*
2190 *Geochronology* 20, 89–98.
- 2191 Le Goff, M., Gallet, Y., 2015. Experimental variability in kinetics of moisture
2192 expansion and mass gain in ceramics. *J. Am. Ceram. Soc.* 98, 398–401.
- 2193 Le Goff, M., Gallet, Y., Warmé, N., Genevey, A., 2020. An updated archeo-
2194 magnetic directional variation curve for France over the past two millennia,

- 2195 following 25 years of additional data acquisition. *Phys. Earth Planet. Inter.*
2196 309, 106592.
- 2197 Le Goff, M., Henry, B., Daly, L., 1992. Practical method for drawing a VGP
2198 path. *Phys. Earth Planet. Inter.* 70 (3), 201–204.
- 2199 Lengyel, S. N., Eighmy, J. L., 2002. A revision to the U.S. Southwest ar-
2200 chaeomagnetic master curve. *J. Arch. Sci.* 29 (12), 1423–1433.
- 2201 Leonhardt, R., Krása, D., Coe, R. S., 2004. Multidomain behavior dur-
2202 ing Thellier paleointensity experiments: a phenomenological model. *Phys.*
2203 *Earth Planet. Inter.* 147, 127–140.
- 2204 Leonhardt, R., Matzka, J., Nichols, A. R. L., Dingwell, D. B., 2006. Cool-
2205 ing rate correction of paleointensity determination for volcanic glasses by
2206 relaxation geospeedometry. *Earth Planet. Sci. Lett.* 243, 282–292.
- 2207 Levi, S., 1977. The effect of magnetite particle size on paleointensity deter-
2208 minations of the geomagnetic field. *Phys. Earth Planet. Inter.* 13, 245–259.
- 2209 Licht, A., Hulot, G., Gallet, Y., Thébaud, E., 2013. Ensembles of low de-
2210 gree archeomagnetic field models for the past three millennia. *Phys. Earth*
2211 *Planet. Inter.* 224, 38–67.
- 2212 Liritzis, L., Lagios, E., 1993. A global archaeomagnetic intensity data bank.
2213 *Eos Trans. AGU* 74 (27), 303–306.
- 2214 Liritzis, Y., Thomas, R., 1980. Palaeointensity and thermoluminescence mea-
2215 surements on Cretan kilns from 1300 to 2000 BC. *Nature* 283, 54–55.

- 2216 Livermore, P. W., Fournier, A., Gallet, Y., 2014. Core-flow constraints on
2217 extreme archeomagnetic intensity changes. *Earth Planet. Sci. Lett.* 387,
2218 145 – 156.
- 2219 Livermore, P. W., Fournier, A., Gallet, Y., Bodin, T., 09 2018. Transdi-
2220 mensional inference of archeomagnetic intensity change. *Geophys. J. Int.*
2221 215 (3), 2008–2034.
- 2222 Livermore, P. W., Gallet, Y., Fournier, A., 2021. Archeomagnetic intensity
2223 variations during the era of geomagnetic spikes in the Levant. *Physics of*
2224 *the Earth and Planetary Interiors* 312, 106657.
- 2225 Lodge, A., Holme, R., 2009. Towards a new approach to archaeomagnetic
2226 dating in Europe using geomagnetic field modelling. *Archaeometry* 51,
2227 309–322.
- 2228 Lopez-Sanchez, J., Palencia-Ortas, A., del Campo, A., McIntosh, G., Ko-
2229 vacheva, M., Martin-Hernandez, F., Carmona, N., Rodriguez De la Fuente,
2230 O., Marin, P., Molina-Cardin, A., Osete, M., 2020. Occurrence of epsilon
2231 iron oxide in archeological materials: Effect on the natural remanent mag-
2232 netization. *Phys. Earth Planet. Inter.* 307, 106554.
- 2233 Mahgoub, A. N., Juárez-Arriaga, E., Böhnell, H., Manzanilla, L. R., Cyphers,
2234 A., 2019. Refined 3600 years palaeointensity curve for Mexico. *Phys. Earth*
2235 *Planet. Inter.* 296, 106328.
- 2236 Mandeau, M., Korte, M., Mozzoni, D., Kotzé, P., 2007. The magnetic field
2237 changing over the southern African continent: a unique behaviour. *South*
2238 *African Journal of Geology* 110, 193–202.

- 2239 Mandeá, M., Olsen, N., 2009. Geomagnetic and archeomagnetic jerks: where
2240 do we stand? *Eos, Transactions American Geophysical Union* 90 (24), 208.
- 2241 Márton, P., 1970. Secular variation of the geomagnetic virtual dipole field
2242 during the last 2000 yr as inferred from the spherical harmonic analysis
2243 of the available archeomagnetic data. *Pure and Applied Geophysics* 81,
2244 163–176.
- 2245 Márton, P., 2003. Recent achievements in archaeomagnetism in Hungary.
2246 *Geophys. J. Int.* 153 (3), 675–690.
- 2247 Márton, P., 2010. Two thousand years of geomagnetic field direction over
2248 central Europe revealed by indirect measurements. *Geophys. J. Int.* 181,
2249 261–268.
- 2250 Mauerberger, S., Schanner, M., Korte, M., Holschneider, M., 2020. Correla-
2251 tion based snapshot models of the archeomagnetic field. *Geophys. J. Int.*
2252 223, 648–665.
- 2253 McElhinny, M. W., Senanayake, W. E., 1982. Variations in the geomagnetic
2254 dipole: I. The past 50 000 years. *J. Geomag. Geoelectr.* 34, 39–51.
- 2255 Merrill, R. T., McElhinny, M. W., McFadden, P. L., 1996. *The Magnetic Field*
2256 *of the Earth: Palaeomagnetism, the core, and the deep mantle. Vol. 63 of*
2257 *International Geophysics Series. Academic Press.*
- 2258 Mitra, R., Tauxe, L., McIntosh, S. K., 2013. Two thousand years of archeoin-
2259 tensity from West Africa. *Earth Planet. Sci. Lett.* 364, 123–133.

- 2260 Molina-Cardín, A., Campuzano, S. A., Osete, M. L., Rivero-Montero, M.,
2261 Pavón-Carrasco, F. J., Palencia-Ortas, A., Martín-Hernández, F., Gómez-
2262 Paccard, M., Chauvin, A., Guerrero-Suárez, S., Pérez-Fuentes, J. C.,
2263 McIntosh, G., Catanzariti, G., Sastre Blanco, J. C., Larrazabal, J.,
2264 Fernández Martínez, V. M., Álvarez Sanchís, J. R., Rodríguez-Hernández,
2265 J., Martín Viso, I., Garcia i Rubert, D., 2018. Updated Iberian archeo-
2266 magnetic catalogue: New full vector paleosecular variation curve for the
2267 last three millennia. *Geochem. Geophys. Geosyst.* 19 (10), 3637–3656.
- 2268 Morales, J., Goguitchaichvili, A., Acosta, G., Gonzalez-Moran, T., Alva-
2269 Valdivia, L., Robles-Camacho, J., del Sol Hernandez-Bernal, M., 2009.
2270 Magnetic properties and archeointensity determination on Pre-Columbian
2271 pottery from Chiapas, Mesoamerica. *Earth Planets Space* 61, 83–91.
- 2272 Morales, J., Goguitchaichvili, A., Aguilar-Reyes, B., Pineda-Duran, M.,
2273 Camps, P., Carvallo, C., Calvo-Rathert, M., 2011. Are ceramics and bricks
2274 reliable absolute geomagnetic intensity carriers? *Phys. Earth Planet. Inter.*
2275 187 (3), 310–321.
- 2276 Nachasova, I. E., Burakov, K. S., 1995. Archaeointensity of the geomagnetic
2277 field in the 5th millennium B.C. in northern Mesopotamia. *Geomagnetism*
2278 *and Aeronomy* 35 (3), 398–402.
- 2279 Nachasova, I. E., Burakov, K. S., 1998. Geomagnetic variations in the VI-V
2280 millenia B.C. *Geomagnetism and Aeronomy* 38 (4), 502–505.
- 2281 Nachasova, I. E., Burakov, K. S., 2012. Variations in geomagnetic intensity

- 2282 and temperature in the second millennium B.C. in Spain. *Izvestiya, Phys.*
2283 *Solid Earth* 48, 434–440.
- 2284 Nachasova, I. E., Burakov, K. S., Bernabeu, J., 2002. Geomagnetic field
2285 intensity variation in Spain. *Izvestiya, Phys. Solid Earth* 38 (5), 371–376.
- 2286 Nachasova, I. E., Burakov, K. S., Molina, F., C]ámara, J. A., 2007. Archaeo-
2287 magnetic study of ceramics from the Neolithic Los Castillejos multilayer
2288 monument (Montefrio, Spain). *Izvestiya, Phys. Solid Earth* 42, 170–176.
- 2289 Nagata, T., Arai, Y., Momose, K., 1963. Secular variation of the geomagnetic
2290 force during the last 5000 years. *J. Geophys. Res.* 68, 5277–5281.
- 2291 Nagata, T., Kobayashi, K., Schwarz, E. J., 1965. Archeomagnetic intensity
2292 studies of South and Central America. *J. Geomag. Geoelectr.* 17, 399–405.
- 2293 Néel, L., 1949. Théorie du traînage magnétique des ferromagnétiques en
2294 grains fins avec applications aux terre cuites. *Ann. Géophys.* 5, 99–136.
- 2295 Neukirch, L. P., Tarduno, J. A., Huffman, T. N., Watkeys, M. K., Scribner,
2296 C. A., Cottrell, R. D., 2012. An archeomagnetic analysis of burnt grain
2297 bin floors from ca. 1200 to 1250 AD Iron-Age South Africa. *Phys. Earth*
2298 *Planet. Inter.* 190-191, 71–79.
- 2299 Nilsson, A., Holme, R., Korte, M., Suttie, N., Hill, M., 2014. Reconstructing
2300 Holocene geomagnetic field variation: new methods, models and implica-
2301 tions. *Geophys. J. Int.* 198, 229–248.
- 2302 Nilsson, A., Suttie, N., Korte, M., Holme, R., Hill, M., 2020. Persistent west-
2303 ward drift of the geomagnetic field at the core-mantle boundary linked to

- 2304 recurrent high-latitude weak/reverse flux patches. *Geophys. J. Int.* 222 (2),
2305 1423–1432.
- 2306 Noel, M., Batt, C. M., 1990. A method for correcting geographically sep-
2307 arated remanence directions for the purpose of archaeomagnetic dating.
2308 *Geophys. J. Int.* 102 (3), 753–756.
- 2309 Osete, M. L., Catanzariti, G., Chauvin, A., Pavón-Carrasco, F. J., Roperch,
2310 P., Fernández, V. M., 2015. First archaeomagnetic field intensity data from
2311 Ethiopia, Africa (1615 ± 12 AD). *Phys. Earth Planet. Inter.* 242, 24–35.
- 2312 Palencia-Ortas, A., Molina-Cardín, A., Osete, M. L., Gómez-Paccard, M.,
2313 Martín-Hernández, F., Chauvin, A., Roperch, P., 2021. Inclination flat-
2314 tening effect in highly anisotropic archaeological structures from Iberia. In-
2315 fluence on archaeomagnetic dating. *Phys. Earth Planet. Inter.*, 106762.
- 2316 Palencia-Ortas, A., Osete, M., Campuzano, S., McIntosh, G., Larrazabal, J.,
2317 Sastre, J., Rodríguez-Aranda, J., 2017. New archaeomagnetic directions
2318 from Portugal and evolution of the geomagnetic field in Iberia from Late
2319 Bronze Age to Roman Times. *Phys. Earth Planet. Inter.* 270, 183–194.
- 2320 Panovska, S., Korte, M., Constable, C. G., 2019. One hundred thousand years
2321 of geomagnetic field evolution. *Reviews of Geophysics* 57 (4), 1289–1337.
- 2322 Paterson, G. A., Tauxe, L., Biggin, A. J., Shaar, R., Jonestrask, L. C., 2014.
2323 On improving the selection of Thellier-type paleointensity data. *Geochem.*
2324 *Geophys. Geosyst.* 15 (4), 1180–1192.
- 2325 Pavón-Carrasco, F., Osete, M., Torta, J., Gaya-Piqué, L., Lanos, P., 2008.

- 2326 Initial SCHA.DI.00 regional archaeomagnetic model for Europe for the last
2327 2000 years. *Phys. Chem. Earth* 33, 596–608.
- 2328 Pavón-Carrasco, F. J., Osete, M. L., Torta, J. M., 2010. Regional model-
2329 ing of the geomagnetic field in Europe from 6000 to 1000 B.C. *Geochem.*
2330 *Geophys. Geosyst.* 11, Q11008.
- 2331 Pavón-Carrasco, F. J., Osete, M. L., Torta, J. M., De Santis, A., 2014. A
2332 geomagnetic field model for the Holocene based on archaeomagnetic and
2333 lava flow data. *Earth Planet. Sci. Lett.* 388, 98–109.
- 2334 Pavón-Carrasco, F. J., Osete, M. L., Torta, J. M., Gaya-Piqué, L. R., 2009.
2335 A regional archeomagnetic model for Europe for the last 3000 years,
2336 SCHA.DIF.3K: Applications to archeomagnetic dating. *Geochem. Geo-*
2337 *phys. Geosyst.* 10, Q03013.
- 2338 Pavón-Carrasco, F. J., Rodríguez-González, J., Osete, M. L., Torta, J. M.,
2339 2011. A matlab tool for archaeomagnetic dating. *Journal of Archaeological*
2340 *Science* 38 (2), 408–419.
- 2341 Poletti, W., Hartmann, G. A., Hill, M. J., Biggin, A. J., Trindade, R. I. F.,
2342 2013. The cooling-rate effect on microwave archeointensity estimates. *Geo-*
2343 *phys. Res. Lett.* 40 (15), 3847–3852.
- 2344 Poletti, W., Trindade, R. I., Hartmann, G. A., Damiani, N., Rech, R. M.,
2345 2016. Archeomagnetism of Jesuit Missions in South Brazil (1657-1706 AD)
2346 and assessment of the South American database. *Earth Planet. Sci. Lett.*
2347 445, 36–47.

- 2348 Reimer, P., Austin, W., Bard, E., Bayliss, A., Blackwell, P., Ramsey, C.,
2349 Butzin, M., Cheng, H., Edwards, R., Friedrich, M., Grootes, P., Guilderson,
2350 son, T., Hajdas, I., Heaton, T., Hogg, A., Hughen, K., Kromer, B., Manning,
2351 S., Muscheler, R., Palmer, J., Pearson, C., van der Plicht, J., Reimer,
2352 R., Richards, D., Scott, E., Southon, J., Turney, C., Wacker, L., Adolphi,
2353 F., Büntgen, U., Capano, M., Fahrni, S., Fogtmann-Schulz, A., Friedrich,
2354 R., Köhler, P., Kudsk, S., Miyake, F., Olsen, J., Reinig, F., Sakamoto, M.,
2355 Sookdeo, A., Talamo, S., 2020. The IntCal20 Northern Hemisphere radio-
2356 carbon age calibration curve (0-55 Cal kBP). *Radiocarbon* 62, 725–757.
- 2357 Reimer, P. J., Bard, E., Bayliss, A., Beck, J. W., Blackwell, P. G., Bronk
2358 Ramsey, C., Buck, C. E., Cheng, H., Edwards, R. L., Friedrich, M.,
2359 Grootes, P. M., Guilderson, T. P., Hafidason, H., Hajdas, I., Hatté, C.,
2360 Heaton, T. J., Hoffmann, D. L., Hogg, A. G., Hughen, K. A., Kaiser,
2361 K. F., Kromer, B., Manning, S. W., Niu, M., Reimer, R. W., Richards,
2362 D. A., Scott, E. M., Southon, J. R., Staff, R. A., Turney, C. S. M., van der
2363 Plicht, J., 2013. IntCal13 and Marine13 radiocarbon age calibration age
2364 curves 0-50,000 years cal BP. *Radiocarbon* 55, 1869–1887.
- 2365 Riisager, P., Riisager, J., 2001. Detecting multidomain magnetic grains in
2366 Thellier palaeointensity experiments. *Phys. Earth Planet. Inter.* 125, 111–
2367 117.
- 2368 Rivero-Montero, M., Gómez-Paccard, M., Pavón-Carrasco, F., Cau-
2369 Ontiveros, M., Fantuzzi, L., Martín-Hernández, F., Palencia-Ortas, A.,
2370 Aidona, E., Tema, E., Kondopoulou, D., Mas-Florit, C., Ramon-Torres,
2371 J., 2021. Refining geomagnetic field intensity changes in Europe between

- 2372 200CE and 1800 CE. New data from the Mediterranean region. *Phys. Earth*
2373 *Planet. Inter.* 317, 106749.
- 2374 Roberts, A. P., Hu, P., Harrison, R. J., Heslop, D., Muxworthy, A. R., Oda,
2375 H., Sato, T., Tauxe, L., Zhao, X., 2019. Domain state diagnosis in rock
2376 magnetism: Evaluation of potential alternatives to the Day diagram. *Journal of Geophysical Research: Solid Earth* 124 (6), 5286–5314.
2377
- 2378 Roberts, R., Jacobs, Z., Li, B., Jankowski, N., Cunningham, A., 2015. Opti-
2379 cal dating in archaeology: thirty years in retrospect and grand challenges
2380 for the future. *J. Arch. Sci.* 56, 41–60.
- 2381 Rogers, J., Fox, J., Aitken, M. J., 1979. Magnetic anisotropy in ancient
2382 pottery. *Nature* 277, 644–646.
- 2383 Rolph, T. C., Shaw, J., 1985. A new method of paleofield magnitude correc-
2384 tion for thermally altered samples and its application to Lower Carbonif-
2385 erous lavas. *Geophys. J. R. astr. Soc.* 80, 773–781.
- 2386 Roperch, P., Chauvin, A., Lara, L. E., Moreno, H., 2015. Secular variation
2387 of the earth’s magnetic field and application to paleomagnetic dating of
2388 historical lava flows in chile. *Phys. Earth Planet. Inter.* 242, 65–78.
- 2389 Sakai, H., 1980. Variation of geomagnetic field deduced from analysis of re-
2390 manent magnetization of archaeological objects. Ph.D. thesis, Osaka Uni-
2391 versity.
- 2392 Sakai, H., Hirooka, K., 1986. Archaeointensity determinations from Western
2393 Japan. *J. Geomag. Geoelectr.* 38 (12), 1323–1329.

- 2394 Salnaia, N., Gallet, Y., O.N., G., Gavryshukin, D., 2017. New archeointensity
2395 results on a baked-clay tile collection from the New Jerusalem Monastery
2396 (Moscow region, Russia). *Geophysical Research* 18, 83–94.
- 2397 Sanchez, S., Fournier, A., Aubert, J., Cosme, E., Gallet, Y., 2016. Modelling
2398 the archaeomagnetic field under spatial constraints from dynamo simu-
2399 lations: a resolution analysis. *Geophysical Journal International* 207 (2),
2400 983–1002.
- 2401 Sasajima, S., 1965. Geomagnetic secular variation revealed in the baked
2402 earths in West Japan. Part 2 Change of the field intensity. *J. Geomag.*
2403 *Geoelectr.* 17, 413–416.
- 2404 Schnepf, E., Lanos, P., 2005. Archaeomagnetic secular variation in Germany
2405 during the past 2500 years. *Geophys. J. Int.* 163 (2), 479–490.
- 2406 Schnepf, E., Leonhardt, R., Korte, M., Klett-Drechsel, J., 2016. Validity of
2407 archaeomagnetic field recording: an experimental pottery kiln at Copen-
2408 grave, Germany. *Geophys. J. Int.* 205 (1), 622–635.
- 2409 Schnepf, E., Pucher, R., Goedicke, C., Manzano, A., Müller, U., Lanos,
2410 P., 2003. Paleomagnetic directions and thermoluminescence dating from a
2411 bread oven-floor sequence in Lübeck (germany): A record of 450 years of
2412 geomagnetic secular variation. *J. Geophys. Res.* 108 (B2).
- 2413 Schnepf, E., Thallner, D., Arneitz, P., Leonhardt, R., 2020a. New archeo-
2414 magnetic secular variation data from Central Europe, II: Intensities. *Phys.*
2415 *Earth Planet. Inter.* 309, 106605.

- 2416 Schnepp, E., Thallner, D., Arneitz, P., Mauritsch, H., Scholger, R., Rolf,
2417 C., Leonhardt, R., 10 2020b. New archaeomagnetic secular variation data
2418 from Central Europe. I: directions. *Geophys. J. Int.* 220 (2), 1023–1044.
- 2419 Schwarz, E. J., Christie, K. W., 1967. Original remanent magnetization of
2420 Ontario potsherds. *J. Geophys. Res.* 72, 3263–3269.
- 2421 Selkin, P. A., Tauxe, L., 2000. Long-term variations in palaeointensity. *Philos.*
2422 *Trans. R. Soc. Lond. A* 358, 1065–1088.
- 2423 Shaar, R., Bechar, S., Finkelstein, I., Gallet, Y., Martin, M. A. S., Ebert,
2424 Y., Keinan, J., Gonen, L., 2020. Synchronizing geomagnetic field intensity
2425 records in the Levant between the 23rd and 15th Centuries BCE: Chrono-
2426 logical and methodological implications. *Geochem. Geophys. Geosyst.*
2427 21 (12), e2020GC009251.
- 2428 Shaar, R., Ben-Yosef, E., Ron, H., Tauxe, L., Agnon, A., Kessel, R., 2011.
2429 Geomagnetic field intensity: How high can it get? How fast can it change?
2430 Constraints from Iron Age copper slag. *Earth Planet. Sci. Lett.* 301, 297–
2431 306.
- 2432 Shaar, R., Hassul, E., Raphael, K., Ebert, Y., Segal, Y., Eden, I., Vaknin,
2433 Y., Marco, S., Nowaczyk, N. R., Chauvin, A., Agnon, A., 2018. The first
2434 catalog of archaeomagnetic directions from Israel with 4,000 years of geo-
2435 magnetic secular variations. *Frontiers in Earth Science* 6, 164.
- 2436 Shaar, R., Ron, H., Tauxe, L., Kessel, R., Agnon, A., Ben-Yosef, E., Feinberg,
2437 J. M., 2010. Testing the accuracy of absolute intensity estimates of the

2438 ancient geomagnetic field using copper slag material. *Earth Planet. Sci.*
2439 *Lett.* 290 (1), 201–213.

2440 Shaar, R., Tauxe, L., Ben-Yosef, E., Kassianidou, V., Lorentzen, B., Fein-
2441 berg, J. M., Levy, T. E., 2015. Decadal-scale variations in geomagnetic field
2442 intensity from ancient Cypriot slag mounds. *Geochem. Geophys. Geosyst.*
2443 16 (1), 195–214.

2444 Shaar, R., Tauxe, L., Ron, H., Ebert, Y., Zuckerman, S., Finkelstein, I.,
2445 Agnon, A., 2016. Large geomagnetic field anomalies revealed in Bronze to
2446 Iron Age archeomagnetic data from Tel Megiddo and Tel Hazor, Israel.
2447 *Earth Planet. Sci. Lett.* 442, 173–185.

2448 Shaw, J., 1974. A new method of determining the magnitude of the palaeo-
2449 magnetic field. Application to five historic lavas and five archaeological
2450 samples. *Geophys. J. R. astr. Soc.* 39, 133–141.

2451 Shaw, J., Yang, S., Rolph, T. C., Sun, F. Y., 1999. A comparison of ar-
2452 chaeointensity results from Chinese ceramics using microwave and conven-
2453 tional Thellier’s and Shaw’s methods. *Geophys. J. Int.* 136, 714–718.

2454 Shaw, J., Yang, S., Wei, Q. Y., 1995. Archaeointensity variations for the past
2455 7,500 years evaluated from ancient Chinese ceramics. *J. Geomag. Geo-*
2456 *electr.* 47 (1), 59–70.

2457 Shuey, R. T., Cole, E. R., Mikulich, M. J., 1970. Geographic correction of
2458 archeomagnetic data. *J. Geomag. Geoelectr.* 22 (4), 485–489.

2459 Simon, Q., Thouveny, N., Bourlès, D. L., Valet, J.-P., Bassinot, F.,
2460 Ménabréaz, L., Guillou, V., Choy, S., Beaufort, L., 2016. Authigenic

- 2461 $^{10}\text{Be}/^9\text{Be}$ ratio signatures of the cosmogenic nuclide production linked
2462 to geomagnetic dipole moment variation since the Brunhes/Matuyama
2463 boundary. *Journal of Geophysical Research: Solid Earth* 121 (11), 7716–
2464 7741.
- 2465 Smith, P. J., 1967. Ancient geomagnetic field intensities-I Historic and ar-
2466 chaeological data: Sets H1-H9. *Geophys. J. R. astr. Soc.* 13, 417–419.
- 2467 Soler Arechalde, A., Caballero Miranda, C., Osete López, M., López Delgado,
2468 V., Goguitchaichvili, A., Barrera Huerta, A., Urrutia Fucugauchi, J., 2019.
2469 An updated catalog of pre-hispanic archaeomagnetic data for north and
2470 central Mesoamerica: Implications for the regional paleosecular variation
2471 reference curve. *Boletín de la Sociedad Geológica Mexicana* 71 (2), 497–
2472 518.
- 2473 Stark, F., Cassidy, J., Hill, M. J., Shaw, J., Sheppard, P., 2010. Establishing
2474 a first archaeointensity record for the SW Pacific. *Earth Planet. Sci. Lett.*
2475 298, 113–124.
- 2476 Sternberg, R. S., 1989a. Archaeomagnetic paleointensity in the American
2477 Southwest during the past 2000 years. *Phys. Earth Planet. Inter.* 56 (1),
2478 1–17.
- 2479 Sternberg, R. S., 1989b. Secular variation of archaeomagnetic direction in the
2480 American Southwest, A.D. 750-1425. *J. Geophys. Res. Solid Earth* 94 (B1),
2481 527–546.
- 2482 Stillinger, M. D., Feinberg, J. M., Frahm, E., 2015. Refining the archaeo-
2483 magnetic dating curve for the Near East: new intensity data from Bronze

- 2484 Age ceramics at Tell Mozan, Syria. *Journal of Archaeological Science* 53,
2485 345–355.
- 2486 Tangborn, A., Kuang, W., 2018. Impact of archeomagnetic field model data
2487 on modern era geomagnetic forecasts. *Phys. Earth Planet. Inter.* 276, 2–9.
- 2488 Tarduno, J. A., 2018. Subterranean clues to the future of our planetary
2489 magnetic shield. *Proceedings of the National Academy of Sciences* 115 (52),
2490 13154–13156.
- 2491 Tarduno, J. A., Watkeys, M. K., Huffman, T. H., Cottrell, R. D., Blackman,
2492 E. G., Wendt, A., Scribner, C. A., Wagner, C. L., 2015. Antiquity of
2493 the South Atlantic Anomaly and evidence for top-down control on the
2494 geodynamo. *Nature Communications* 6, 7865.
- 2495 Tarling, D. H., 1989. *Geomagnetic secular variation in Britain during the*
2496 *last 2000 years*. Kluwer Academic Publishers, Dordrecht, pp. 55–62.
- 2497 Tauxe, L., 2006. Long-term trends in paleointensity: The contribution of
2498 DSDP/ODP submarine basaltic glass collections. *Phys. Earth Planet. In-*
2499 *ter.* 156, 223–241.
- 2500 Tauxe, L., Banerjee, S., Butler, R., van der Voo, R., 2018. *Essentials of*
2501 *Paleomagnetism*, 5th Web Edition.
- 2502 Tauxe, L., Shaar, R., Jonestrask, L., Swanson-Hysell, N. L., Minnett, R.,
2503 Koppers, A. A. P., Constable, C. G., Jarboe, N., Gaastra, K., Fairchild,
2504 L., 2016. PmagPy: Software package for paleomagnetic data analysis and
2505 a bridge to the Magnetism Information Consortium (MagIC) Database.
2506 *Geochem. Geophys. Geosyst.* 17 (6), 2450–2463.

- 2507 Tauxe, L., Yamazaki, T., 2015. 5.13 - Paleointensities. In: Schubert, G. (Ed.),
2508 Treatise on Geophysics (Second Edition). Elsevier, Oxford, pp. 461–509.
- 2509 Tchibinda Madingou, B., Hervé, G., Perrin, M., M'Mbogori, F. N., Gue-
2510 mona, D., Mathé, P.-E., Rochette, P., Williamson, D., Mourre, V., Robion-
2511 Brunner, C., 2020. First archeomagnetic data from Kenya and Chad: Anal-
2512 ysis of iron furnaces from Mount Kenya and Guéra Massif. *Phys. Earth*
2513 *Planet. Inter.* 309, 106588.
- 2514 Tema, E., Hedley, I., Lanos, P., 2006. Archaeomagnetism in Italy: a com-
2515 pilation of data including new results and a preliminary Italian reference
2516 curve. *Geophys. J. Int.* 167, 1160–1171.
- 2517 Tema, E., Herrero-Bervera, E., Lanos, P., 2017. Geomagnetic field secular
2518 variation in Pacific Ocean: A Bayesian reference curve based on Holocene
2519 Hawaiian lava flows. *Earth Planet. Sci. Lett.* 478, 58–65.
- 2520 Tema, E., Lanos, P., 2020. New Italian directional and intensity archaeomag-
2521 netic reference curves for the past 3000 years: Insights on secular variation
2522 and implications on dating. *Archaeometry*.
- 2523 Terra-Nova, F., Amit, H., Hartmann, G., Trindade, R., 2016. Using archaeo-
2524 magnetic field models to constrain the physics of the core: robustness
2525 and preferred locations of reversed flux patches. *Geophys. J. Int.* 206 (3),
2526 1890–1913.
- 2527 Terra-Nova, F., Amit, H., Hartmann, G., Trindade, R., Pinheiro, K., 2017.
2528 Relating the South Atlantic Anomaly and geomagnetic flux patches. *Phys.*
2529 *Earth Planet. Inter.* 266, 39–53.

- 2530 Thébault, E., Gallet, Y., 2010. A bootstrap algorithm for deriving the archeo-
2531 magnetic field intensity variation curve in the Middle East over the past 4
2532 millennia BC. *Geophys. Res. Lett.* 37, L22303.
- 2533 Thellier, E., 1938. Sur l'aimantation des terres cuites et ses applications
2534 géophysiques. *Ann. Inst. Globe Univ. Paris* 16, 157–302.
- 2535 Thellier, E., 1941. Sur les propriétés de l'aimantation thermorémanente des
2536 terres cuites. *C. R. Acad. Sci. Paris* 213, 1019–1022.
- 2537 Thellier, E., 1946. Sur l'intensité du champ magnétique terrestre, en France,
2538 à l'époque gallo-romaine. *C. R. Acad. Sci. Paris* 222, 905–907.
- 2539 Thellier, E., 1977. Early research on the intensity of the ancient geomagnetic
2540 field. *Phys. Earth Planet. Inter.* 13, 241–244.
- 2541 Thellier, E., 1981. Sur la direction du champ magnétique terrestre, en France,
2542 durant les deux derniers millénaires. *Phys. Earth Planet. Inter.* 24 (2), 89–
2543 132.
- 2544 Thellier, E., Thellier, O., 1959. Sur l'intensité du champ magnétique terrestre
2545 dans le passé historique et géologique. *Ann. Géophys.* 15, 285–376.
- 2546 Trindade, R. I. F., Jaqueto, P., Terra-Nova, F., Brandt, D., Hartmann, G. A.,
2547 Feinberg, J. M., Strauss, B. E., Novello, V. F., Cruz, F. W., Karmann, I.,
2548 Cheng, H., Edwards, R. L., 2018. Speleothem record of geomagnetic South
2549 Atlantic Anomaly recurrence. *Proceedings of the National Academy of*
2550 *Sciences* 115 (52), 13198–13203.

- 2551 Troyano, M., Gallet, Y., Genevey, A., Pavlov, V., Fournier, A., Niyazova, M.,
2552 Mirzaakhmedov, D., 2020. Constraining the axial dipole moment variations
2553 during the historical period from new archeointensity results obtained in
2554 Bukhara (Uzbekistan, Central Asia). *Phys. Earth Planet. Inter.* 309, TBD.
- 2555 Tsunakawa, H., Shaw, J., 1994. The Shaw method of palaeointensity deter-
2556 minations and its application to recent volcanic rocks. *Geophys. J. Int.*
2557 118, 781–787.
- 2558 Turner, G. M., King, R., McFadgen, B., Gevers, M., 2020. The first ar-
2559 chaeointensity records from New Zealand: evidence for a fifteenth century
2560 AD archaeomagnetic ‘spike’ in the SW Pacific Region? Geological Society,
2561 London, Special Publications 497.
- 2562 Usoskin, I. G., Gallet, Y., Lopes, F., Kovaltsov, G. A., Hulot, G., 2016. Solar
2563 activity during the Holocene: the Hallstatt cycle and its consequence for
2564 grand minima and maxima. *Astronomy and Astrophysics* 587, A150.
- 2565 Usoskin, I. G., Korte, M., Kovaltsov, G. A., 2008. Role of centennial geo-
2566 magnetic changes in local atmospheric ionization. *Geophys. Res. Lett.* 35,
2567 L05811.
- 2568 Usoskin, I. G., Mironova, I. A., Korte, M., Kovaltsov, G. A., 2010. Regional
2569 millennial trend in the cosmic ray induced ionization of the troposphere.
2570 *J. Atmos. Sol. Terr. Phys.* 72, 19–25.
- 2571 Usoskin, I. G., Solanki, S. K., Korte, M., 2006. Solar activity reconstructed
2572 over the last 7000 years: The influence of geomagnetic field changes. *Geo-
2573 phys. Res. Lett.* 33, L08103.

- 2574 Valet, J.-P., Herrero-Bervera, E., LeMoüel, J.-L., Plenier, G., 2008. Secular
2575 variation of the geomagnetic dipole during the past 2000 years. *Geochem.*
2576 *Geophys. Geosyst.* 9, Q01008.
- 2577 Veitch, R., Hedley, I., Wagner, J., 1984. An investigation of the intensity of
2578 the geomagnetic field during Roman times using magnetically anisotropic
2579 bricks and tiles. *Arch. Sci. Genève* 37, 359–373.
- 2580 Walton, D., 1977. Archaeomagnetic intensity measurements using a SQUID
2581 magnetometer. *Archaeometry* 19 (2), 192–200.
- 2582 Walton, D., Snape, S., Rolph, T., Shaw, J., Share, J., 1996. Application of
2583 ferrimagnetic resonance heating to palaeointensity determinations. *Phys.*
2584 *Earth Planet. Inter.* 94 (3), 183–186.
- 2585 Wardinski, I., Korte, M., 2008. The evolution of the core-surface flow over
2586 the last seven thousands years. *J. Geophys. Res.* 113, B05101.
- 2587 Watanabe, N., 1958. Secular variation in the direction of geomagnetism as
2588 the standard scale for geomagnetochemistry in Japan. *Nature* 182 (3-4),
2589 383–384.
- 2590 Watanabe, N., Dubois, R. L., 1965. Some results of an archaeomagnetic study
2591 on the secular variation in the southwest of North America. *J. Geomag.*
2592 *Geoelectr.* 17 (3-4), 395–397.
- 2593 Wei, Q. Y., Li, D. J., Cao, G. Y., Zhang, W. S., Wang, S. P., 1982. Intensity
2594 of the geomagnetic field near Loyang, China between 500 BC and AD 1900.
2595 *Nature* 296, 728–729.

- 2596 Wei, Q. Y., Li, D. J., Cao, G. Y., Zhang, W. X., Wei, S. F., 1986. The total
2597 intensity of geomagnetic field in southern China for the period from 4500
2598 B.C. to A.D. 1500. *J. Geomag. Geoelectr.* 38, 1311–1322.
- 2599 Wilson, M. A., Carter, M. A., Hall, C., Hoff, W. D., Ince, C., Savage, S. D.,
2600 Mckay, B., Betts, I. M., 2009. Dating fired-clay ceramics using long-term
2601 power law rehydroxylation kinetics. *Proceedings of the Royal Society of*
2602 *London A* 465 (2108), 2407–2415.
- 2603 Wilson, R. L., 1961. Paleomagnetism in Northern Ireland, Part I, The thermal
2604 demagnetization of natural magnetic moments in rocks. *Geophys. J. R.*
2605 *astr. Soc.* 5, 45–58.
- 2606 Yamamoto, Y., Tsunakawa, H., 2005. Geomagnetic field intensity during the
2607 last 5 Myr: LTD-DHT Shaw palaeointensities from volcanic rocks of the
2608 Society Islands, French Polynesia. *Geophys. J. Int.* 162, 79–114.
- 2609 Yamamoto, Y., Tsunakawa, H., Shibuya, H., 2003. Palaeointensity study of
2610 the Hawaiian 1960 lava: implications for possible causes of erroneously
2611 high intensities. *Geophys. J. Int.* 153, 263–276.
- 2612 Yang, S., Odah, H., Shaw, J., 2000. Variations in the geomagnetic dipole
2613 moment over the last 12000 years. *Geophys. J. Int.* 140, 158–162.
- 2614 Yang, T., Shaw, J., Wei, Q. Y., 1993. A comparison of archaeointensity
2615 results from Chinese ceramics using Thellier's and Shaw's palaeointensity
2616 methods. *Geophys. J. Int.* 113, 499–508.
- 2617 Yu, Y., Tauxe, L., Genevey, A., 2004. Toward an optimal geomagnetic

- 2618 field intensity determination technique. *Geochem. Geophys. Geosyst.* 5,
2619 Q02H07.
- 2620 Yutsis-Akimova, S., Gallet, Y., Amirov, S., 2018a. Rapid geomagnetic field
2621 intensity variations in the Near East during the 6th millennium BC: New
2622 archeointensity data from Halafian site Yarim Tepe II (northern Iraq).
2623 *Earth Planet. Sci. Lett.* 482, 201–212.
- 2624 Yutsis-Akimova, S., Gallet, Y., Petrova, N., Nowak, S., Le Goff, M., 2018b.
2625 Geomagnetic field in the Near East at the beginning of the 6th millennium
2626 BC: Evidence for alternating weak and strong intensity variations. *Phys.*
2627 *Earth Planet. Inter.* 282, 49–59.
- 2628 Zanella, E., Gurioli, L., Chiari, G., Ciarallo, A., Cioni, R., De Carolis, E.,
2629 Lanza, R., 2000. Archaeomagnetic results from mural paintings and py-
2630 roclastic rocks in Pompeii and Herculaneum. *Phys. Earth Planet. Inter.*
2631 118 (3), 227–240.
- 2632 Zeigen, C., Shaar, R., Ebert, Y., Hovers, E., 2019. Archaeomagnetism of
2633 burnt cherts and hearths from Middle Palaeolithic Amud Cave, Israel:
2634 Tools for reconstructing site formation processes and occupation history.
2635 *Journal of Archaeological Science* 107, 71–86.